



**Universitat**  
de les Illes Balears

## **MASTER'S THESIS**

# **SYNTHESIS AND CHARACTERIZATION OF GOLD-NUCLEIC BASES COMPLEXES**

**Jordi Buils Casanovas**

**Master's Degree in Chemical Science and Technology**

**(Specialisation/Pathway *Biological chemistry / Organic Chemistry*)**

**Centre for Postgraduate Studies**

**Academic Year 2020-21**

# **Synthesis and characterization of gold-nucleic bases complexes**

**Jordi Buils Casasnovas**

**Master's Thesis**

**Centre for Postgraduate Studies**

**University of the Balearic Islands**

**Academic Year 2020-21**

Key words:

Gold complexes, bioinorganic chemistry, nucleic acids, coordination chemistry, nucleic bases, cytosine, uracil

*Thesis Supervisor's Name Dr. Àngel Terrón Homar*



## **Acknowledgments:**

I would like to thank my family for their emotional support during the realization of this work, without which it would have been harder to accomplish. Also I'd like to thank my partner for unconditional help and support.

I would like to thank Dr. Angel García Raso for his help with the obtention and elucidation of NMR spectrum, also for his countless tips on my TFM and life in general.

I would like to thank Dr. Juan Jesús Fiol Arbós for his tips on general coordination chemistry and for his general advice.

I would like to thank in a special way the indispensable collaboration of Dr. Miquel Barceló Oliver without which this TFM would not be finished. Also I'd like to thank him for carrying out the X-ray diffraction studies over my complexes, and for the elucidation of its structure.

Last, I would like to thank Dr. Àngel Terrón Homar for his guidance and help during the completion of my TFM. Also I'd like to thank him for these two and a half years of collaboration, during which I've learned lots of things related to chemistry, history, and other subjects. Not only he has been my tutor, but also, he has been a mentor to me, introducing me to the investigation career, and teaching things about how life works. For his countless talks, for his support on my last years of the chemistry degree, for his understanding of my personal problems. For all these things, I want to thank Dr. Terrón.

# Content's index

Abstract.....	6
1 Introduction .....	7
1.1 Historical Precedents: topic's motivation.....	7
1.2 Bioinorganic chemistry .....	8
1.3 Nucleic Acids.....	8
1.3.1 Base Pair .....	12
1.4 Coordination chemistry .....	13
1.4.1 Gold complexes.....	14
1.4.2 Other gold complexes .....	14
1.4.3 Gold red-ox chemistry .....	16
1.5 Weak interactions.....	17
1.5.1 Hydrogen Bond .....	17
1.5.2 Anion- $\pi$ and Cation- $\pi$ .....	17
1.5.3 Stacking forces .....	18
1.5.4 Hydrophobic interactions .....	19
1.5.5 Van der Waals .....	21
1.5.6 Regium bond.....	21
2 Objectives.....	23
3 Methods and Materials.....	24
3.1 Materials and Techniques .....	24
3.2 Synthesis.....	25
4 Results and discussion.....	31
4.1 Synthetic strategies .....	31
4.2 Spectroscopic characterization.....	32
4.2.1 MeCyt complexes.....	32
4.2.2 Cyd complexes .....	34
4.2.3 CytC <sub>6</sub> complexes .....	35
4.3 Structural characterization .....	36
4.3.1 AuCl <sub>3</sub> (CytC <sub>6</sub> ) .....	36
4.3.2 (HCytC <sub>6</sub> ) <sub>2</sub> [AuCl <sub>4</sub> ] Cl .....	43
5 Conclusions .....	48
6 Annexes.....	49
6.1 Annex I: Abbreviations .....	50
6.1 Annex II: IR spectrum .....	53
6.2 Annex III: <sup>1</sup> H-NMR spectrum.....	61
6.3 Annex IV: ESI-HRMS spectrums .....	69
6.4 Annex V: Crystallographic data and X-Ray structures .....	73

# Abstract

*All abbreviations used in this work are summarised in Annex I: Abbreviations*

1. Some new coordination complexes of gold (III) with nucleic bases and their derivatives have been synthesized and characterised:
  - 1.1. The MeCyt-Au 1:2 derivative has been synthesized and spectroscopic data induces thinking of trans isomer being formed.
  - 1.2. The Cyt-Au 1:1 and 1:2 derivatives have been synthesized but any of these complexes have crystalized.
  - 1.3. A 1:1 derivative of CytC<sub>6</sub>-Au, crystalized in a different packing, being a polymorph of the already described coordination compound<sup>10</sup>. In this case, water was used as solvent instead of acetonitrile.
2. A new outer-sphere complex of CytC<sub>6</sub> has been obtained and studied by High Resolution Single Crystal X-ray diffraction.
3. A new line of investigation has been opened, after seeing the reaction of uracil derivatives with Au(III).

This work enhances the knowledge of the gold interaction with nucleic bases and opens new perspectives for futures work in this field that to this day so much is still yet unknown. In concrete the possibility to crystalize a 1:2 derivative of cytosine with gold would be a major hit, as it would possibly resemble DNA structure.

# 1 Introduction

## 1.1 Historical Precedents: topic's motivation

This work is a follow up of my graduate degree's final project, where I started studying the coordination chemistry of complexes with nucleic bases and its derivatives. The coordination chemistry of nucleic bases and metal ions is a topic with high interest among the bioinorganic chemists<sup>1,2,3,4</sup>. It has been studied for the last decades<sup>5</sup>, and recently studied intensively due to all the possible applications of these compounds. Its applications include anticancer drugs, antiarthritic medicines and new nanomaterials development<sup>6,7,8</sup>, all of this with unique properties. Few bibliographic references have been published about gold and nucleic bases complexes.

The precedents that motivate this TFM are the publication of new coordination complex of nucleic bases and derivatives with silver<sup>9</sup> and gold<sup>10</sup>. Silver structures were obtained with different cytosine derivatives: N<sup>1</sup>-hexylcytosine, methyl-cytosine<sup>11</sup> and cytidine<sup>12</sup>, while gold structure was obtained with N<sup>1</sup>-hexylcytosine. This project will be aimed to design and optimize the synthesis of new coordination compounds, based on the poor information related. Also, structural characterization has been done with suitable X-ray diffraction crystals, during the realization of this TFM. Very few spectroscopic data is published about this type of compounds, and owing to this reason, the characterization of new gold complexes is both very important and very hard.

---

<sup>1</sup> Lippert, B.; Sanz Miguel, P. J. Merging Metal–Nucleobase Chemistry With Supramolecular Chemistry. *Advances in Inorganic Chemistry* 2018, 71, 277–326.

<sup>2</sup> Lippert, B.; Sanz Miguel, P. J. The Renaissance of Metal–Pyrimidine Nucleobase Coordination Chemistry. *Accounts of Chemical Research* 2016, 49 (8), 1537–1545.

<sup>3</sup> Sigel, A. and Sigel, H. Eds. *Metal Ions in Biological Systems. Interactions of Metal Ions with Nucleotides, Nucleic Acids, and Their Constituents*, Marcel Dekker Inc., vol 32, New York. 1996.

<sup>4</sup> A. Sigel; H. Sigel; R.K.O. Sigel (eds); *Interplay between metal ions and nucleic acids*, *Metal Ions in Life Sciences*, vol 10, Springer, (2012).

<sup>5</sup> Lusty, J. R.; Wearden, P. *Handbook of Nucleobase Complexes. Transition Metal Complexes of Naturally Occurring Nucleobases and Their Derivatives*. CRC PRESS Bocarratón 1990, I and II.

<sup>6</sup> Zhou, P.; Shi, R.; Yao, J.-feng; Sheng, C.-fang; Li, H. *Supramolecular Self-Assembly OF Nucleotide–Metal coordination complexes: From Simple Molecules to Nanomaterials*. *Coordination Chemistry Reviews* 2015, 292, 107–143.

<sup>7</sup> Pu, F.; Ren, J.; Qu, X. *Nucleobases, Nucleosides, and Nucleotides: Versatile Biomolecules for Generating Functional Nanomaterials*. *Chemical Society Reviews* 2018, 47 (4), 1285–1306.

<sup>8</sup> Zhang, Y.; Jiang, H.; Ge, W.; Li, Q.; Wang, X. *Cytidine-Directed Rapid Synthesis of Water-Soluble and Highly Yellow Fluorescent Bimetallic AuAg Nanoclusters*. *Langmuir* 2014, 30 (36), 10910–10917.

<sup>9</sup> Terrón, A.; Moreno-Vachiano, B.; Bauzá, A.; García-Raso, A.; Fiol, J. J.; Barceló-Oliver, M.; Molins, E.; Frontera, A. *X-Ray Crystal Structure of a Metalled Double-Helix Generated by Infinite and Consecutive C\*–AgI–C\* (C\*:N1-Hexylcytosine) Base Pairs through Argentophilic and Hydrogen Bond Interactions*. *Chemistry - A European Journal* 2017, 23 (9), 2103–2108.

<sup>10</sup> Terrón, A.; Buils, J.; Mooibroek, T. J.; Barceló-Oliver, M.; García-Raso, A.; Fiol, J. J.; Frontera, A. *Synthesis, X-Ray Characterization and Regium Bonding Interactions of a Trichlorido(1-Hexylcytosine) Gold (III) Complex*. *Chemical Communications* 2020, 56 (24), 3524–3527.

<sup>11</sup> Linares, F.; García-Fernández, E.; López-Garzón, F. J.; Domingo-García, M.; Orte, A.; Rodríguez-Diéguez, A.; Galindo, M. A. *Multifunctional Behavior of Molecules Comprising Stacked Cytosine–AgI–Cytosine Base Pairs; towards Conducting and Photoluminescence Silver-DNA Nanowires*. *Chemical Science* 2019, 10 (4), 1126–1137.

<sup>12</sup> Mistry, L.; El-Zubir, O.; Dura, G.; Clegg, W.; Waddell, P. G.; Pope, T.; Hofer, W. A.; Wright, N. G.; Horrocks, B. R.; Houlton, A. *Addressing the Properties of "Metallo-DNA" with a Ag(I)-Mediated Supramolecular Duplex*. *Chemical Science* 2019, 10 (11), 3186–3195.

## 1.2 Bioinorganic chemistry

Bioinorganic chemistry is the field that studies the roles of metals and inorganic elements in biological systems, in other words, it correlates biological activity of inorganic system inside organic environment with all its characteristics. Bioinorganic chemistry is a multidisciplinary area situated in between biochemistry, inorganic chemistry, organic chemistry, physical chemistry, and medicine. Biology is usually associated with organic chemistry because most present elements in living beings are Carbon, Nitrogen, Oxygen and Hydrogen. But there at least other 20 chemical elements, which have important roles inside living systems, called elemental elements. Excess or deficiency of this elements is translated into functional deficiencies and prevents organisms from growing. Then, elements can be classified as essential, toxic or of pharmacological interest.

Coordination complexes involving elements such as Platinum, Gold, Palladium, Gallium or Silver have a pharmacological interest as possible anti-cancer drug. Cisplatin was the first of many to fight different kinds of cancer. Bioinorganic chemistry studies different areas such as transport, storage and biomineralization of transition metals; electron transfer or metal/nucleic-acid interactions. Some of these are the synthesis of new nanomaterials, creation of MOFs (metal organic framework) or new metallodrugs. S. J. Lippard<sup>13</sup> defined the main guidelines of bioinorganic chemistry:

1. Study of the function of bio-metals and of their mechanisms of action.
2. Synthesis of simple models that try to reproduce the behaviour of more complex systems to understand its functioning.
3. Addition of metal ions or coordination complexes to biological systems to carry out structure and function tests.

These last studies are the ones I have focused on. The metal-nucleic acids complexes have been studied due to the wide range of applications: from nanomaterials to new drugs against cancer. Platinum drugs are used as anticancer medicines, gold drugs are used to treat arthritis, and lithium is used for depression treatment.

## 1.3 Nucleic Acids

Nucleic acids are biopolymers essential to all forms of life, composed of nucleotides which are the monomers. These nucleotides are formed by three different biomolecules: a 5 carbon atoms pentose, a phosphate group, and a nucleobase. Nucleobases or nitrogenous base are cyclic organic compounds that contain at least two nitrogen atoms. The nucleobases in nucleic acids are the following: Adenine, Thymine, Guanine, Cytosine and Uracil. These nucleobases are classified into 2 different groups depending on its structures: pyrimidines and purines. In Table 1 nucleobases, sugars and phosphate are classified according to its structure and in which nucleic acid are found, while in Table 2 it is shown the  $pK_a$  of nucleobases and its natural derivatives:

---

<sup>13</sup> Lippard, S. J.; Berg, J. M. Principles of bioinorganic chemistry; University Science Books: Mill Valley, California, 1994.



Table 1 Nucleobases, sugars and phosphate found in nucleic acids

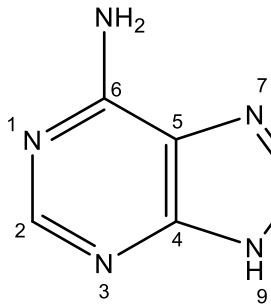
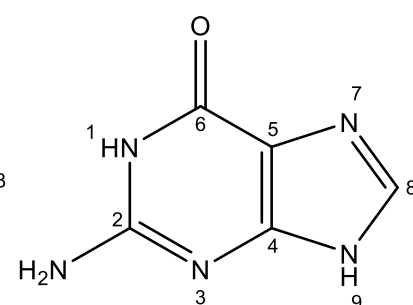
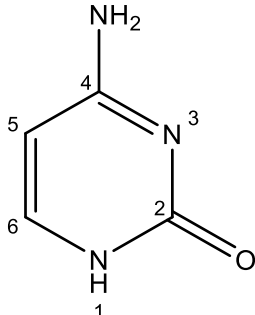
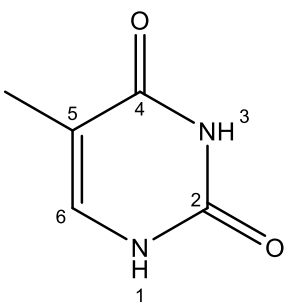
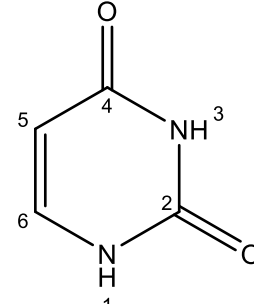
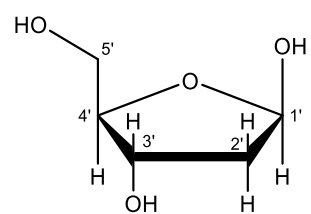
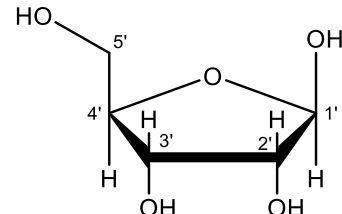
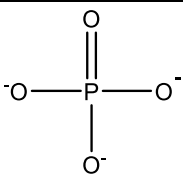
		DNA	RNA
Nucleobases	Purines	 <p>Adenine (A)</p>	 <p>Guanine (G)</p>
	Pyrimidines	 <p>Cytosine (C)</p>	
		 <p>Thymine (T)</p>	 <p>Uracil (U)</p>
	Sugar	 <p>2'-Deoxyribose</p>	 <p>Ribose</p>
Phosphate	 <p>Phosphate</p>		

Table 2 Nucleobase's acidity constants for nucleic bases, nucleosides, and nucleotides <sup>14</sup>.

Nucleobase	Site	pK <sub>a</sub> at 25°C and [I]=0.1M		
		Base	Nucleoside	Nucleotide
Adenine	N7	-	-1.6	-
	N1	4.1	3.6	3.8
	N9	9.7	-	-
Guanine	N7	2.9	2.2	2.4
	N1	8.8	8.7	8.9
Cytosine	N3	4.5	4.3	4.4
Uracil	N3	9.5	9.3	9.6
Thymine	N3	9.8	9.6	9.9
Free Phosphate			~6.3	

Other nitrogenous bases such as 5-methylcytosine or N<sup>6</sup>-methyladenine can be found in DNA. But it is in t-RNA where more nucleobases derivatives are found. Among these derivatives are inosine, which is a derivative of hypoxanthine, dihydrouridine and 7-methylguanosine which structures are shown in Figure 1:

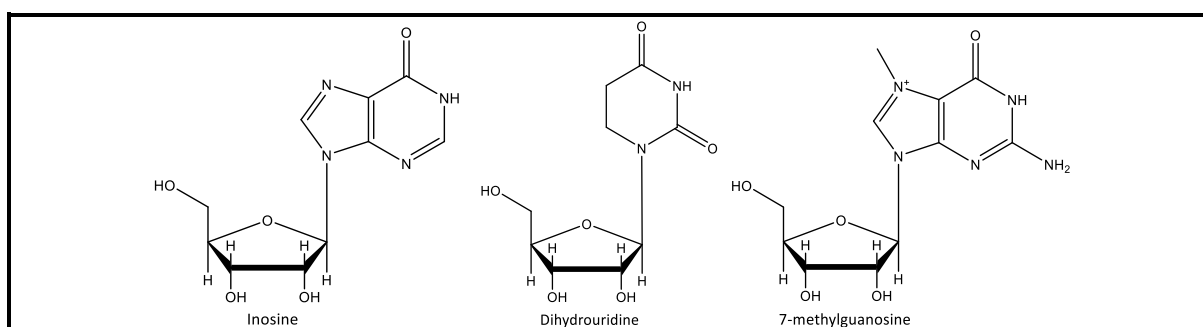
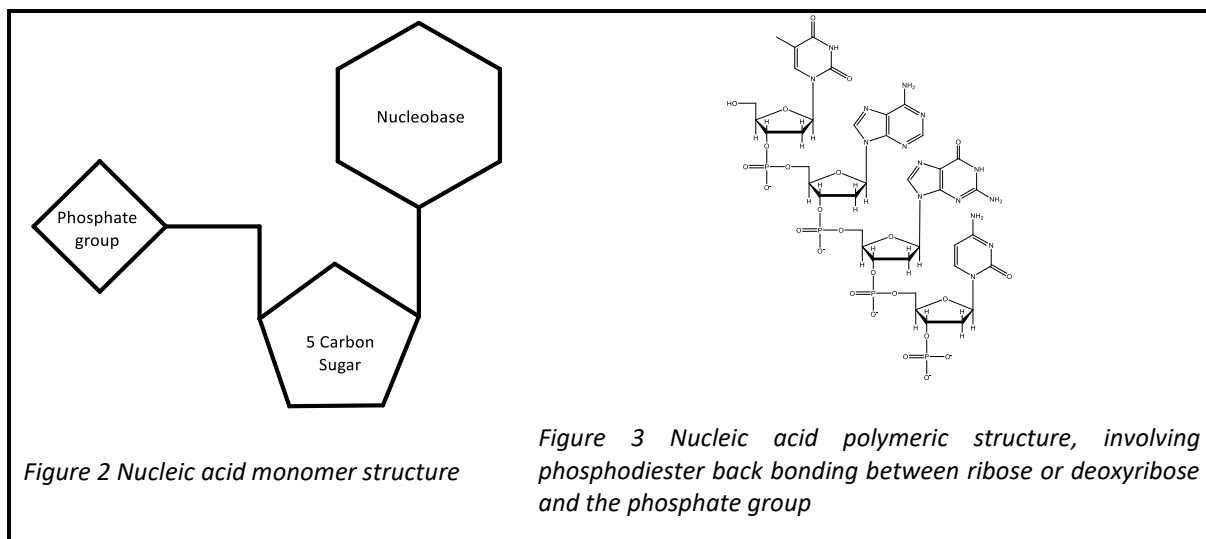


Figure 1 Inosine, dihydrouridine and 7-methylguanosine structures.

There are two main classes of nucleic acid, deoxyribonucleic acid (DNA) and ribonucleic acid (RNA). This is determined by the sugar in the nucleotide, if the sugar is ribose the polymer is RNA and if the sugar is a deoxyribose the polymer is DNA. These polymers form helicoidal structures through consecutive nucleotides linked by phosphodiester bonding. RNA can also comply for a huge number of different structures. The DNA contains the genetic code used by the organisms to functionally live. In the other hand RNA converts the genetic information from genes into the amino-acid sequence that form proteins. In Figure 2 and Figure 3 monomeric and polymeric structure of DNA and RNA is shown:

<sup>14</sup> Martin, R. B. Nucleoside Sites for Transition Metal Ion Binding; Accounts of Chemical Research, 1985, 18, 32–38.



Nucleic acids' structures consist of single-stranded or doubled-stranded polymers. Double-stranded DNA keeps its structure due to hydrogen bonding between opposite chains. This hydrogen bonding complies mainly for 3 types of interaction. DNA structure presents three different types of structures which are type A, type B and type Z. Type B DNA is the most common form in vivo. B type is narrower and more elongated than A type, which makes the major groove more accessible to proteins. The most favoured conformations happen at higher water concentrations, and base pairs interact perpendicularly to the helix axis. On the other hand, A type DNA occurs in dehydration conditions. Z type DNA structures rarely happen, and the difference with A and B type is the rotation of the helix, which in Z type is opposite. In high salt concentrations, Z-type conformation is most favoured. These conformations are shown in Figure 4 and in Table 3 basic conformational parameters are presented:

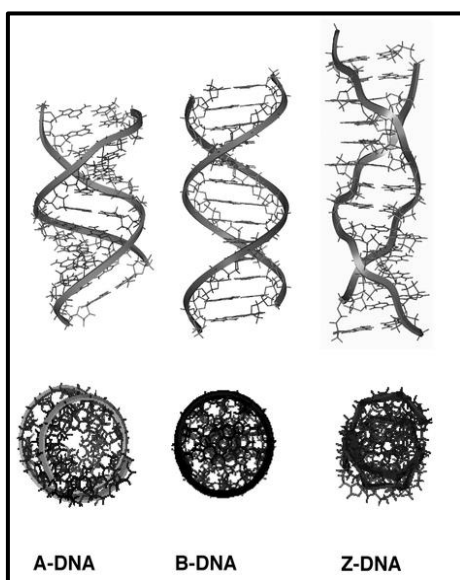


*Figure 4 Nucleic acid conformation. The main differences lie in the increase in the distance between bases, the length of the turn of the DNA helix, the decrease in the diameter of the helix and the variation in the number of bases per turn<sup>15</sup>.*

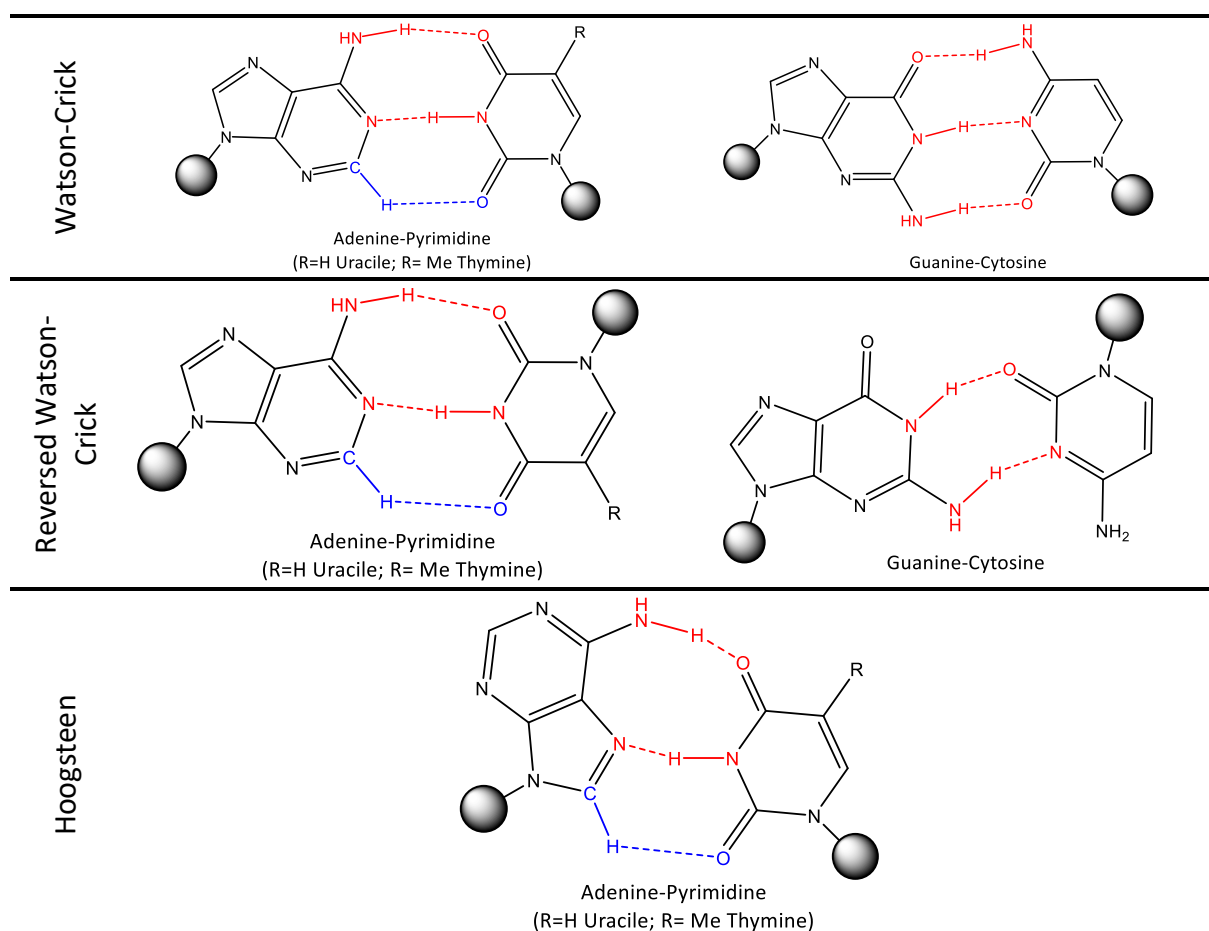
<sup>15</sup> Belmont, P.; Constant, J. F.; Demeunynck, M. Nucleic Acid Conformation Diversity: from Structure to Function and Regulation. Chemical Society Reviews 2001, 30 (1), 70–81.

Table 3 DNA conformational parameters from A type, B type and Z type DNA<sup>15</sup>.

<i>Parameter</i>	<b>A-DNA</b>	<b>B-DNA</b>	<b>Z-DNA</b>
<b>Helix sense</b>	Right	Right	Left
<b>Residue per turn</b>	11	10.5	11.6
<b>Axial rise</b>	2.55 Å	3.4 Å	3.7 Å
<b>Diameter of helix</b>	23 Å	20 Å	18 Å

### 1.3.1 Base Pair

As commented previously, DNA's structure is held by hydrogen bonding between bases. Opposite base pairs interactions can be classified according to how the hydrogen bond is formed, and according to the position of the nucleobase. In Figure 5 it is shown most common base pair interactions:



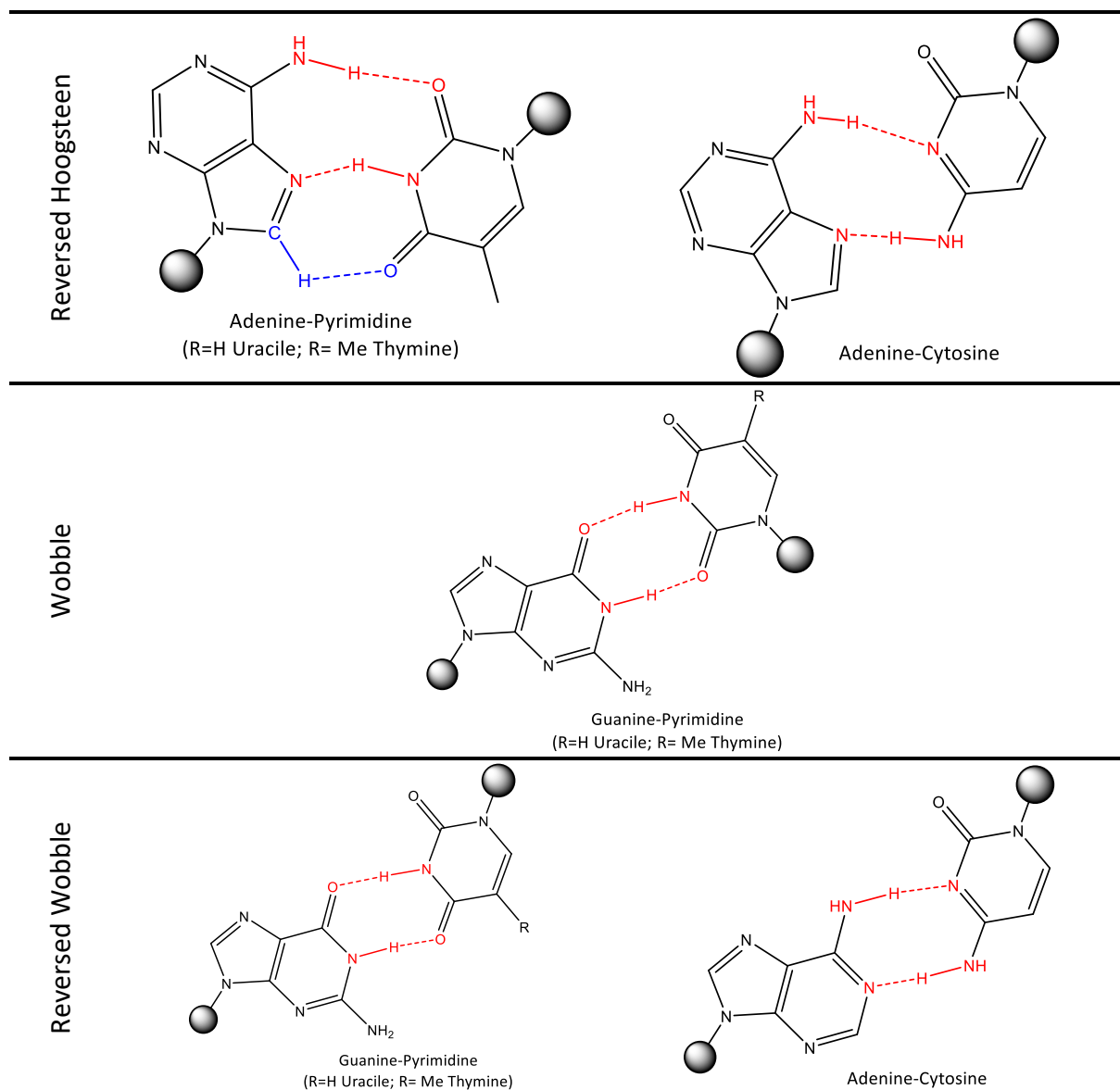


Figure 5 Most common base pair interactions models. Note that in Adenine-Pyrimidine interactions, there is one hydrogen bond from a carbon atom shown in blue.

## 1.4 Coordination chemistry

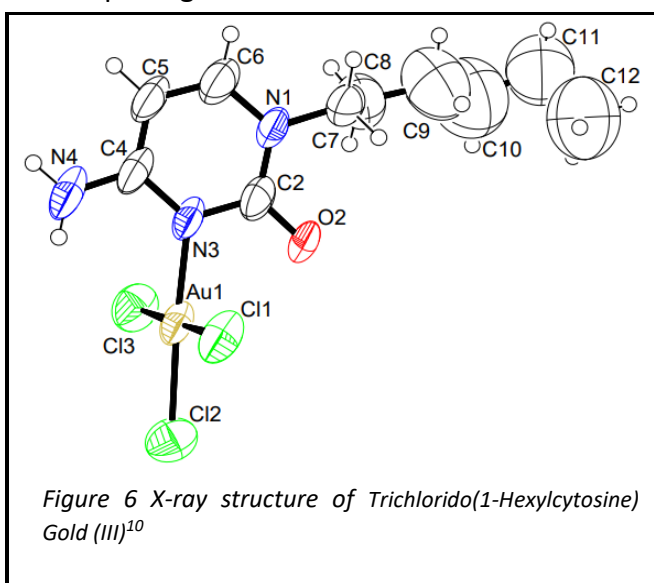
Coordination chemistry is the branch of chemistry that studies the bonds of a molecule with a central atom (usually a metal ion) and the atoms that surround it, which are called ligands. These ligands are directly bind to the central atom donating at least on pair of free electrons to it. Most of the metal compounds in block “d” are coordination complexes. Metal ion complexes have a huge variety of geometries, colors, and electronic properties. These properties depend on central atom, oxidation state, isomerism (for instance,  $\text{cis-Co(IDA)}_2$  and  $\text{trans-Co(IDA)}_2$  where IDA means iminodiacetate, show different colors, one is purple, and the other is brown) and the ligands that can bind to central atom in different ways. Molecular Orbital Theory as well as Crystal Field Theory, Ligand Field Theory, VSEPR (Valence shell electron pair repulsion) Theory and Valence Bond Theory try to explain coordination complexes geometries and structures, electronic properties, and vibrational states. Coordination complexes have been known for long time, even though they were not

understood at all. These kinds of compounds are now used in metal-drugs such as cisplatin, auranofin or chelating drugs as EDTA, BAL etc. These drugs are used in medicine to treat a variety of diseases and illnesses, other are used in imaging techniques. Some metal complexes are also found inside biological world: hemoglobin, B12 vitamin, DNA zinc fingers, and a lot of other proteins and enzymes.

#### 1.4.1 Gold complexes

Gold is the 79<sup>th</sup> element of the periodic table and is comprised in the noble metals group. It is a transition metal and in its natural state does not react with most reagents. It is found in nature as gold nuggets or grains, in rocks and in alluvial deposits. Gold is not soluble in nitric acid unlike silver and other metals, but it is in “aqua regia” which forms tetrachloridoaurate anion, which will be the initial gold compound used in the experimental process. Oxidation states go from -3 to +3, being Au<sup>0</sup>, Au<sup>+1</sup> and Au<sup>+3</sup> the most common. Gold (III) complexes usually comply for a square planar geometry while Gold (I) complexes tend to form linear geometries.

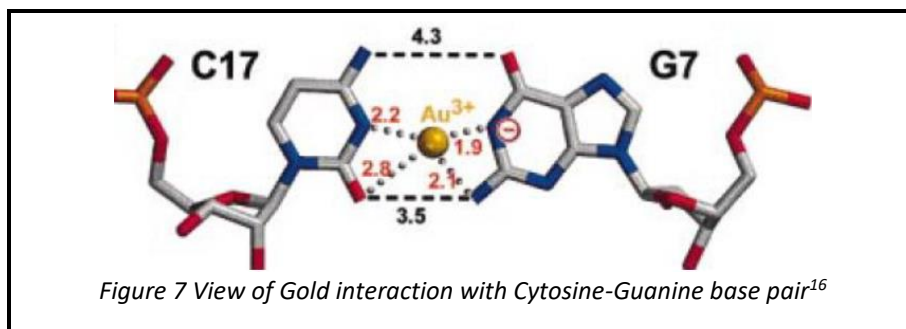
Pearson’s classification sort cations and anions by their hardness which depends on the size and charge of the ion. Gold (I) is classified as soft ion and gold (III) is classified as intermedium. This implies that interaction between gold (I) and ligands will be ruled by orbital coefficients and thus the gold will seek to bind itself to soft atoms like sulfur or phosphorus in phosphines. On the other hand, gold (III) can interact with soft and hard ions and atoms like phosphates or pyridine-like nitrogen. This interaction between gold and heterocyclic nitrogen is the one that will allow the gold-nucleobases complexes to form. Purines will bond preferably by N<sup>7</sup>, and pyrimidines will do it by N<sup>3</sup>. An example of this is the recently published, by our research team, gold N<sup>1</sup>-hexylcytosine coordination complex<sup>10</sup> and it is shown in Figure 6.



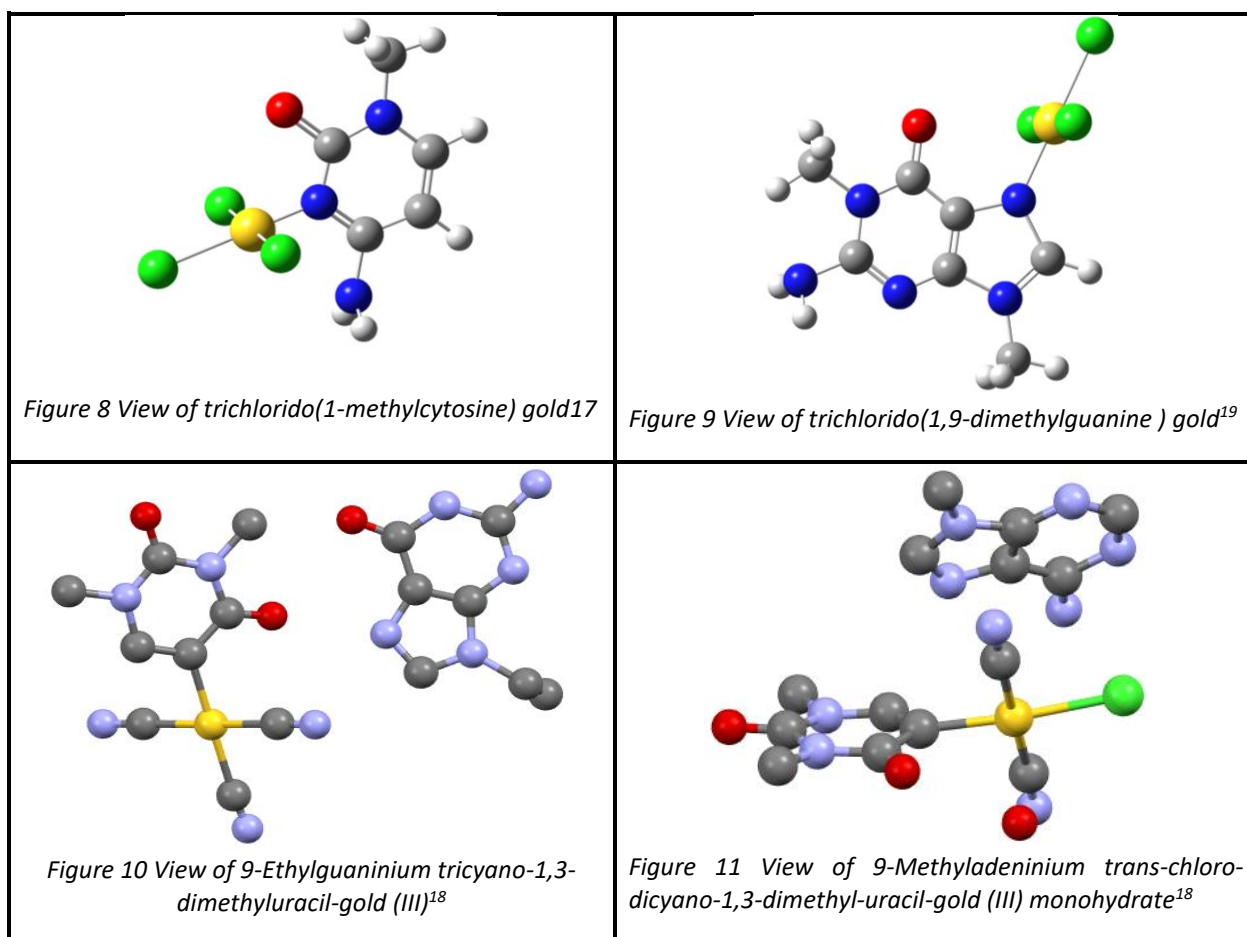
#### 1.4.2 Other gold complexes

The amount of well characterized by X-ray diffraction gold-nucleic bases or its derivatives complexes is quite low. There is one structure published where gold binds to a Cytosine-Guanine base pair within an RNA structure (Figure 7), but resolution is too low to assure either oxidation state of gold or coordination positions<sup>16</sup>.

<sup>16</sup> Ennifar, E. A Crystallographic Study of the Binding of 13 Metal Ions to Two Related RNA Duplexes. *Nucleic Acids Research* 2003, 31 (10), 2671–2682.



Apart from this structure, there are few other coordination complexes, but only one involving methyl-cytosine<sup>17</sup> (Figure 8), apart from the coordination compound published by my research team<sup>10</sup> very recently, with my participation. Other important structures are two organometallic uracil-gold complexes<sup>18</sup> (Figure 10 and Figure 11). Also, a guanine derivative gold complex was published<sup>19</sup> (Figure 9):



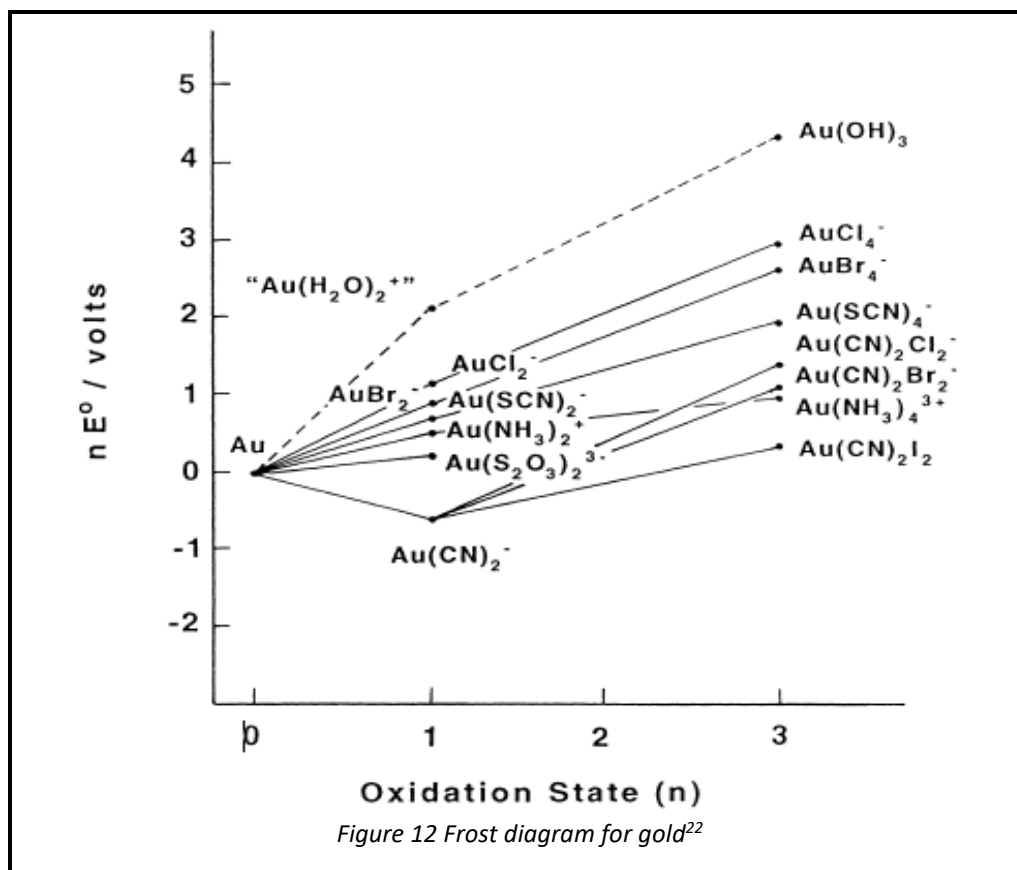
<sup>17</sup> Holowczak, M. S.; Stancl, M. D.; Wong, G. B. Trichloro(1-Methylcytosinato)Gold(III). Model for Gold-DNA Interactions. *Journal of the American Chemical Society* 1985, 107 (20), 5789–5790.

<sup>18</sup> Zamora, F.; Zangrando, E.; Furlan, M.; Randaccio, L.; Lippert, B. Au (III), Binding to C5 of the Model Nucleobase 1,3-Dimethyluracil (1,3-DimeU): Preparation and X-Ray Crystal Structures of Trans-K[Au(CN)<sub>2</sub>Cl(1,3-DimeU)] and of Two Derivatives. *Journal of Organometallic Chemistry* 1998, 552 (1-2), 127–134.

<sup>19</sup> Schimanski, A.; Freisinger, E.; Erxleben, A.; Lippert, B. Interactions between [AuX<sub>4</sub>]<sup>-</sup> (X = Cl, CN) and Cytosine and Guanine Model Nucleobases: Salt Formation with (Hemi-) Protonated Bases, Coordination, and Oxidative Degradation of Guanine. *Inorganica Chimica Acta* 1998, 283 (1), 223–232.

### 1.4.3 Gold red-ox chemistry

The coordination chemistry of gold presents two basic oxidation states which are gold (I) and gold (III). Gold (III) red-ox chemistry can be difficult with biological ligands due to the red-ox properties that affect the stability and reactivity of gold compounds<sup>20</sup>. In fact, it is demonstrated that gold coordinated to guanine can carry out the degradation of guanine<sup>19</sup>. Moreover, it has been described in water solution the degradation of GMP coordinated to gold complexes<sup>21</sup>. A Frost diagram of different gold species is indicated in Figure 12<sup>22</sup>.



For these reason solvents as methanol can't be used normally in the synthesis of gold compounds.

<sup>20</sup> Đurović, M. D.; Bugarčić, Ž. D.; van Eldik, R. Stability and Reactivity of Gold Compounds – From Fundamental Aspects to Applications. *Coordination Chemistry Reviews* 2017, 338, 186–206.

<sup>21</sup> Zhu, S.; Gorski, W.; Powell, D. R.; Walmsley, J. A. Synthesis, Structures, and Electrochemistry of Gold(III) Ethylenediamine Complexes and Interactions with Guanosine 5'-Monophosphate. *Inorganic Chemistry* 2006, 45 (6), 2688–2694.

<sup>22</sup> Sadler, P.J.; Sue, R.E., *Metal-based drugs*, 1994, 1, 107-144



## 1.5 Weak interactions

Weak interactions are responsible for maintaining three-dimensional structures and packings. Complexes that get to crystallize are directed by these forces, also solutions that tend to form gels are directed by this kind of interactions. Among the weak interactions can be found ionic interactions, hydrogen bonding, anion/cation- $\pi$ , stacking forces, hydrophobic interactions, Van der Waals forces and regium bond can also be found in noble metal complexes.

### 1.5.1 Hydrogen Bond

Hydrogen bond is an attractive electrostatic force between a donor atom and a receptor atom. Donor and acceptor atoms need to meet a series of properties. Donor atoms must have higher electronegativity than hydrogen and be covalently bound to it. Acceptor atom must have higher electronegativity and a lone pair of electrons. Mainly, atoms involved in hydrogen bonding are fluorine, oxygen, and nitrogen but also chlorine and carbon atoms can be involved. This interaction can be intermolecular between different molecules or intramolecular among different parts of the same molecule. The energy of a hydrogen bond depends on donor and acceptor nature, also depends on geometry and environment. Even so, it is less energetic than pure covalent or ionic bonding, but more than Van der Waals forces. In some cases, the total amount of hydrogen bonds can rule the geometries like tertiary structures in proteins or double strand DNA. Hydrogen bonding can be classified according to the strength<sup>23</sup> as strong, moderate, or weak and are summarised in Table 4:

Table 4 Hydrogen bond classification, general characteristics, bond distances, angles, and energy.

	<b>Strong</b>	<b>Moderate</b>	<b>Weak</b>
<b>Interaction nature</b>	Strongly Covalent	Mostly Electrostatic	Dispersion
<b>Bond length H...A (Å)</b>	1.2-1.5	1.5-2.2	>2.2
<b>Bond length D-A (Å)</b>	0.08-0.25	0.02-0.08	<0.02
<b>Bond angle D-H...A (°)</b>	170-180	>130	>90
<b>Directionality</b>	Strong	Moderate	Weak
<b>Bond energy (kcal/mol)</b>	15-40	4-15	<4

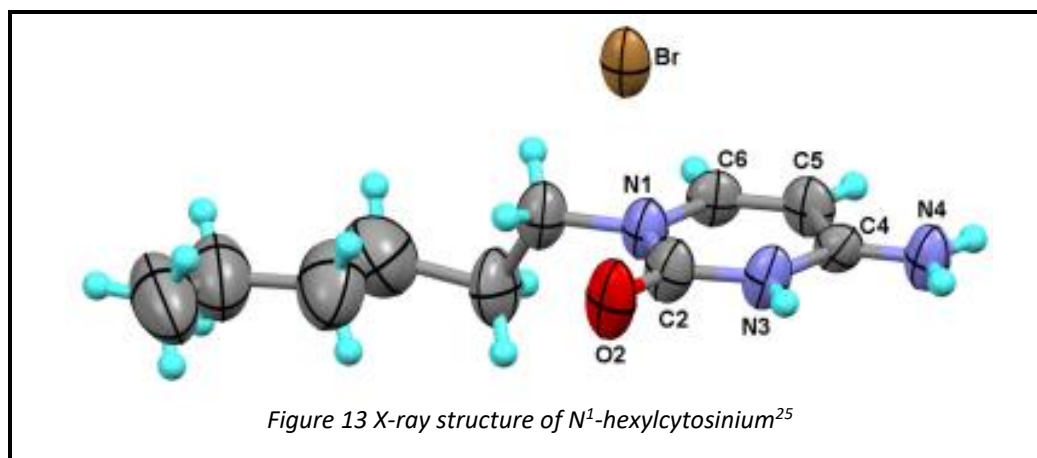
### 1.5.2 Anion- $\pi$ and Cation- $\pi$

Anion- $\pi$  interactions are non-covalent favourable contacts between electron deficient aromatic system and an anion. The interaction is dominated by electrostatic and anion-induced polarization contributions. Electrostatic component is correlated with the permanent quadrupole of the electron deficient aromatic ring<sup>24</sup>. In N<sup>1</sup>-hexylcytosine synthesis, N<sup>1</sup>-

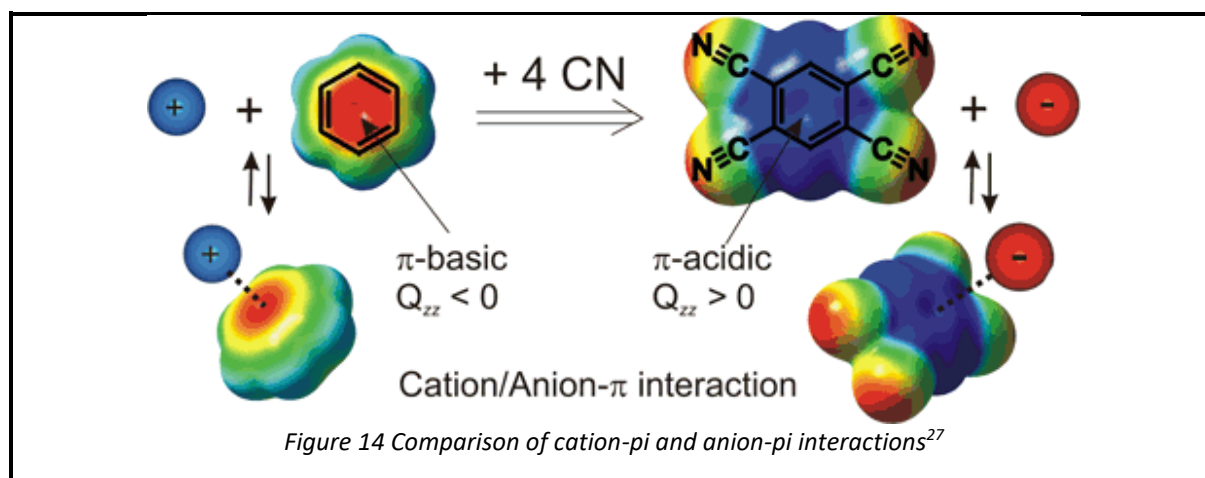
<sup>23</sup> Steiner, T. The Hydrogen Bond in the Solid State. *Angewandte Chemie International Edition* 2002, 41 (1), 48–76.

<sup>24</sup> Schottel, B. L.; Chifotides, H. T.; Dunbar, K. R. Anion- $\pi$  Interactions. *Chem. Soc. Rev.* 2008, 37 (1), 68–83.

hexylcytosinium bromide (Figure 13) was formed due to the bromide- $\pi$  interaction. Neutralization with  $\text{Na}_2\text{CO}_3$  in methanol is needed to form the neutral cytosine<sup>25</sup>.



Cation- $\pi$  interactions, in the other hand, is a non-covalent molecular interaction between an electron rich  $\pi$  system and a cation. This kind of interaction has an important role in protein structure and its bonding energies can be of the same order of magnitude as hydrogen bonding in some cases. Bond strength is influenced by cation's nature, solvation effects and  $\pi$  system's nature<sup>26</sup>. In Figure 14 a comparison of anion- $\pi$  and cation- $\pi$  interaction is shown<sup>27</sup>:



### 1.5.3 Stacking forces

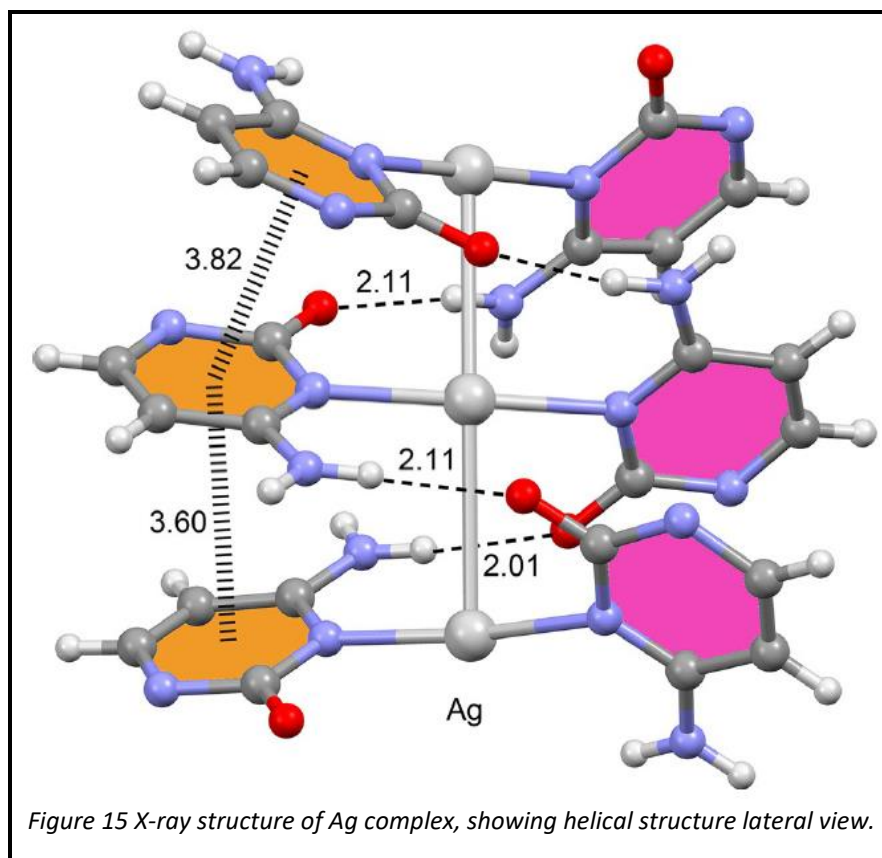
Also noun as  $\pi$ -stacking or  $\pi$ - $\pi$  interactions refers to a noncovalent interaction between aromatic rings, through the  $\pi$  cloud. These interactions are present between consecutive bases of the same DNA helix, protein folding, among others. Stacking interactions are present in metallated double-helix, generated by infinite and consecutive  $\text{C}^*-\text{Ag}-\text{C}^*$  ( $\text{C}^*$  means

<sup>25</sup> Fiol, J. J.; Barceló-Oliver, M.; Tasada, A.; Frontera, A.; Terrón, À.; García-Raso, Á. Structural Characterization, Recognition Patterns and Theoretical Calculations of Long-Chain N-Alkyl Substituted Purine and Pyrimidine Bases as Ligands: On the Importance of Anion- $\pi$  Interactions. *Coordination Chemistry Reviews* 2013, 257 (19-20), 2705–2715.

<sup>26</sup> Dougherty, D. A. The Cation- $\pi$  Interaction. *Accounts of Chemical Research* 2012, 46 (4), 885–893.

<sup>27</sup> Ballester, P. Anions and  $\pi$ -Aromatic Systems. Do They Interact Attractively? *Recognition of Anions, Structure and Bonding*, 2007, 129, 127–174.

N<sup>1</sup>-hexylcytosine)<sup>9</sup> (Figure 15). In this structure, there are other forces like argentophilic bonding or hydrogen bonding.



Stacking forces can be classified based on the geometry of the interaction (Figure 16):

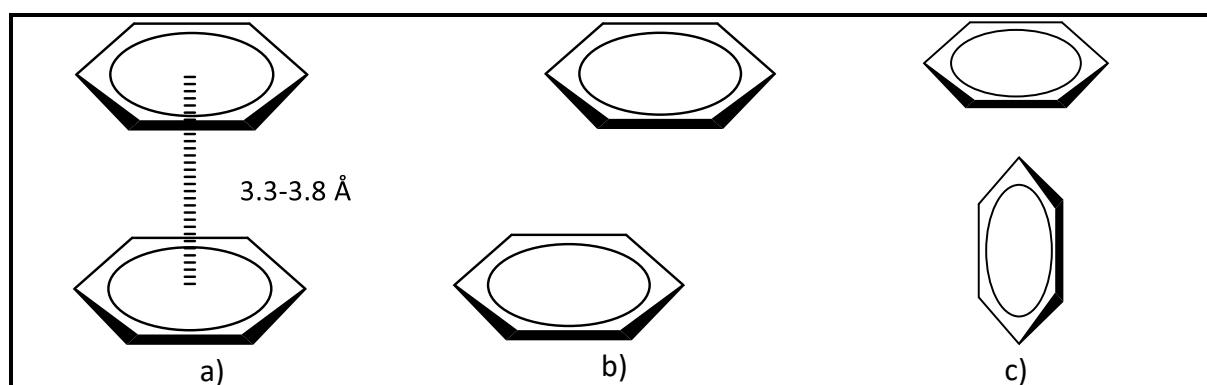


Figure 16 Geometry of possible stacking forces: a) face to face perfectly aligned b) parallel displaced c) point to face, T-shaped

#### 1.5.4 Hydrophobic interactions

Hydrophobic interaction is the tendency of nonpolar substances to exclude water molecules and aggregate. This interaction maximizes hydrogen bonding in water molecules and minimizes contact surface between nonpolar molecules and water. Thermodynamically speaking, hydrophobic interactions is the free energy change of water surrounding a solute. If

water surrounding solute implies a positive change of free energy it is because of hydrophobic effect, while negative change of free energy implies hydrophilic effect.<sup>28</sup>

This interaction is responsible for many proteins structure and folding, because of hydrophobic amino acids that aggregate together inside the folded protein while hydrophilic residues remain outside the protein to interact with water molecules<sup>29</sup> (Figure 17). In this paperwork this interaction is important due to the use of nonpolar ligands as N<sup>1</sup>-hexylcytosine, which has a C<sub>6</sub>H<sub>13</sub> alkyl residue, which is totally nonpolar, and will avoid water molecules contact. In fact, previously described gold-N<sup>1</sup>-hexylcytosine complex, the crystallographic structure shows hydrophobic interaction of alkyl residues<sup>10</sup>.

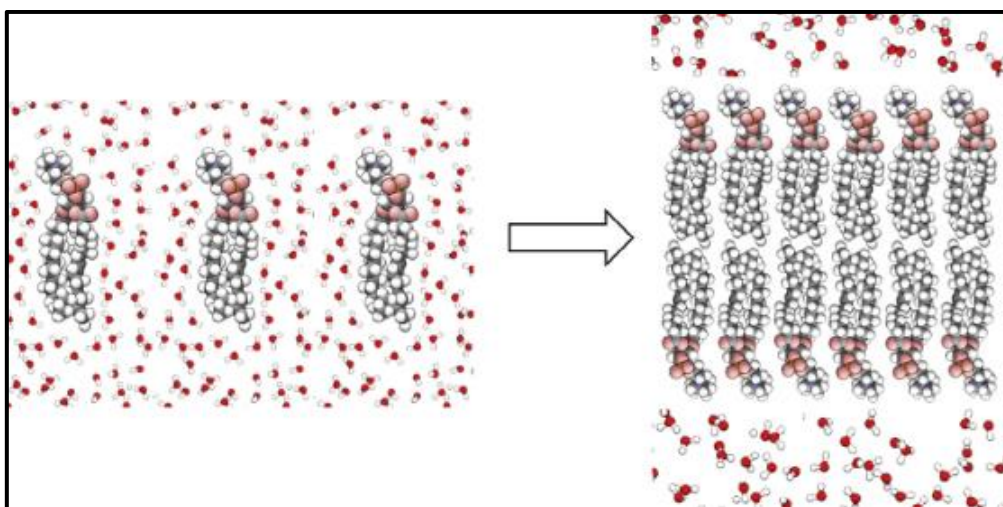


Figure 17 Molecular alignment of hydrophobic residues to decrease contact surface with water molecules<sup>30</sup>

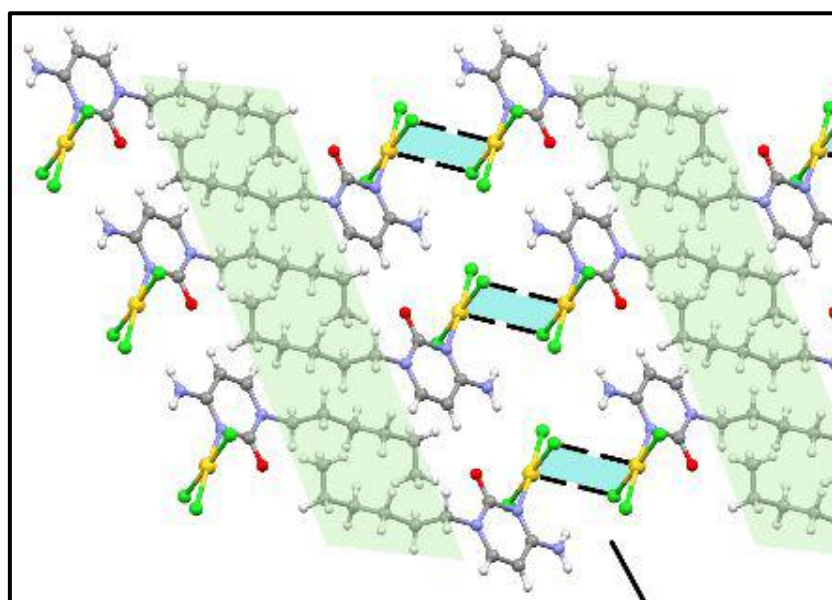


Figure 18 Hydrophobic interactions in solid state in Trichlorido(N<sup>1</sup>-Hexylcytosine) Gold (III) 10

<sup>28</sup> Bogunia, M.; Makowski, M. Influence of Ionic Strength on Hydrophobic Interactions in Water: Dependence on Solute Size and Shape. *The Journal of Physical Chemistry B* 2020, 124 (46), 10326–10336.

<sup>29</sup> Lindman, B.; Medronho, B.; Alves, L.; Norgren, M.; Nordenskiöld, L. Hydrophobic Interactions Control the Self-Assembly of DNA and Cellulose. *Quarterly Reviews of Biophysics* 2021, 54.

<sup>30</sup> de Jesus, A. J.; Yin, H. Supramolecular Membrane Chemistry. *Comprehensive Supramolecular Chemistry II* 2017, 311–328.

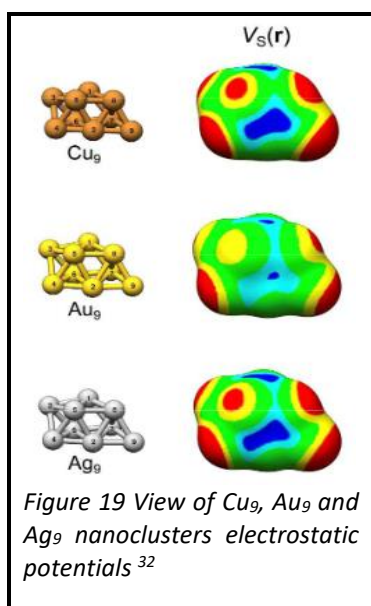
### 1.5.5 Van der Waals

Van der Waals force is a distance-dependent interaction between molecules. This attractive interaction does not result from a chemical bond and compared to ionic or covalent bonds it is weak interaction and therefore more susceptible to disturbance. Van der Waals force plays a fundamental role in supramolecular chemistry, structural biology, polymer science, nanotechnology, among others. This interaction is usually described as a combination of London dispersion forces between instantaneously induced dipoles, Debye forces between permanent dipoles and induced dipoles.<sup>31</sup>

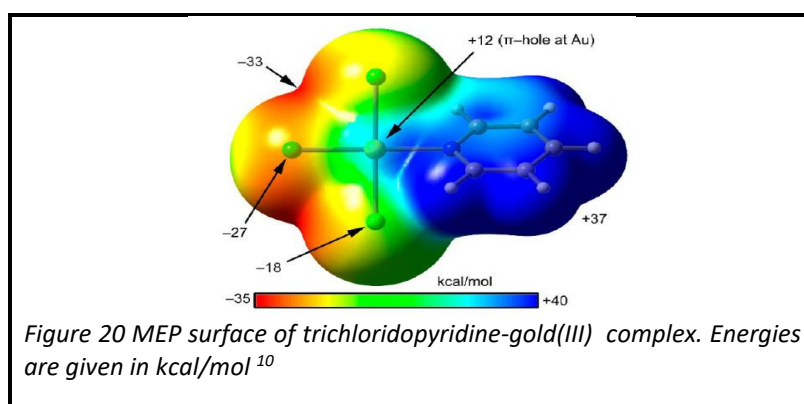
### 1.5.6 Regium bond

Transition metals nanoparticles and nanoclusters have emerged in the last decades as versatile materials for a wide range in catalysis, medical therapy, and solar energy harvesting<sup>32</sup>. Size and shape catalytic properties of gold nanoparticles have been explained using electrostatic potentials of nanoparticles. In other studies of MEPs,  $\sigma$ -holes were denoted as positive potentials by a density depletion at the end of a halogen due to the polarization of the  $\sigma$ -orbitals. This is also present in homonuclear diatomic as  $\text{Cl}_2$ .

Orbital polarization's influence on the surface electrostatic potential is easier to interpret in small molecules when only  $\sigma$ -orbitals contribute to bonding such as in  $\text{H}_2$ . This results in positive potentials at the ends and negative potentials at the centre of diatomic molecules. This is denoted as  $\sigma$ -holes and  $\sigma$ -lumps.  $\text{Li}_2$  has a similar tendency, but with stronger  $\sigma$ -holes, and more diffused  $\sigma$ -lumps. Noble metals as Ag, Au or Cu diatomic molecules also follow this tendency but with higher electrostatic potentials values.  $\text{Ag}_2$  potential surface demonstrates the preference to interact end-on with Lewis bases and side-on with Lewis acids. Clusters of group XI metals show the same behaviour, and corner and vertices show  $\sigma$ -holes (Figure 19).



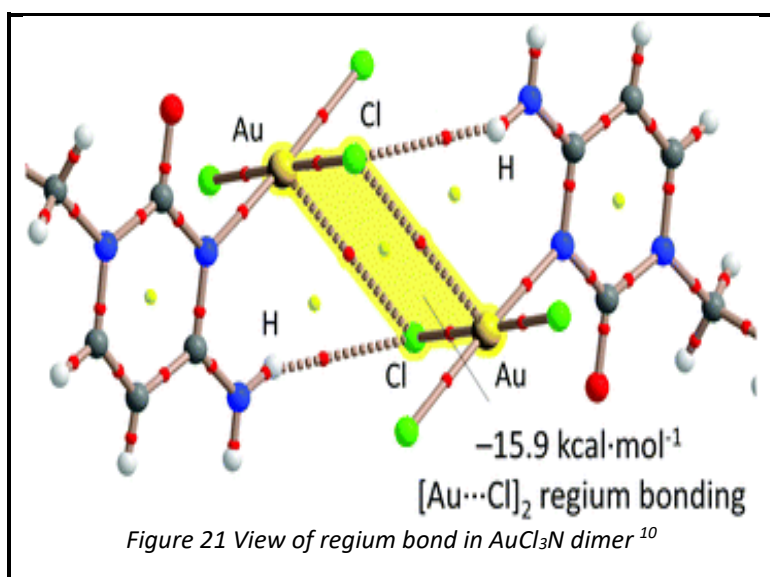
Similarly to  $\sigma$ -holes, it is denoted that a positive electrostatic potential located in the direction perpendicular to a  $\sigma$ -framework of the molecular entity as  $\pi$ -hole. One example of this  $\pi$ -hole was found after computational calculations in  $\text{AuCl}_3\text{N}(\text{Py})$  fragment (Figure 20):



<sup>31</sup> Van der Waals force. [https://en.wikipedia.org/wiki/Van\\_der\\_Waals\\_force](https://en.wikipedia.org/wiki/Van_der_Waals_force) (accessed Jul 17, 2021).

<sup>32</sup> Halldin Stenlid, J.; Johansson, A. J.; Brinck, T.  $\sigma$ -Holes and  $\sigma$ -Lumps Direct the Lewis Basic and Acidic Interactions of Noble Metal Nanoparticles: Introducing Regium Bonds. *Physical Chemistry Chemical Physics* 2018, 20 (4), 2676–2692.





This MEP (Figure 21) clearly shows the existence of a positive electrostatic potential both above and below Au atom.

Thus, regium bonds are controlled by  $\sigma$ -orbitals polarization, and takes place between charge acceptor (noble metals) showing high electrostatic potential like sigma-holes and pi-holes with electron donor with negative electrostatic potential like chlorines and nitrogen with free pair of electrons<sup>32</sup>.

It was thought that regium bonds were only present in noble metals in their oxidation state of 0, but in this paper, it was shown that oxidated forms of gold can also participate in this kind of interactions which are very important for the solid-state structure to be held.

Last, weak interactions apply for different natures and energies and are summarised in Table 5:

Table 5 Summary of different weak interactions approximate energies and nature

Interaction	Interaction's nature	Energy (kcal/mol)	Distance (Å)
Hydrogen bond	Electrostatic (dipole-dipole)	4-40 <sup>23</sup>	1-3
Anion- $\pi$	Electrostatic (charge-quadrupole)	15-40 <sup>33</sup>	2-5 <sup>34</sup>
Cation- $\pi$	Electrostatic (charge-quadrupole) and covalent	18-230 <sup>33</sup>	2-5 <sup>34</sup>
$\pi$ - $\pi$ stacking forces	Quadrupole-quadrupole and dispersion	1-15 <sup>33</sup>	2-5.5 <sup>34</sup>
Hydrophobic interactions	Dispersion and polarization	1-2 <sup>35</sup>	3.8-9.5 <sup>35</sup>
Van der Waals forces	Dispersion and polarization (London forces)	1-2 <sup>35</sup>	3-6 <sup>35</sup>
Regium bond	Electrostatic	10-30 <sup>10,32</sup>	2-4 <sup>10,32</sup>

<sup>33</sup> Quiñonero, D.; Garau, C.; Frontera, A.; Ballester, P.; Costa, A.; Deyà, P. M. Structure and Binding Energy of Anion- $\pi$  and Cation- $\pi$  Complexes: A Comparison of MP2, RI-MP2, DFT, and DF-DFT Methods. *The Journal of Physical Chemistry A* 2005, 109 (20), 4632-4637.

<sup>34</sup> Lucas, X.; Bauzá, A.; Frontera, A.; Quiñonero, D. A Thorough Anion- $\pi$  Interaction Study in Biomolecules: On the Importance of Cooperativity Effects. *Chemical Science* 2016, 7 (2), 1038-1050.

<sup>35</sup> Lodish, H.; Berk, A.; Zipursky, S.L.; Matsudaira, P.; Baltimore, D.; Darnell, J., *Molecular Cell Biology* (4<sup>th</sup> ed.), Freeman & Co., New York 2000, ISBN 0-7167-3136

## 2 Objectives

General objective of this work is aimed to study the interaction modes presents in metal-nucleobase complexes.

- a) Gold was chosen to synthesize new coordination complexes with nucleobases or their derivatives, biological or synthetic.
- b) Cytosine-based ligands (Cyd, dCyd, CMP, MeCyt and CytC<sub>6</sub>)<sup>36</sup> were the first step of our study. The second part is to test the interaction of gold with Uracil-based ligands (UraC<sub>6</sub>, Ura<sub>2</sub>C<sub>3</sub> and (F-Ura)<sub>2</sub>C<sub>3</sub>). Last, Cytidine-Guanosine base pair interactions with gold were tested. Thus, a major part of the work was centered in pyrimidine bases.
- c) Spectroscopic and structural characterization of new coordination compounds was carried out since very few data is published about this kind of complexes.

---

<sup>36</sup> Abbreviations are summarised in Annex I: Abbreviations

## 3 Methods and Materials

### 3.1 Materials and Techniques

Some of the reagents were obtained from commercial products from Sigma-Aldrich (Cyd, dCyd, MeCyt and CMP)<sup>36</sup> and VWR CHEMICALS (NaAuCl<sub>4</sub> and HAuCl<sub>4</sub>) without further purification. Other ligands were synthesized as described procedures that will be indicated in its proper complex.

Elemental analysis was carried out by "Servei de Microanàlisi del CSIC Barcelona". Carbon, hydrogen, and nitrogen were determined using Carlo-Erba (1106-1108) and Microanalyzer Thermo Finnigan Flash 1112.

IR spectra was obtained in a Bruker Tensor 27 between 4000-400 cm<sup>-1</sup> in KBr tablets.

<sup>1</sup>H-RMN were obtained in a Bruker AMX 300 (300MHz). d<sup>6</sup>-DMSO (referred to residual DMSO; <sup>1</sup>H NMR  $\delta$ =2.50 ppm) was used as solvent for obtaining RMN data.

ESI-HRMS data was determined in a Orbitrap mass spectrometer (ThermoFischer Scientific) using a heated-electrospray ionization probe (HESI) and registered in positive or negative mode. Capillary transference temperature of ions was fixed at 320°C, spray voltage was fixed at 2,9kV for negative mode and 3,9 kV for the positive mode. Direct injection in Full Scan as acquisition mode in a range comprised in between 190 and 1000 m/z and was carried out with a resolution of 140000.

Single crystals of two compounds were selected, covered with Parabar 10320 (formally known as Paratone N) and mounted on a Cryoloop on a D8 Venture diffractometer, with a Photon III 14 detector, using an Incoatec high brilliance  $\mu$ S DIAMOND Cu equipped with an Incoatec Helios MX multilayer optics. The crystals were kept at 100.0 K during data collection. Data reduction and cell refinements were performed using the Bruker APEX3 program.<sup>20</sup> Scaling and absorption corrections were carried out using the SADABS program in all cases.<sup>20</sup> Using Olex2,<sup>21</sup> the structure was solved with the XT structure solution program<sup>18</sup> using Intrinsic Phasing and refined with the XL refinement package<sup>22</sup> using Least Squares minimization. All non-hydrogen atoms were refined with anisotropic thermal parameters by full-matrix least-squares calculations on F<sup>2</sup>. Hydrogen atoms were generally inserted at calculated positions and refined as riders, except those of water molecules and protonation sites, which were located using a Fourier difference map and refined isotropically. The structures were checked for higher symmetry with help of the program PLATON.<sup>23</sup> The graphical material have been prepared with the help of Mercury software.<sup>24</sup>

Theoretical calculations were carried out on LanL2DZ basis set and B3LYP DFT functional. Calculations and MEP surfaces have been carried out with Gaussian-09W and GaussView.



## 3.2 Synthesis

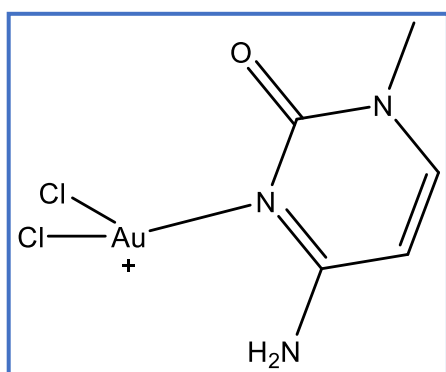
**Synthesis of Complex I: AuCl<sub>3</sub>(MeCyt):** Compound was obtained in a reaction made in different steps. The first step was the activation of the gold salt (NaAuCl<sub>4</sub>) with AgNO<sub>3</sub> the resulting of this is the nitrate form of the gold salt. This form is more suitable for the reaction with a nucleobase. Once we have the nitrate form, the final product is obtained by mixing with stirring for 24 h an equimolar amount of the nitrate gold salt with methyl cytosine in 30mL of water. The AuCl<sub>3</sub>MeCyt precipitated as a yellow powder which was then filtered and analysed.

**C:** exp 14.15% (calc 14,02)<sup>37</sup>      **H:**1.61% (1.65)      **N:**9.56% (9.81)

**IR (cm<sup>-1</sup>):** 3400 (s) 3323 (s) 3225 (s) 3095 (m) 3078 (m) 2949 (w) 1680 (s) 1640 (vs) 1511 (vs) 1425 (m) 1383 (s) 1337 (s) 1243 (m) 1199 (m) 1151 (m) 1118 (m) 1063 (w) 982 (m) 783 (m) 760 (m)

**RMN [DMSO-d<sub>6</sub>]**

**δ (ppm):** 9.39 (bs, 1H, NH); 9.07 (bs, 1H, NH); 7.82 (d, 1H, J= 7.5 Hz, C<sub>6</sub>-H); 5.97 (d, 1H, J= 7.5 Hz, C<sub>5</sub>-H); 3.36 (s, 3H, C<sub>1</sub>-H)



**HRMS-ESI: Main peak can be identified as Figure 22**  
**Calculated for C<sub>5</sub>H<sub>7</sub>AuCl<sub>2</sub>N<sub>3</sub>O** 391.96262 daltons  
**Experimental** 391.96251 daltons  
**δ = -0.27 ppm**

Figure 22 Structure calculated for main peak at ESI-HRMS

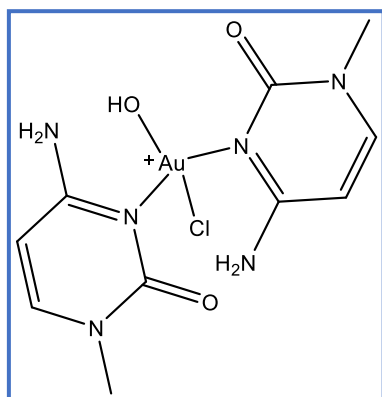
**Synthesis of Complex II: AuCl(NO<sub>3</sub>)<sub>2</sub>(MeCyt)<sub>2</sub>:** Compound was obtained by mixing in a 1:2 molar proportion of gold (III) salt and the methyl cytosine. Previously the commercial gold reagent (NaAuCl<sub>4</sub>) was activated by elimination of two chlorides with AgNO<sub>3</sub>. The resulting gold product was then mixed in a water solution with methyl-cytosine. A precipitate was formed and removed from the solution. After the solution dried, we recovered the powder remaining.

**C:** 20.09% (19.80)    **H:** 2.54% (2.33)    **N:**19.53% (18.47)

**IR:** 3332(m) 3132 (m) 3074 (w) 1724(s) 1679 (s) 1640 (s) 1543 (m) 1385 (s) 1328 (s) 1186 (w) 1155 (w) 1045 (w) 991 (w) 822 (w) 792 (w) 759 (m) 614 (m)

**RMN [DMSO-d<sub>6</sub>] δ (ppm):** 9.25 (bs, 1H, H(4a)); 8.16 (bs, 1H, H(4b)); 7.926 (d, 1H, J= 7.5 Hz, C<sub>6</sub>-H); 5.96 (d, 1H, J= 7.5 Hz, C<sub>5</sub>-H); 3.31 (s, 3H, C<sub>1</sub>-H)

<sup>37</sup> Elemental analysis, in () calculated percentage



**HRMS-ESI: Main peak can be identified as:** Figure 23

**Calculated for**  $C_{10}H_{15}AuClN_6O_3$  :499.05542 daltons

**Experimental:** 499.05537 daltons

**$\delta$  = -0.09 ppm**

Figure 23 Structure calculated for main peak at ESI-HRMS

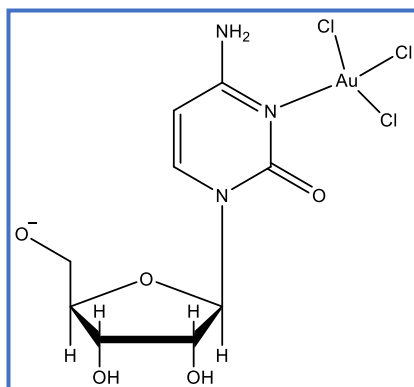
**Synthesis of Complex III  $AuCl_3Cyd$ :** The compound was obtained by mixing an aqueous solution of 0,5mmol of  $NaAuCl_4$  with a 0.5 mmol of cytidine in water solution. The mixing was stirred for one night after which some precipitate appeared corresponding to the final product. The elemental analysis coincided perfectly with what we were looking for:

**C:**19.24% (19.78)      **H:** 2.54% (2.40)      **N:**7.03% (7.69)

**IR ( $cm^{-1}$ ):** 3556 (s) 3506 (s) 3420 (s) 3385 (s) 3196 (m) 3177 (m) 3080 (m) 2945 (w) 2895 (m) 1653 (vs) 1512 (s) 1280 (m) 1102 (s) 1052 (m) 878 (w)

**RMN [DMSO- $d_6$ ]**

**$\delta$  (ppm):** 9.63 (bs, 1H, NH); 9.29 (bs, 1H, NH); 8.152 (d, 1H,  $J$ = 7.5 Hz,  $C_6$ -H); 6.077 (d, 1H,  $J$ = 7.5 Hz,  $C_5$ -H) 5.76 (d, 1H,  $J$ =3.9Hz,  $C_{1'}$ -H)



**HRMS-ESI: An anionic peak can be identified as:** Figure 24

**Calculated for the anion** 543.95135 daltons

**Experimental** 543.94528 daltons

**$\delta$  = -0.11 ppm**

Figure 24 Structure calculated for main peak at ESI-HRMS

**Synthesis of Complex IV:  $Na[AuCl_2Cyd_2(SbF_6)_2]$ :** The compound was obtained by mixing an aqueous solution of 0,5mmol of  $NaAuCl_4$  with a 0.5 mmol of cytidine in water solution. The mixing was stirred for one hour, and then another 0,5mmol of cytidine in water solution was added. After 1 day of stirring the mix, 0.5mmol of  $NaSbF_6$  in MeOH solution were added. It was stirred and heated under reflux for 3 hours after which some precipitate appeared corresponding to the final product. The elemental analysis coincided perfectly with what we were looking for:

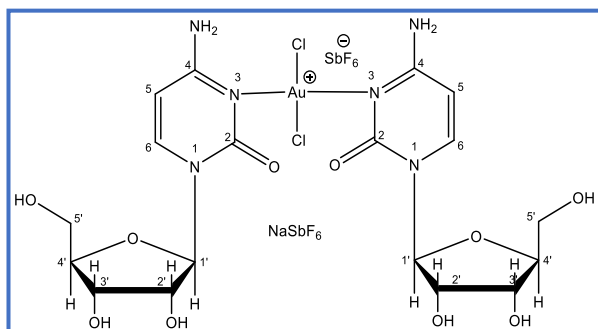


Figure 25 Structure proposed for this elemental analysis

**C:**17.48% (17.31) **H:** 2.14% (2.10) **N:**6.74% (6.73) (Figure 25)

**IR (cm<sup>-1</sup>):** 3383 (s) 2925 (m) 1723 (m) 1675(s) 1644 (s) 1541 (m) 1449 (w) 1275 (m) 1079 (m) 759 (w) 628 (m)

**RMN [DMSO-d<sub>6</sub>]**

**δ (ppm):** Complex low solubility in conventional solvents did not allow the proper resolution in NMR to elucidate the spectrum.

**Synthesis of Complex V: AuCl<sub>3</sub>(dCyd):** Compound was obtained by reaction of NaAuCl<sub>4</sub> with 2'-deoxycytidine. A water solution of the gold salt was mixed with a water solution of dCyd in equimolar proportion. The mixture was stirred overnight. A powdered precipitate appeared and was collected and dried. The final product was analysed, and elemental analysis confirm the product.

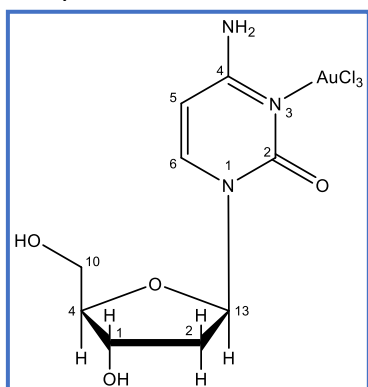


Figure 26 Structure proposed for this elemental analysis

**C:** 20.76% (20.38) **H:** 2.56% (2.47) **N:**7.92% (7.92) (Figure 26)

**IR:** 3346 (m)br 2926 (m) 1642 (s) 1515 (m) 1276 (m) 1088 (m) 1051 (m) 954 (w) 785 (w) 758 (w)

**Synthesis of Complex VIa: AuCl<sub>3</sub>(CytC<sub>6</sub>):** New synthesis path is described. Compound was originally described by QUIMIBIO<sup>38</sup> very recently, as a direct reaction of sodium tetrachloridoaurate. Compound was obtained in two different steps: first step was activation of gold initial reagent by reaction with silver nitrate. Second step was the reaction of gold activated compound with N<sup>1</sup>-hexylcytosinium bromide. Fine yellow needles appeared from solution, resulting in the described complex (Figure 27). Single crystal x-ray diffraction confirmed this product was the same described in bibliography (Table 6). Thus, further characterization is not needed. N<sup>1</sup>-hexylcytosine and N<sup>1</sup>-hexylcytosinium bromide were synthesized according to bibliography<sup>39</sup>.

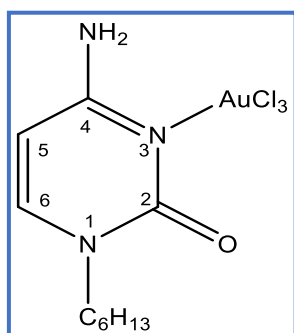


Figure 27 View of X-ray structure for AuCl<sub>3</sub>(CytC<sub>6</sub>)

<sup>38</sup> UIB Bioinorganic and Bioorganic Chemistry investigation group

<sup>39</sup> Barceló-Oliver, M.; Baquero, B. A.; Bauzá, A.; García-Raso, A.; Terrón, A.; Mata, I.; Molins, E.; Frontera, A. Experimental and Theoretical Study of Thymine and Cytosine Derivatives: the Crucial Role of Weak Noncovalent Interactions. CrystEngComm 2012, 14 (18), 5777.

Table 6 Unit cell parameters of  $\text{AuCl}_3(\text{CytC}_6)$

<b>Unit cell dimensions</b> <b>Space group:</b> <b>P21/c</b>	<b>a (Å)</b>	7.004
	<b>b (Å)</b>	15.654
	<b>c (Å)</b>	16.326
	<b><math>\beta</math> (°)</b>	115.41
	<b>Volume (Å<sup>3</sup>)</b>	1617

**Synthesis of Complex VIb:  $\text{AuCl}_3(\text{CytC}_6)$ :** A polymorphic new complex was obtained by reaction of sodium tetrachloridoaurate with  $\text{N}^1$ -hexylcytosinium hexafluoroantimoniate. Ligand was obtained by reaction of  $\text{N}^1$ -hexylcytosinium bromide with silver hexafluoroantimoniate, filtration is needed to remove silver bromide formed in reaction. Fine yellow needle of gold complex appears in a minimal yield (Table 7). Further details on structural characterization and comparison in Results and discussion.

**Ligand's AE for :  $(\text{HCytC}_6)\text{SbF}_6$ : C:** 27.10 % (27.80) **H:** 4.13% (4.20) **N:**9.23 % (9.73)

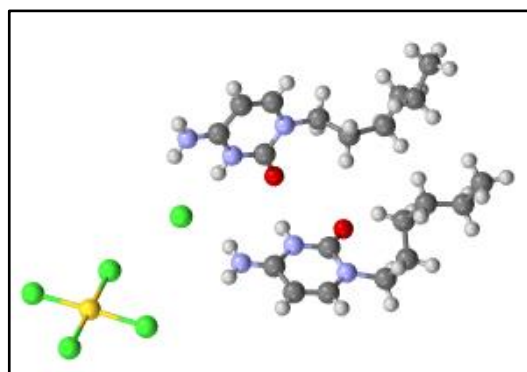
**$\text{C}_{10}\text{H}_{18}\text{F}_6\text{N}_3\text{OSb} (\text{HCytC}_6)\text{SbF}_6$  IR:** 3451 (s) 3339 (m) 3219 (m) 2957 (m) 2930 (m) 2860 (w) 1722 (s) 1651 (vs) 1607 (vs) 1534 (m) 1501 (m) 1397 (w) 1194 (w) 1083 (s) 787 (m) 662 (vs) 617 (m)

Spectroscopic data has not been obtained because the reaction's yield was too low, and only few suitable crystals for X-ray diffraction were obtained.

Table 7 Unit cell parameters of  $\text{AuCl}_3(\text{CytC}_6)$  polymorphism

<b>Unit cell dimensions</b> <b>Space group:</b> <b>P21/c</b>	<b>a (Å)</b>	16.147
	<b>b (Å)</b>	8.475
	<b>c (Å)</b>	11.769
	<b><math>\beta</math> (°)</b>	105.40
	<b>Volume (Å<sup>3</sup>)</b>	1553

**Synthesis of complex VII:  $(\text{HCytC}_6)_2 [\text{AuCl}_4] \text{Cl}$ :** Complex was obtained after direct reaction between sodium tetrachloridoaurate and  $\text{N}^1$ -hexylcytosinium bromide in equimolar proportion. Orange precipitate appears in a yellow solution. Precipitate is washed in HCl 2N at reflux for 2 hours. From this new solution suitable single crystals appear, which turn out to be 1:2 outer sphere complex, confirmed by SC-XRD (Table 8).



**C:** 31.48% (31.33) **H:** 4.57% (4.73) **N:**10.53% (10.96)  
 Elemental analysis calculated for asymmetric unit (Figure 28)

**IR:** 3433 (m) 3371 (m) 3212 (m) 2955 (m) 2920 (m) 2852 (m) 1922 (w) 1726 (s) 1682 (m) 1649 (s) 1490 (m) 1374 (m) 1200 (w) 788 (m) 616 (m) 502 (w)

Figure 28 X-ray structure for  $(\text{HCytC}_6)_2 [\text{AuCl}_4] \text{Cl}$

Table 8 Unit cell parameters for complex VII

<b>Unit cell dimensions</b> <b>Space group:</b> <b>P 1</b>	<b>a (Å)</b>	6.869
	<b>b (Å)</b>	10.718
	<b>c (Å)</b>	20.600
	<b>α (°)</b>	84.71
	<b>β (°)</b>	86.89
	<b>γ (°)</b>	72.36
	<b>Volume (Å<sup>3</sup>)</b>	1439

**Synthesis of complex VIII: [AuCl<sub>2</sub>(CytC<sub>6</sub>)<sub>2</sub>] Cl:** Compound obtention reaction was taken in two different steps. Firstly, AuCl<sub>3</sub>CytC<sub>6</sub> compound was obtained by direct reaction of sodium tetrachloridoaurate and N<sup>1</sup>-hexylcytosine in water. After 2 days of stirring, compound had completely precipitated, and it was dried in a rotary evaporator until all water was gone. In second place, more CytC<sub>6</sub> was added in MeOH solution giving place to a brown solution which was dried until all MeOH was evaporated. Afterwards, product was recrystallized in iPrOH, which dried and completely evaporated, leaving a brown precipitate which was analysed:

**C:** 35.51 % (34.62)                      **H:** 5.18 % (4.94)                      **N:** 12.09 % (12.11)

**IR:** 3380 (m) 3217 (m) 2956 (m) 2926 (m) 2856 (m) 1717 (m) 1643 (vs) 1537 (m) 1514 (m) 1459 (w) 1263 (m) 798 (m) 765 (m) 613 (w) 586 (w) 453 (m) 413 (s)

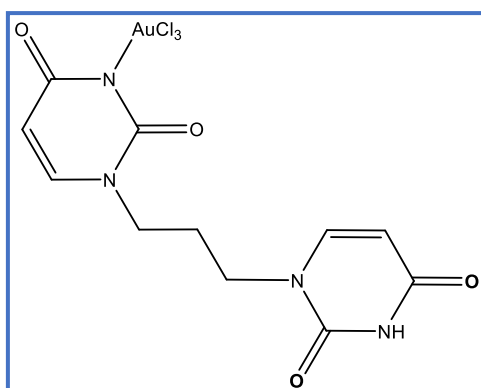
**Synthesis of complex IX: AuCl<sub>3</sub>CMP:** Complex was obtained by direct reaction of sodium tetrachloridoaurate with CMP in water, and pH adjusting to 4 to protonate phosphate group and obtain a neutral coordination complex. Solution is concentrated in a rotary evaporator until all water is evaporated. The formation of gels prevents elemental analysis to be carried out. For the same reason infrared data or nuclear magnetic resonance is not possible. After recrystallization in acetonitrile-dioxane suitable crystals for X-ray studies appear in the solution. Crystallographic studies reveal CMP degradation under presence of gold, as it was previously described with GMP<sup>21</sup>.

**Synthesis of Complex X: AuCl<sub>3</sub>(UraC<sub>6</sub>):** Ligand was synthesized as in bibliography<sup>40</sup>. Compound is obtained by direct reaction of sodium tetrachloridoaurate with N<sup>1</sup>-hexyluracil in water. Mixture is stirred for a whole day, after which it is left to concentrate in a crystallizer. To this day it has not precipitate so far.

**Synthesis of Complex XI: AuCl<sub>3</sub>(Ura<sub>2</sub>C<sub>3</sub>):** Complex is obtained by direct reaction of N<sup>1</sup>, N<sup>1</sup>-trimethylene-bis-uracil with sodium tetrachloridoaurate. Ligand was obtained as in

<sup>40</sup> Barceló-Oliver, M.; Estarellas, C.; García-Raso, A.; Terrón, A.; Frontera, A.; Quiñonero, D.; Molins, E.; Deyà, P. M. Lone Pair-π vs π-π Interactions in 5-Fluoro-1-Hexyluracil and 1-Hexyluracil: a Combined Crystallographic and Computational Study. *CrystEngComm* 2010, 12 (2), 362–365.

bibliography<sup>41</sup>. Ligand is completely insoluble in water, but by reaction with gold it was completely solubilized in a yellow transparent solution. After concentrating in the air it was analysed:



**C:** 23.46 % (23.32) **H:** 2.40 % (1.96) **N:** 9.60 % (9.89)  
(Figure 29)

**IR:** 3462 (s) 3047 (m) 3018 (m) 2839 (m) 1680 (vs) 1482 (m) 1424 (m) 1353 (m) 1244 (m) 1181 (m) 1041 (w) 872 (m) 821 (m) 758 (w) 726 (w) 564 (m) 430 (w)

Figure 29 Structure proposed for elemental analysis

**Synthesis of Complex XII: AuCl<sub>3</sub>(F-Ura<sub>2</sub>C<sub>3</sub>):** Compound was obtained by direct reaction of N<sup>1</sup>, N<sup>1</sup>-trimethylene-bis-(5-fluorouracil) with sodium tetrachloridoaurate. Milky yellow solution is formed after stirring. Solution is filtered and after concentration it was impossible to analyse due to low yield of the reaction.

**Synthesis of Complex XIII: AuCl<sub>2</sub>(Cyd-Gua):** Reaction is carried out from Au-Cyd complex. AuCl<sub>3</sub>Cyd complex in water solution is mixed with a guanosine aqueous solution. After one day stirring, brown precipitate is formed resulting in a degradation of ligand, already described<sup>21</sup>.

<sup>41</sup> Barceló-Oliver, M.; PhD Thesis: Interaccions entre ions metàl·lics i composts d'interès biològic (halouracils i derivats sintètics, hipurats i aciclovir). Interaccions metàl·liques que desenvolupen noves molècules anticanceroses; Universitat de les Illes Balears; 2009; <http://hdl.handle.net/11201/2558>

## 4 Results and discussion

### 4.1 Synthetic strategies

We have tested different strategies to obtain the purest compounds, the highest yield possible and suitable crystals for X-ray diffraction.

#### a) Cytosine-based complexes in 1:1 (Metal-Ligand) proportion

For the different cytosine-based ligands (Cyd, CMP, dCyd, MeCyt and CytC<sub>6</sub>) a direct reaction with NaAuCl<sub>4</sub> in equimolar proportion results in the 1:1 compound in most of the cases. The exception is the CMP and dCyd derivatives that tends to form a gel due to the stacking possibilities.

General speaking, more pure products are obtained activating the gold initial compound with silver nitrate and filtering to remove the silver chloride precipitate. The exception for this activation is the cytidine derivative that has a trend to crystalize in presence of nitrate as cytidinium nitrate, as it was confirmed several times by X-ray structural study

#### b) Cytosine-based complexes in 1:2 proportion

In general, the preparations between the tetrachloridoaurate anion and two mol of ligand have a trend to produce a mixture of products. In case of the CytC<sub>6</sub> gold complex 1:2 the recrystallization in acetonitrile of the raw precipitate does not work. We have isolated a cytosinium-cytosine base pair that we previously acknowledged in previous works.

The equilibrium between the different chemical species and its different solubility makes the problem more complex than expected. For this reason the best form to obtain the 1:2 derivative is a two-step reaction. In the first step we obtain the 1:1 complex, and in the second step of the reaction, the isolated 1:1 complex reacts with an equimolar amount of ligand. By this way we have obtained the 1:2 derivatives of methyl cytosine and cytidine with a reasonable purity; unfortunately the obtention of crystals for X-ray studies was not possible. For the dCyd derivative it has been impossible to obtain a solid product of the 1:2 complex due to the formation of gels.

The difficulty to tackle with 1:2 derivatives can be seen in Lippert's work with uracil where the chloride in trans with uracil is not substituted, instead, the complex precipitates using the adeninium cation as counter-ion<sup>18</sup> (Figure 10 and Figure 11).

#### c) Gold (III) capability to deprotonate the nucleobases, more precisely uracil derivatives

It was observed that N<sup>1</sup>-hexylcytosinium bromide can react with the sodium tetrachloridoaurate to give the deprotonated complex. More surprisingly the uracil derivatives, that are very insoluble in water, react with the gold compound to give complexes

in solution. It is necessary to consider that pKa of uracil in water is more than 9 to see the ability of gold to deprotonate nucleobases.

d) Guanosine-Cytidine base pair

It was tried to recreate a gold complex involving a cytidine-guanosine base pair<sup>16</sup>. Redox side reaction degraded the guanosine ligand as in other literature references<sup>21</sup>.

## 4.2 Spectroscopic characterization

### 4.2.1 MeCyt complexes

AuCl<sub>3</sub>MeCyt complex was obtained to have data for comparison, although this complex had been previously described and characterised by X-ray<sup>17</sup>. C=O stretching and C=N stretching ring bands were shifted to higher wavenumber owing to the coordination of gold with N<sup>3</sup> of cytosine. For the AuCl(NO<sub>3</sub>)<sub>2</sub>(MeCyt)<sub>2</sub> complex the shift is also increased due to the gold coordination. Gold coordination has the same effect as protonation, which increases the wavenumber in HCytC<sub>6</sub> (C=O → 1719 cm<sup>-1</sup>; C=N → 1670 cm<sup>-1</sup>). Nitrate tension band appears at 1385cm<sup>-1</sup><sup>42</sup> confirming the presence of a free NO<sub>3</sub> in 1:2 complex. The second nitrate seems to be coordinated due to nitrate band-splitting about 1440 cm<sup>-1</sup> (sh) and 1329 cm<sup>-1</sup> that are consistent with an unidentate nitrate. In Table 9 IR data is summarised:

Table 9 MeCyt and MeCyt complexes IR assignment and comparison

Compound	Nu C=O + C-C (cm <sup>-1</sup> )	v C-C + C=N, δ NH2 (cm <sup>-1</sup> )
MeCyt	1664	1621
AuCl <sub>3</sub> MeCyt	1678	1640
AuCl(NO <sub>3</sub> ) <sub>2</sub> (MeCyt) <sub>2</sub>	1722	1680 and 1640
[CHC]Br <sup>39</sup>	1722	1668

In fact, the system seems more like the bridge Cytosinium-Cytosine that was previously described with the ligand N<sup>1</sup>-hexylcytosine<sup>39</sup>. In this case the area of the ring bands gives 3 signals at 1722, 1688 and 1610sh. It was also described a proton-bound dimer of 1-methylcytosine, but IR data was not comparable to our data because it was carried out in gas phase and not in KBr tablet. In our case the MeCyt-Au-MeCyt systems gives the bands at frequencies 1722, 1680 and 1640 sh. The infrared data agree with a trans coordination of Cyt-Au-Cyt. Furthermore we have located a peak by HRMS corresponding to the 1:2 complex.

<sup>1</sup>H-NMR data agrees with the coordination of gold (III) with N<sup>3</sup> in the 1:1 complex, the signals are shifted to higher ppm that can be compared to protonation on same nitrogen. On the other hand, the signals of amino group are lower in 1:2 complex than in 1:1<sup>43</sup>. The semblance with the N<sup>1</sup>-hexylcytosine-N<sup>1</sup>-hexylcytosinium derivative, that was crystallized<sup>39</sup>, supports this

<sup>42</sup> Nakamoto, K., 1986. Infrared and Raman Spectra of Inorganic and Coordination Compounds. 4th Edition. Jhon Wiley & Sons, Inc., 5 Ed. ed. New York/ Chichester/ Weinheim/ Brisbane/ Singapore/ Toronto.

<sup>43</sup> Baquero-Romero, B. A.; Master Thesis: "Estudio del ligando N1-hexilcitosina y sus derivador metálicos. La importancia del reconocimiento anion-pi"; Universitat de les Illes Balears; 2012.



similarity. Specially the signals due to the NH<sub>2</sub> groups that are fixed by hydrogen bonds. One of the NH<sub>2</sub> protons appears in a lower field, compared to H(6) and the other in higher field. In the case of a simple protonation the two hydrogens from the amino group appear a higher ppm than the H(6) signal. Table 10 summarises <sup>1</sup>H-NMR data:

Table 10 MeCyt and MeCyt complexes <sup>1</sup>H-NMR assignment and comparison

Compound	H5	H6
Cyt <sup>44</sup>	5.52	7.26
AuCl <sub>3</sub> MeCyt	5.96	7.83
AuCl(NO <sub>3</sub> ) <sub>2</sub> (MeCyt) <sub>2</sub>	5.96	7.92
HCytC <sub>6</sub> Br <sup>39</sup>	5.96	7.97
[CHC]Br <sup>39</sup>	5.77	7.75
[CHC]NO <sub>3</sub> <sup>39</sup>	5.77	7.75

In conclusion, all spectroscopic evidence supports the coordination of gold (III) to N<sup>3</sup> of two cytosines in trans-conformation as indicated in Figure 30

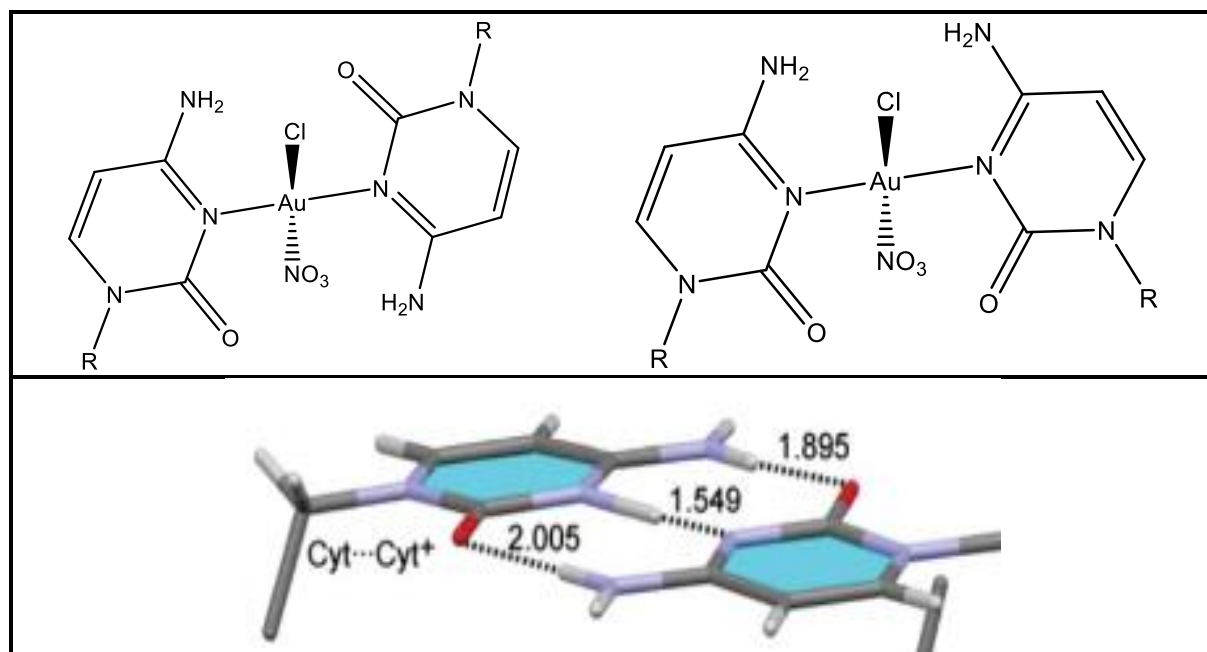


Figure 30 Structure of trans Cyt-Au-Cyt and X-ray structure of Cyt-H-Cyt<sup>39</sup>

It is impossible to discern between the forms that appear on Figure 30 without an X-ray study. In the hemi-protonated form of N<sup>1</sup>-hexylcytosine, a pair of hydrogen bonds is formed between carbonyl and amino group with distance of 2.005 and 1.889 Å, a third hydrogen bond is formed within N<sup>3</sup>-H-N<sup>3</sup> with a distance of 1.55 Å. Theoretical study was carried by me considering formation of dimers with cytosine rings that were coplanar and the Cl-Au-ONO<sub>2</sub> perpendicular to the cytosine rings.

The study was carried out to discern between these two conformations. For this study, a scan was performed, going from one conformation to the other, modifying the dihedral angle of

<sup>44</sup> Cytosine is used to compare data as MeCyt NMR was not carried out.

the two cytosine planes. Results obtained during this study are just estimations as no X-ray structure was obtained, thus the position of the atoms may not be correct. Even so, this study can give more clues of what structures we could obtain. The first conformation would have the two cytosines in an antiparallel position, that means that amino group and carbonyl group are opposite to each other. The second conformation would have the two cytosines in parallel position, having carbonyl and amino groups watching to opposite same group (Figure 31).

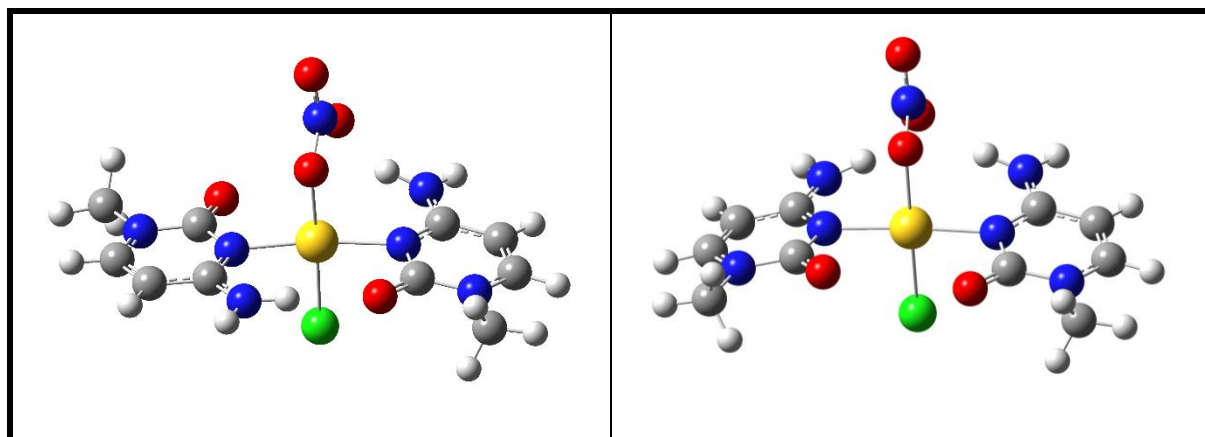


Figure 31 Antiparallel and parallel conformation of MeCyt-Au-MeCyt

Calculated conformations show a difference of energy of 4 kcal/mol. Moreover, the first conformation forms two hydrogen bonds, one involving carbonyl group with opposite amino group, and the second hydrogen bond is formed from the amino group and the oxygen of the nitrate. In the second conformation, two possible hydrogen bonds are formed involving the nitrate oxygen and the amino group of the two cytosines. A different study has been carried out, studying how the N-Au-N affects to the energy in both conformations, finding out the minimum energy is found at 2.06 Å. Conversely, the maximum energy difference between antiparallel and parallel conformations is found at 1.72 Å.

#### 4.2.2 Cyt complexes

Although AuCl<sub>3</sub>Cyd was previously described in my TFG, it was synthesized for three reasons: to optimize synthetic path, to crystalize the Au-Cyd complex, and to have it as reagent for the synthesis of 1:2 derivatives. For the 1:1 complex, high resolution mass spectrometry and <sup>1</sup>H-NMR agree for a coordination of gold at N<sup>3</sup> of cytosine. IR bands agree with a N3 coordination of gold in 1:1 complex and 1:2 complex even though 1:2 complex IR spectrum is not as clean as 1:1. The infrared spectrum of 1:2 derivatives of cytidine and methyl cytosine are similar, but the insolubility of cytidine derivative make impossible the obtention of more conclusions. Unfortunately, for the same reason, it was not possible to carry out an ESI-HRMS or a <sup>1</sup>H-NMR (Table 11 and Table 12).

Table 11 Cytidine and cytidine complexes IR assignation and comparison

Compound	Nu C=O + C-C (cm <sup>-1</sup> )	v C-C + C=N, δ NH2 (cm <sup>-1</sup> )
Cyd	1647 and 1661	1603
AuCl <sub>3</sub> Cyd	1671	1651
Na [AuCl <sub>2</sub> Cyd <sub>2</sub> (SbF <sub>6</sub> ) <sub>2</sub> ]	1723	1675 and 1644

Table 12 Cytidine and cytidine complexes NMR assignation and comparison

Compound	H5	H6
Cyd	6.04	7.83
AuCl <sub>3</sub> Cyd	6.07	8.15

Cytidine complexes crystallization is quite hard due to the tend to form gels phases before crystalizing, and the crystallization of cytidinium nitrate adds difficulty because 1:2 complexes lose ligand in this crystallization. Thus, it has been impossible to crystalize a gold-cytidine complex

#### 4.2.3 N<sup>1</sup>-hexylcytosine complexes

In the case of CytC<sub>6</sub> complexes we have obtained three different compounds:

- AuCl<sub>3</sub>CytC<sub>6</sub>: which was obtained from the HCytC<sub>6</sub>Br reaction with NaAuCl<sub>4</sub>. Suitable crystals for X-ray diffraction appeared in the solution confirming that its unit cell is the same as the complex already described<sup>10</sup>.
- Starting from HCytC<sub>6</sub> SbF<sub>6</sub> we have obtained a compound with the same formula but with different unit cell. The packing is not the same and the comparison of the two structures will be done later in Structural characterization.
- Finally, adding HCl 2N to the precipitate obtained in the first preparation described, a new outer-sphere complex was obtained with suitable crystals for X-ray diffraction.

IR data of compounds obtained is coherent with the idea of coordination for the first two complexes and for a protonation in case of the outer-sphere complex. NMR gives the same kind of information about complexes obtained. But what gives most information and helps in other cytosine derivatives structural and spectroscopic characterization.

The study of IR bands of the three compounds agrees of gold with N<sup>3</sup> in cases "a" and the protonation in case c. The NMR data is consistent with this affirmation. The fact that in these three cases we have obtained X-ray structure means that we will concentrate the results discussion in structural characterization. Table 13 and Table 14 summarises IR and <sup>1</sup>H-NMR data:

Table 13 CytC<sub>6</sub> and derivatives IR assignation

Compound	Nu C=O + C-C (cm <sup>-1</sup> )	v C-C + C=N, δ NH <sub>2</sub> (cm <sup>-1</sup> )
CytC <sub>6</sub>	1665	1617
HCytC <sub>6</sub> Br	1719	1670
HCytC <sub>6</sub> SbF <sub>6</sub>	1722	1651 and 1604
[CHC] <sup>45</sup> Br <sup>39</sup>	1722	1668
[CHC] NO <sub>3</sub> <sup>39</sup>	1740	1692
AuCl <sub>3</sub> CytC <sub>6</sub>	1725	1681 and 1651
(HCytC <sub>6</sub> ) <sub>2</sub> [AuCl <sub>4</sub> ] Cl	1728	1681 and 1650

Table 14 CytC<sub>6</sub> and derivatives NMR assignation

Compound	H5	H6
CytC <sub>6</sub>	5.62	7.57
HCytC <sub>6</sub> Br	5.96	7.97
[CHC] NO <sub>3</sub>	5.77	7.75
AuCl <sub>3</sub> CytC <sub>6</sub> <sup>46</sup>	6.00	7.90

dCyd, CMP, UraC<sub>6</sub>, Ura<sub>2</sub>C<sub>3</sub> and (F-Ura)<sub>2</sub>C<sub>3</sub> complexes results have not been discussed because not enough data was obtained, or it was not clear enough.

### 4.3 Structural characterization

#### 4.3.1 AuCl<sub>3</sub>(CytC<sub>6</sub>)

A polymorph structure was obtained after direct reaction of tetrachloridoaurate with N<sup>1</sup>-hexylcytosinium hexfluoroantimoniate. This polymorph differs with the previously described complex, in the unit cell parameters and the layout of the asymmetric unit which is the same. This asymmetric unit consist of the complex AuCl<sub>3</sub>CytC<sub>6</sub> (Figure 32).

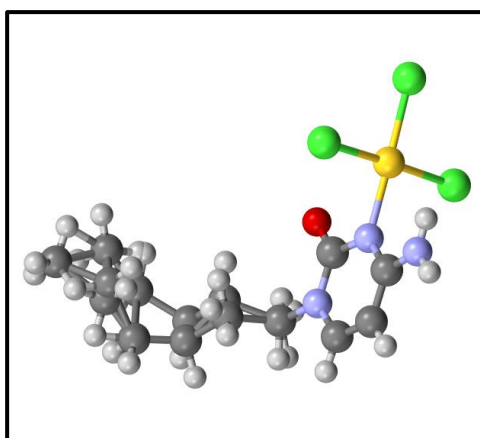


Figure 32 Asymmetric unit of complex VIb

<sup>45</sup> [CHC] means cytosinium-cytosine base pair, which is call hemi protonated form. It was Synthesized in A. Baquero TFM<sup>39</sup>

<sup>46</sup> <sup>1</sup>H-NMR was obtained in CDCl<sub>3</sub>

Dihedral angle of cytosine planes and tetrachloridoaurate anion plane is  $90^\circ$  which differs from the  $75^\circ$  of dihedral angle in complex VIa. Both amino hydrogens stay coplanar with cytosine ring and form an angle of  $120^\circ$  with N(4). Angles around N(4) are all three of  $120^\circ$ , being a plane triangular geometry. Crystal packing consist of 4 complex units interacting by hexyl residues (Figure 33):

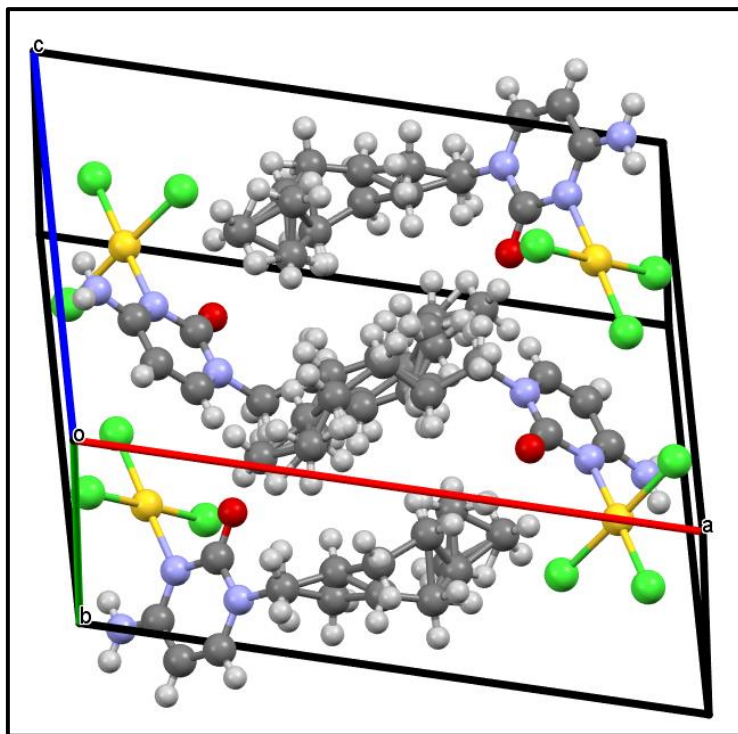


Figure 33 Complex VIb crystal packing

Energy calculations of asymmetric unit, and electrostatic potential map show a high electron density below  $\text{AuCl}_3\text{N}$  plane, next to the oxygen atom of cytosine. On the other hand, the side of the gold-chlorido-nitrogen plane next to the amino group show a positive region of the electron density (Figure 34).

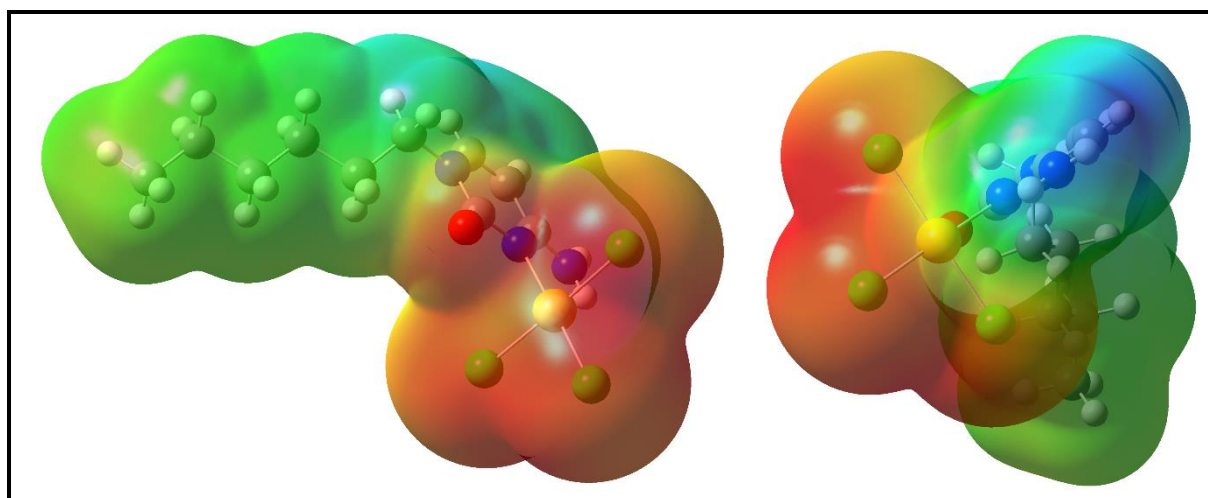


Figure 34 Asymmetric unit of complex VI MEP

Packing of complex VIb contains a  $\text{AuCl}_3\text{CytC}_6$  complex unit nearly perpendicular to a different complex unit. High electron density zones interact with C(6) of a near cytosine in an anion- $\pi$

like interaction, while low electron density zones interact with proximal chlorido. In this interaction, a hydrogen bond between H(4a) and Cl(1). Another hydrogen bond is formed involving H(4b) and a Cl(1) from a different complex unit (Figure 35 and Figure 36).

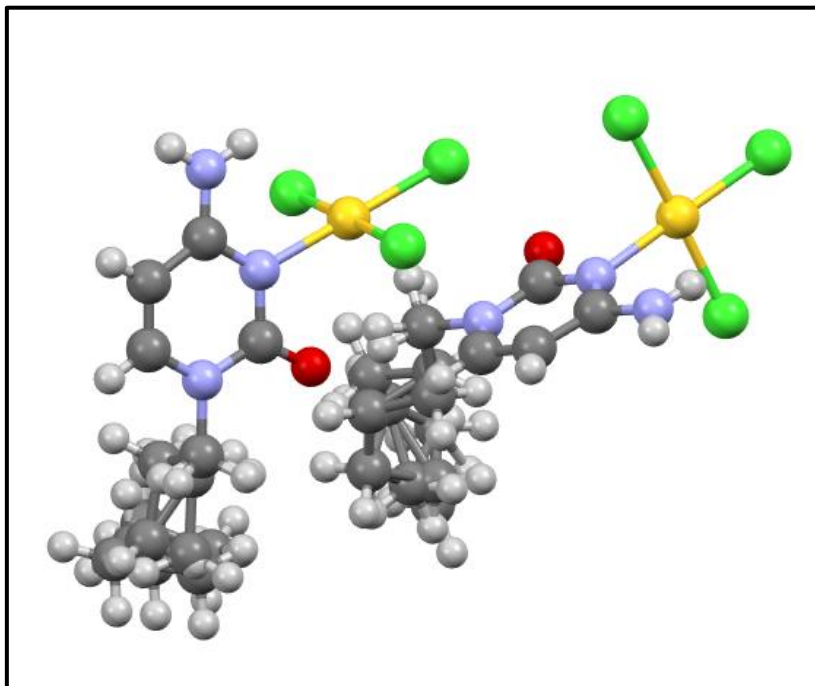


Figure 35 View of anion-pi interaction of two complex units

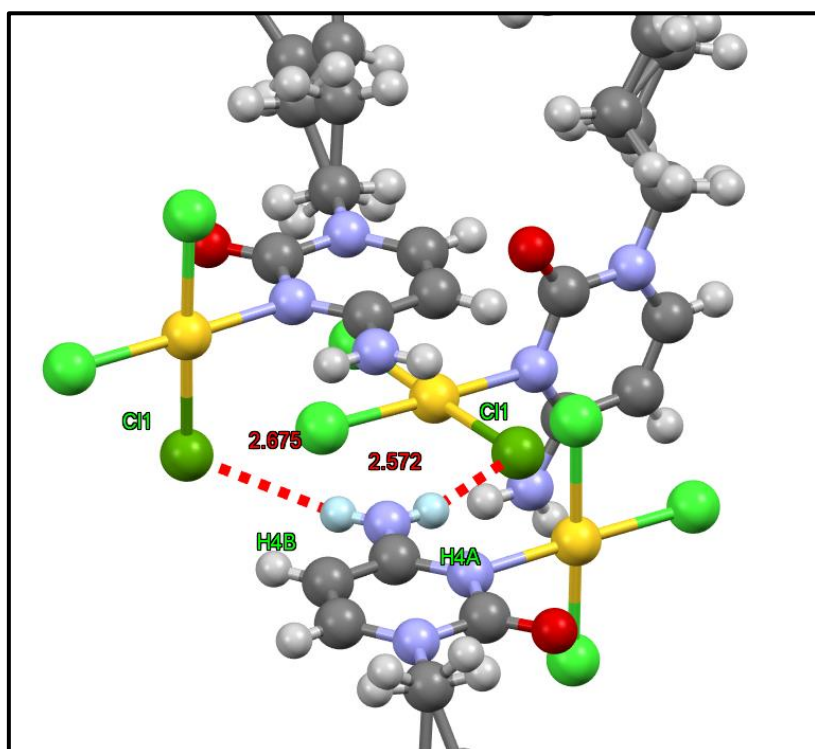


Figure 36 View of hydrogens bond formed from  $\text{NH}_2$  group

The interaction between positive zone and proximal chlorido could be a regium bond interaction between a  $\pi$ -hole on Au, and a  $\pi$ -lump on chlorido. This regium bond would be enhanced by two proximal hydrogens bonds (Figure 37):

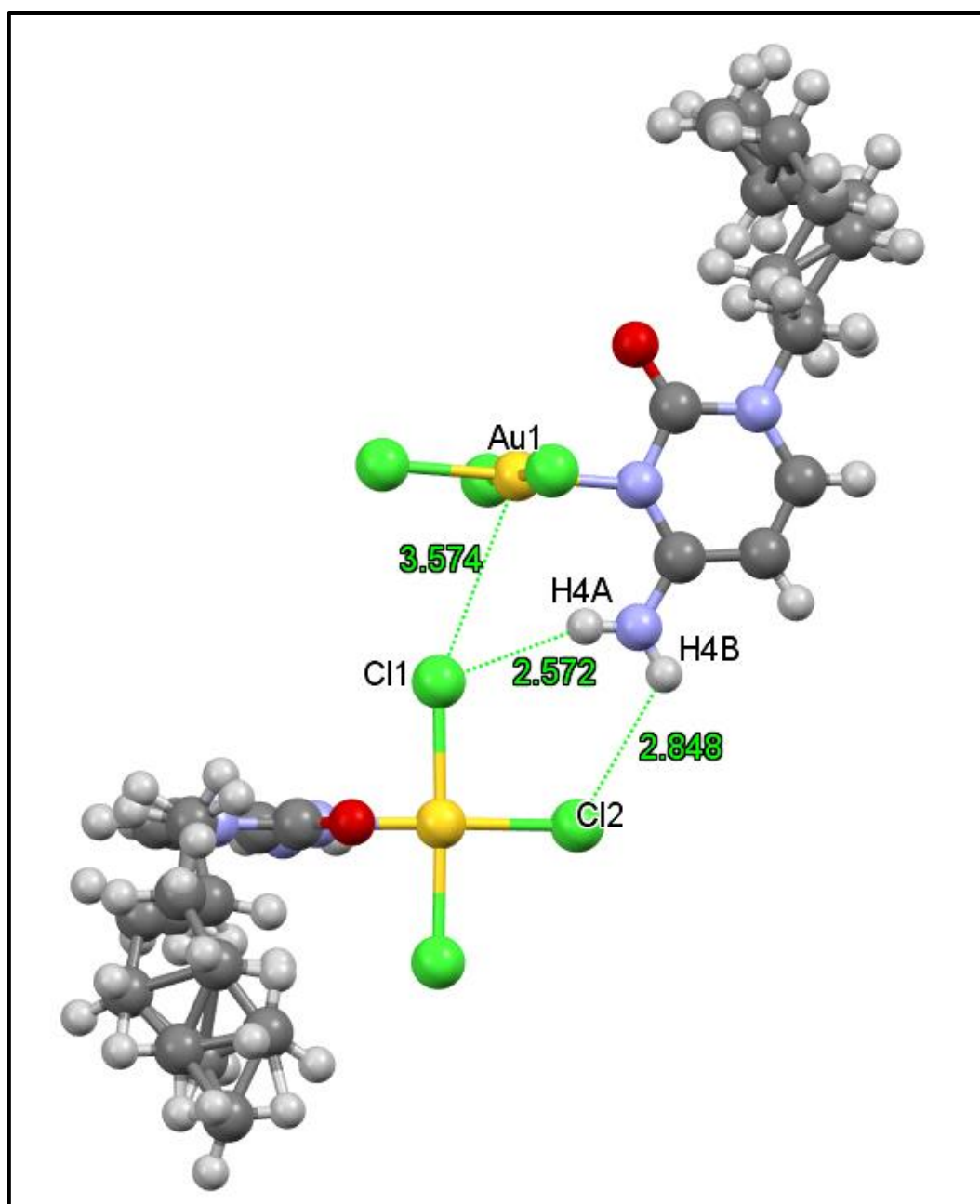


Figure 37 View of regium bond formation and supplementary hydrogen bonds

Regium bond resembles an interaction described within supplementary information provided in complex VIa publication<sup>10</sup>, where an alternative regium bond interaction of a cytosine without amino group was supposed (Figure 38):



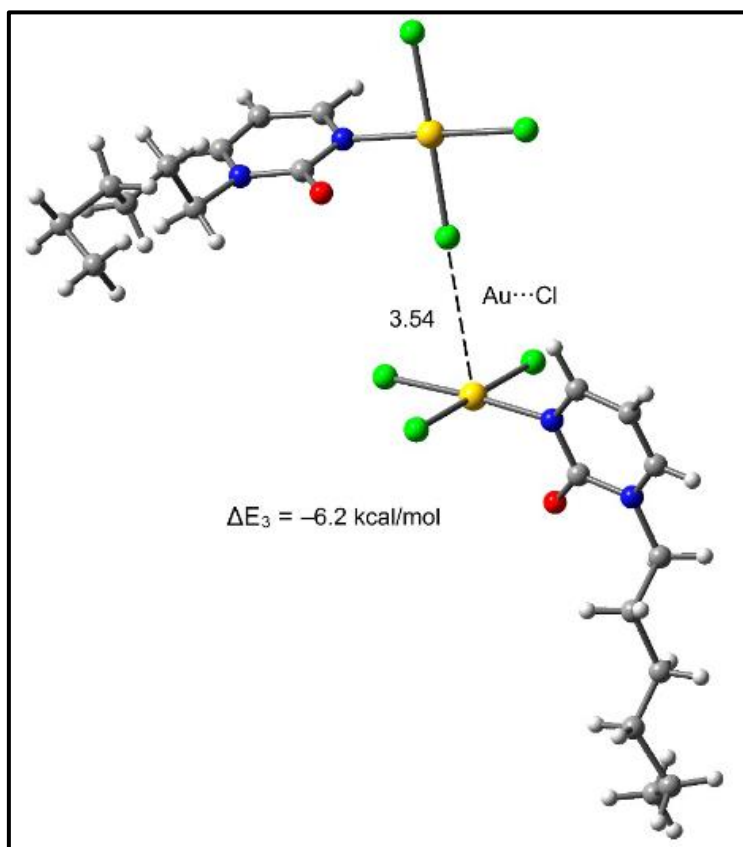


Figure 38 View of alternative regium bond interaction

Last, hydrophobic interactions in crystal packing can be seen in Figure 39:

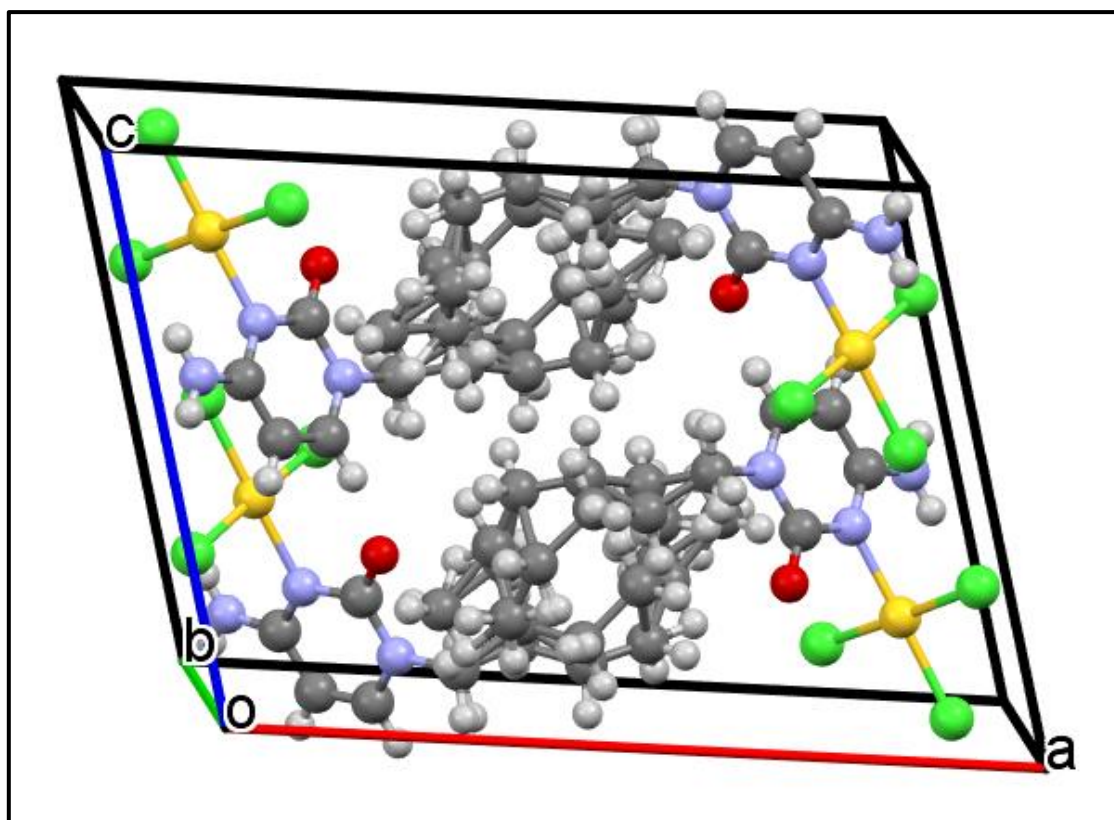


Figure 39 View of hydrophobic interactions in Complex VIb

Bond distances and bond angles of asymmetric unit are summarised in Table 15:



Table 15 Bond distances and angles of complex VIb

Atoms	Distance (Å)	Atoms	Angle (°)
Au-N(3)	2.036	Cl(1)-Au-Cl(2)	91.56
Au-Cl(1)	2.298	Cl(2)-Au-Cl(3)	90.16
Au-Cl(2)	2.245	Cl(3)-Au-N(3)	88.63
Au-Cl(3)	2.254	Cl(1)-Au-N(3)	89.65
N(3)-C(2)	1.394	C(2)-N(3)-Au	111.96
N(3)-C(4)	1.356	C(4)-N(3)-Au	124.23
Cl(1)-N(3)	3.061	N(3)-C(4)-N(4)	119.30
Cl(3)-N(3)	3.001	Cl(1)-Au-N(3)-C(2)	-90.07
Au-H(4a)	2.707		
Au-O(2)	2.911		

Hydrogen bonds and angles in complex VIb are summarised in Table 16:

Table 16 Hydrogen bond distances and angles

D-H...A	d (D-H) (Å)	d (H...A) (Å)	d (D...A) (Å)	< (DHA) (°)
N(4)-H(4a)...Cl(1)	0.880	2.572	3.407	158.86
N(4)-H(4b)...Cl(2)	0.880	2.848	3.374	119.96
N(4)-H(4b)...Cl(1)	0.880	2.675	3.468	150.62
C(6)-H(6)...O(2)	0.950	2.462	3.263	141.93

Complex VIa was already described but a summary will be done to enable a comparison to be made. Structure contained a pair of regium bond between 2 units of complex, and six different hydrogen bonds were formed. Dihedral angle of cytosine ring with tetrachloridoaurate was about 75° and a N-Au distance of 2.02 Å.

Complex VIb is a polymorph of complex VIa. Unit cell differs from complex VIa, interactions present in crystal packing are also slightly different (Table 17) (Figure 40 and Figure 41).

Table 17 Unit cell parameters comparison of two polymorphic complexes

Unit cell dimensions Space group: P21/c		Complex VIa	Complex VIb
	a (Å)	7.004	16.147
	b (Å)	15.654	8.475
	c (Å)	16.326	11.769
	β (°)	115.41	105.40
	Volume (Å <sup>3</sup> )	1617	1553

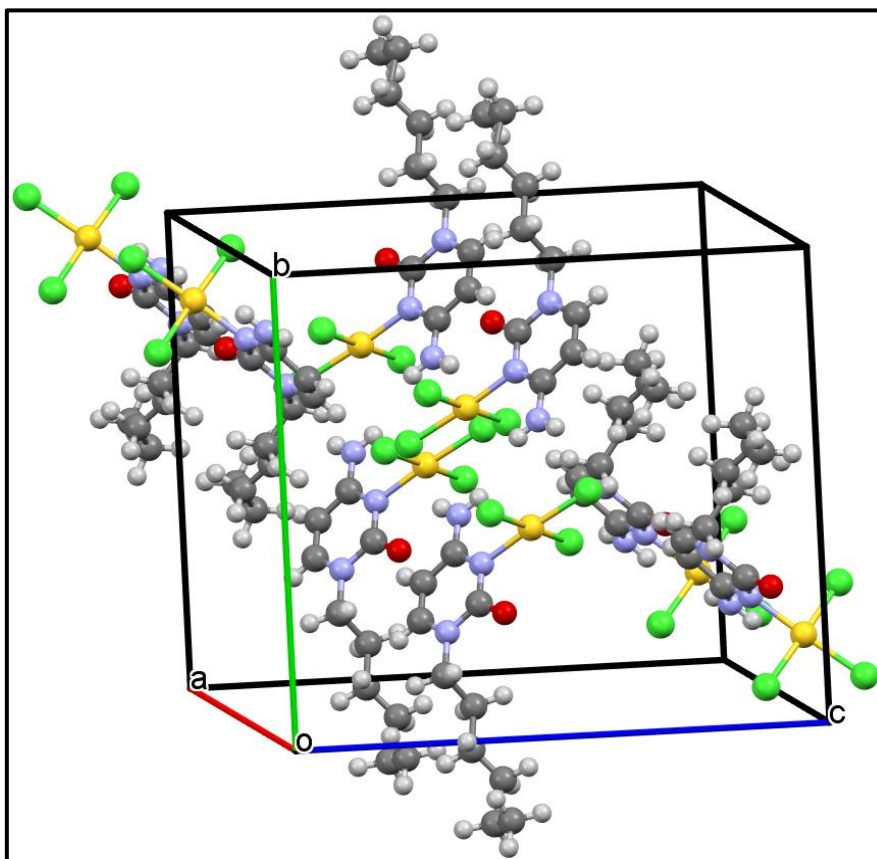


Figure 40 View of X-ray structure of unit cell of complex VIa

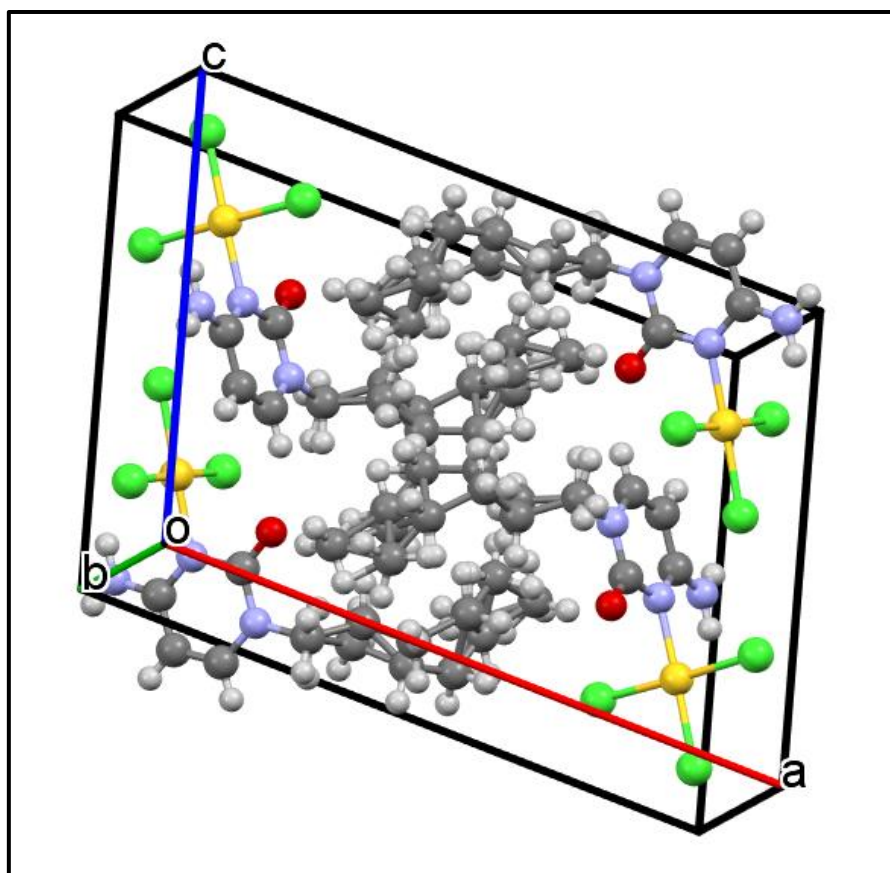


Figure 41 View of X-ray structure of unit cell of Complex VIb

Polymorphic complexes structures differ a little in parameters such as coordination distance, dihedral angles, and bond angles. A summary of these parameters is shown in Table 18:

Table 18 Bond distances, angles, and dihedrals comparison of two polymorphic complexes

Atoms	Complex VIa	Complex VIb
<b>Au-N(3)</b>	2.021 Å	2.036 Å
<b>Au-Cl(1)</b>	2.287 Å	2.298 Å
<b>Au-Cl(2)</b>	2.256 Å	2.245 Å
<b>Au-Cl(3)</b>	2.257 Å	2.254 Å
<b>Au-N(3)-C(2)</b>	112.38 °	111.96 °
<b>Au-N(3)-C(4)</b>	126.47 °	124.23 °
<b>Cl(2)-Au-N(3)</b>	176.07 °	178.72 °
<b>Cl(1)-Au-N(3)-C(2)</b>	72.59 °	89.65 °
<b>H(4a)-N(4)-C(4)-C(5)</b>	0.01 °	0.04 °
<b>H(4b)-N(4)-C(4)-C(5)</b>	3.13 °	0.01 °

#### 4.3.2 (HCytC<sub>6</sub>)<sub>2</sub> [AuCl<sub>4</sub>] Cl

Outer-sphere complex packing consist of two asymmetric units. Asymmetric unit is formed by two protonated cytosines forming an angle of 78°, a tetrachloridoaurate at an angle of 5° with one of the cytosine rings and 82° with the other, and a chloride anion in the intersection of the two cytosine planes (Figure 42).

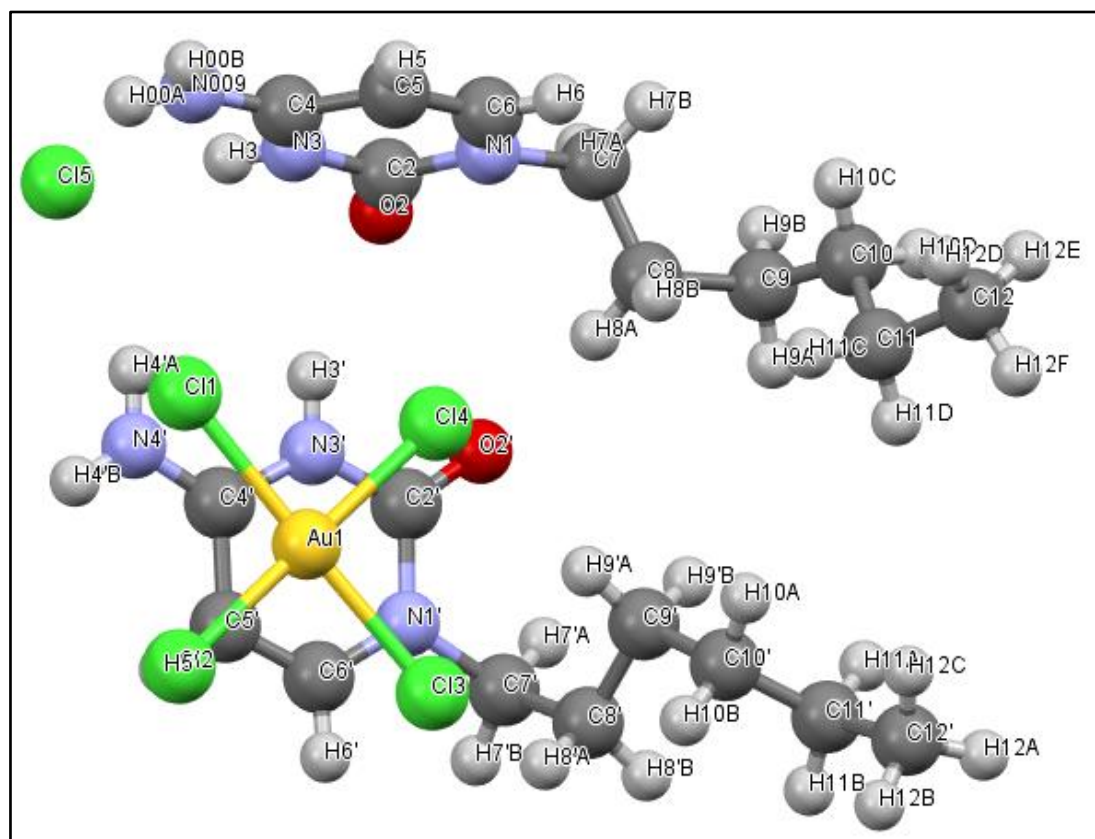


Figure 42 View of asymmetric unit of X-ray structure for complex VII

Bond distances and bond angles of asymmetric unit are included in Table 19:

Table 19 Bond angle and bond distance of complex VII

Atoms	Distance (Å)	Atoms	Angle (°)
<b>Au(1)-Cl (1)</b>	2.288	<b>Cl(1)-Au(1)-Cl(2)</b>	91.22
<b>Au(1)-Cl (2)</b>	2.274	<b>Cl(2)-Au(1)-Cl(3)</b>	89.77
<b>Au(1)-Cl (3)</b>	2.298	<b>Cl(3)-Au(1)-Cl(4)</b>	89.68
<b>Au(1)-Cl (4)</b>	2.273	<b>Cl(4)-Au(1)-Cl(1)</b>	89.32
<b>Au(1)-C (5')</b>	3.554	<b>C(6')-C(5')-Au(1)</b>	99.64
<b>Cl(4)-N(1)</b>	3.377	<b>Cyt<sub>centroid</sub>-C(5')-Au(1)</b>	91.41
<b>Cl(4)-C(2)</b>	3.394	<b>Cyt-Cyt<sup>47</sup></b>	78.41
<b>Cl(1)-N(4)</b>	3.543		

Complex units interact forming an infinite line along “a” axis, consisting of cytosine ring and tetrachloridoaurate anion, stacking on each other. The second cytosine ring remains perpendicular to the planes of first cytosine ring and of tetrachloridoaurate. The hexyl tails unite to decrease the surface exposed to water molecules (Figure 43).

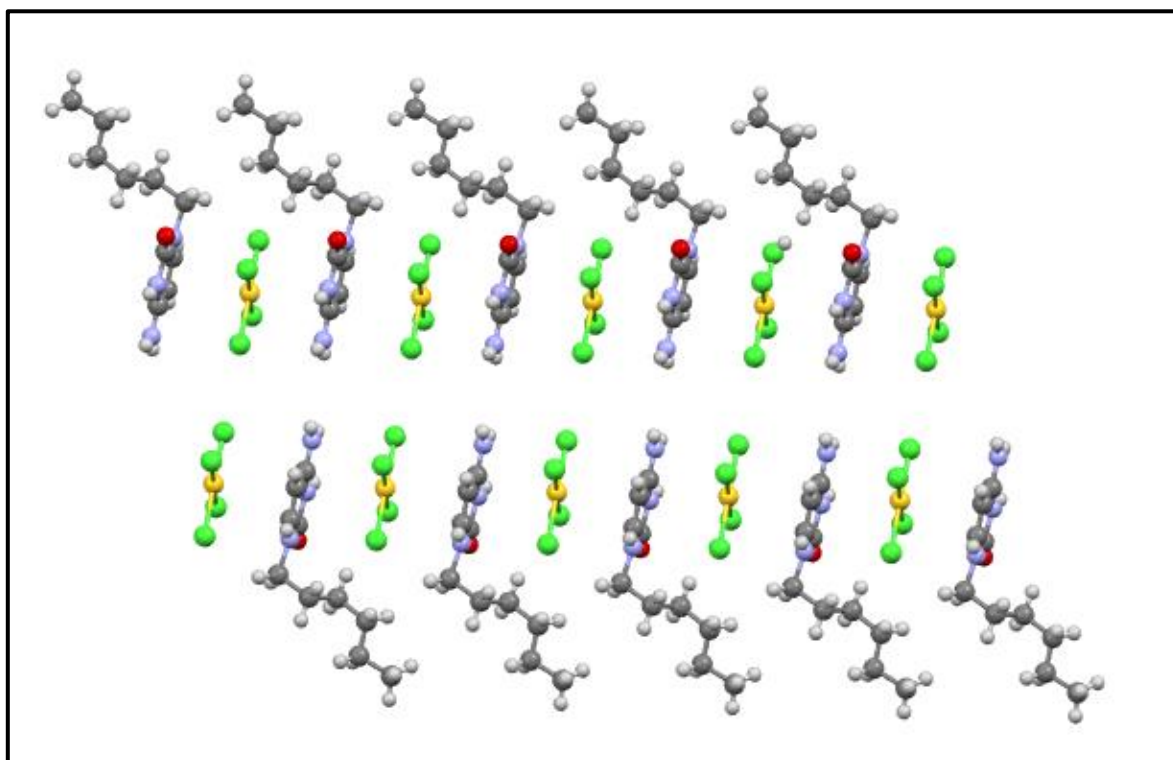


Figure 43 View of crystal growing along “a” axis, with regium bond interaction between cytosine rings and AuCl<sub>4</sub>

Possible hydrogen bonds can be found in this structure. C=O from cytosine ring acts as acceptor of two hydrogen bonds, where the donors are the N<sup>3</sup> from a perpendicular cytosine and C<sup>5</sup> from coplanar cytosine. More hydrogen bond can be found, free chloride from asymmetric unit forms up to 4 hydrogen bonds with 3 amino groups and with one N<sup>3</sup> from a different cytosine. Last, tetrachloridoaurate forms a hydrogen bond, with a chlorido as acceptor. The bond is formed with a C<sup>8</sup> hydrogen (Figure 44 and Table 20):

<sup>47</sup> Angle calculated as the angle of different cytosine planes in asymmetric unit

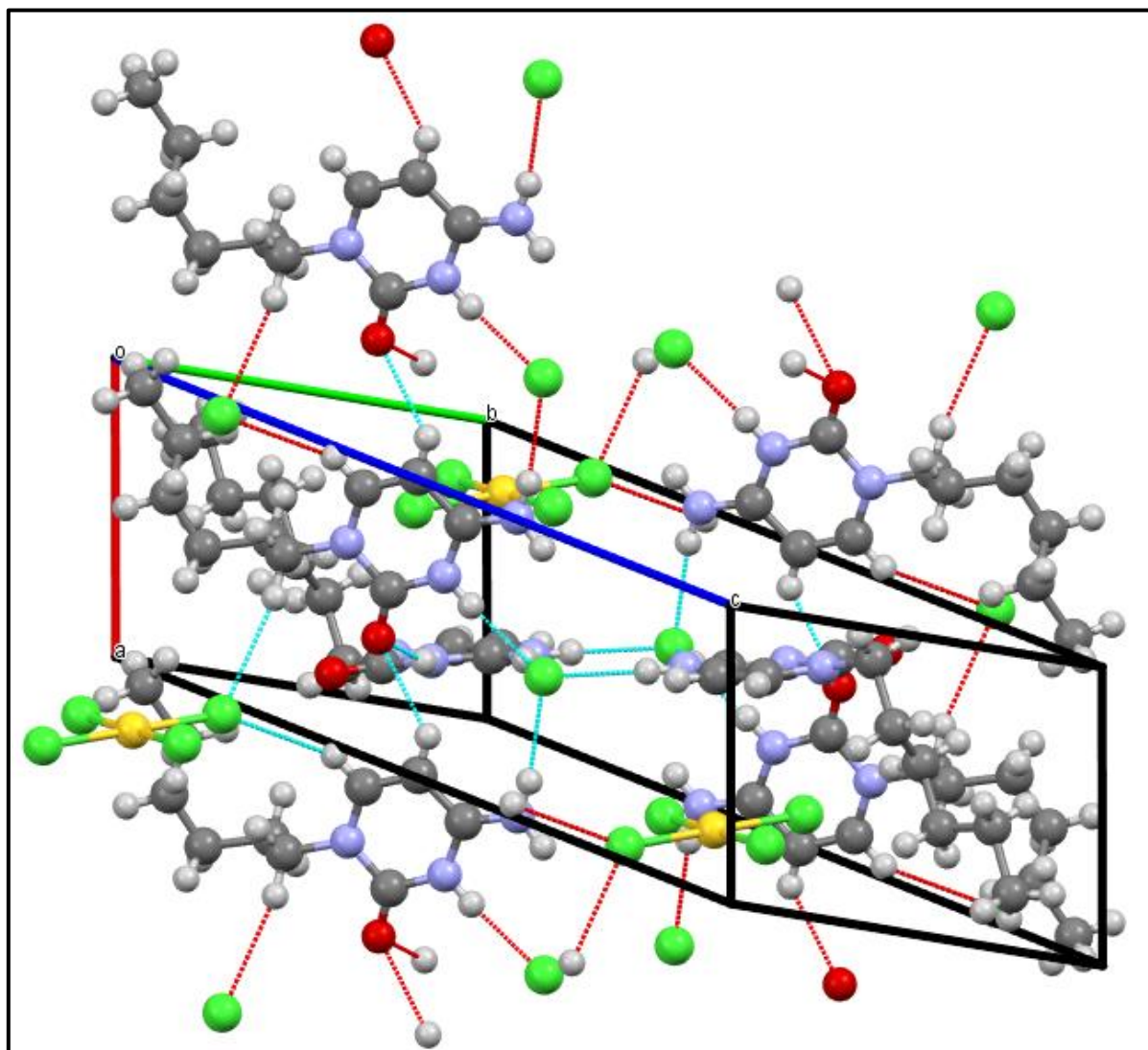


Figure 44 View of possible hydrogen bonds in crystal structure of complex VII

Table 20 Hydrogen bond distances and angles of complex VII

D-H...A	d (D-H) (Å)	d (H...A) (Å)	d (D...A) (Å)	< (DHA) (°)
N(3')-H(3')...O(2)	0.881	2.103	2.928	155.59
C(5)-H(5)...O(2)	0.950	2.429	3.171	134.84
N(4)-H(4b)...Cl(5)	0.880	2.408	3.269	166.19
N(4')-H(4'a)...Cl(5)	0.880	2.377	3.208	157.62
N(4')-H(4'b)...Cl(5)	0.880	2.387	3.267	177.38
N(3)-H(3)...Cl(5)	0.880	2.241	3.120	176.46
C(8)-H(8)...Cl(4)	0.992	3.076	3.426	102.19

Regium bond between tetrachloridoaurate and parallel cytosine ring:  $\pi$ -hole and  $\pi$ -lump regium bond interaction. To study this interaction, electrostatic potential maps have been generated for the tetrachloridoaurate anion and the N1-hexylcytosinium cation (Figure 45 and Figure 46). These MEPs show a  $\pi$ -hole on gold atom in  $\text{AuCl}_4^-$  and a  $\pi$ -lump on C (5) of N<sup>1</sup>-hexylcytosinium.



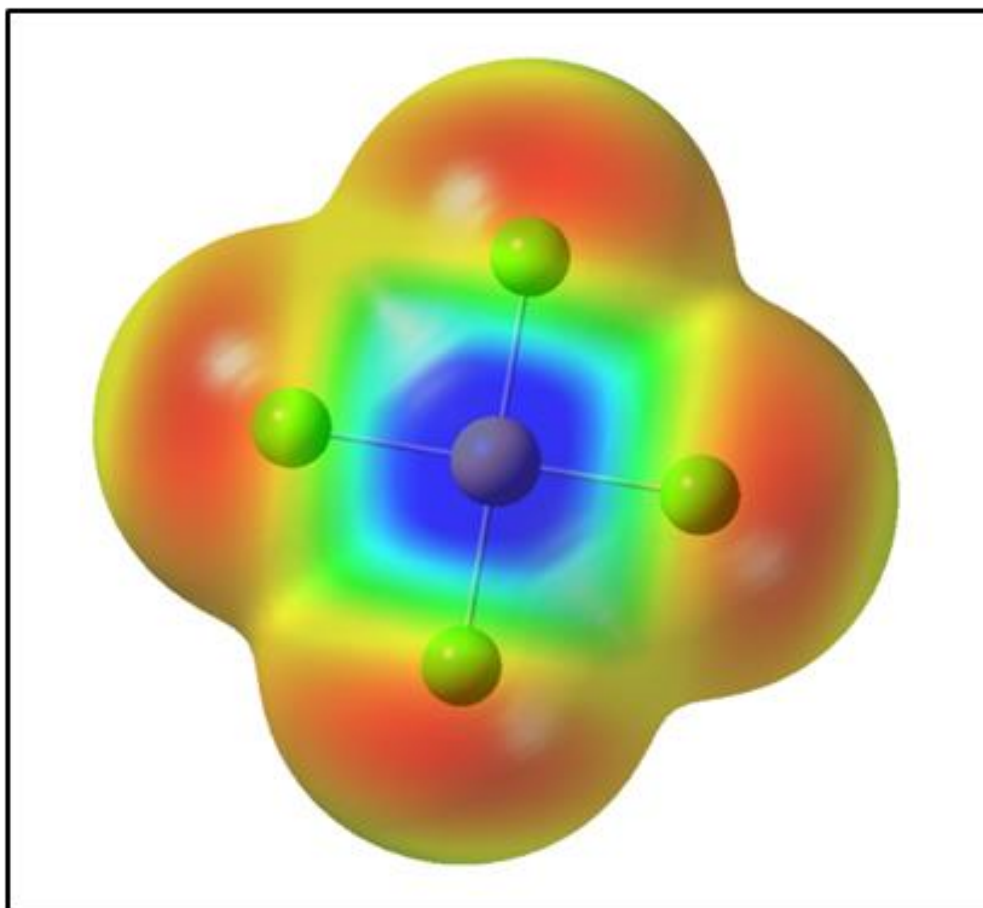


Figure 45  $\text{AuCl}_4^-$  MEP (electrostatic potential map)

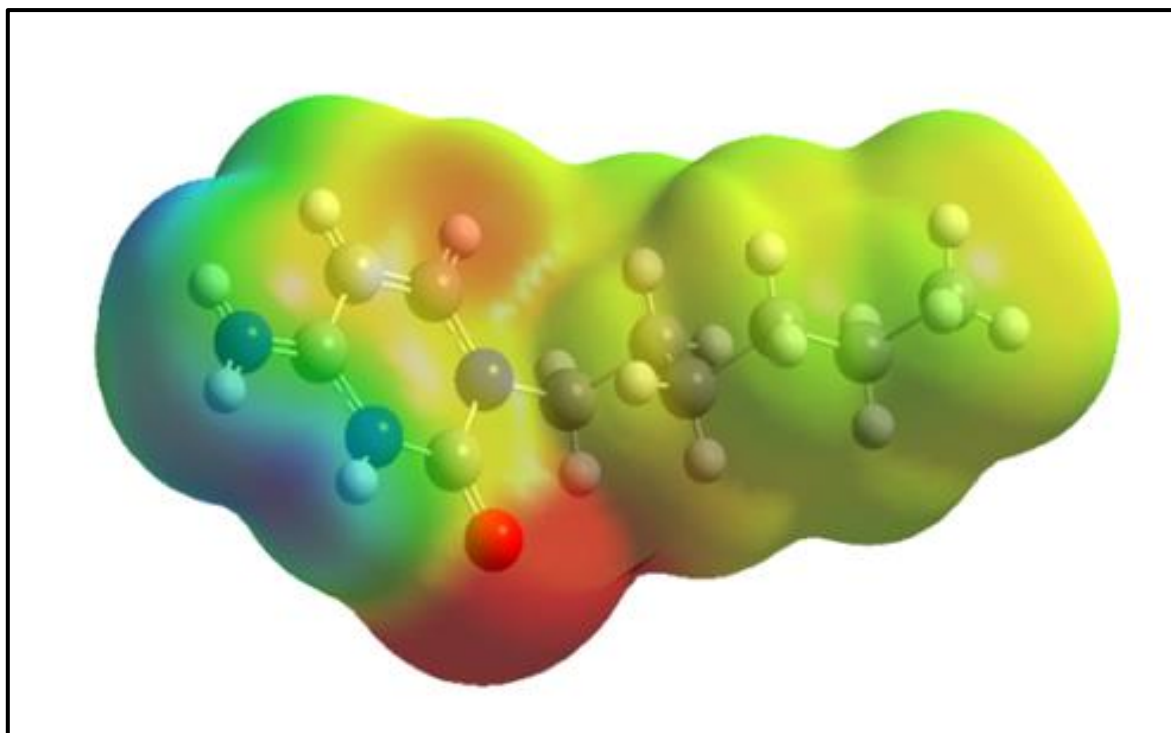


Figure 46  $\text{N}^1$ -hexylcytosinium MEP

In three-dimensional structure, coplanar tetrachloridoaurate and cytosinium ring form a series of regium bonds along axis "a". Every gold can form two bonds, one with cytosine ring

above and one with cytosine ring below. These bonds are not symmetrical since the bond's distances are 3.316 Å and the other is 3.554 Å (Figure 47).

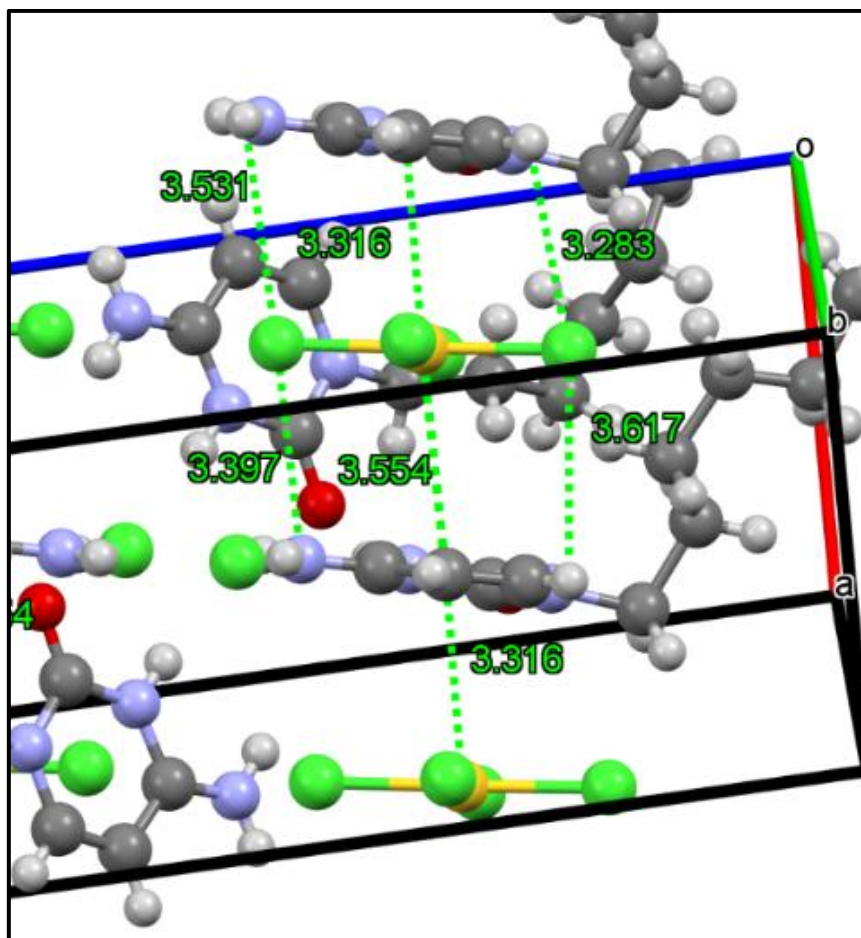


Figure 47 View of Regium Bond interaction with interaction distances

## 5 Conclusions

1. Some new coordination complexes of gold (III) with nucleic bases and their derivatives have been synthesized and characterised using spectroscopic techniques such as AE, HRMS, IR, <sup>1</sup>H-NMR. These are:
  - 1.1. The MeCyt-Au 1:2 derivative has been synthesized and spectroscopic data induces thinking of trans isomer being formed. Even so it is impossible to determine the exact structure of the complex without an x-ray diffraction study
  - 1.2. The Cyt-Au 1:1 and 1:2 derivatives have been synthesized but any of these complexes have crystalized. Spectroscopic data induces thinking of the formation of these coordination compounds, but without any X-ray study it is not possible to elucidate the structure. Even so this work has given clues of new synthesis paths to be followed in the obtention of new coordination compounds with cytidine.
  - 1.3. A 1:1 derivative of CytC<sub>6</sub>-Au, crystalized in a different packing, being a polymorph of the already described coordination compound<sup>10</sup>. These results confirm the capability of long n-alkyl nucleic bases derivatives in the obtention of coordination complexes. Moreover, it encourages to continue working with this ligand in the obtention of 1:2 derivatives.
2. A new outer-sphere complex of CytC<sub>6</sub> has been obtained and studied by High Resolution Single Crystal X-ray diffraction. Although there is not a coordination bond in this complex, we have found a way to obtain this kind of derivatives, using tetrachloridoaurate as a counter ion of a cytosinium-cytosine base pair.
3. A new line of investigation has been opened, after seeing the reaction of uracil derivatives with gold(III). This investigation has not been deepened enough in this work due to the lack of time, as uracil derivatives were the last ligand used in this work. Low quantities used added to low reaction yields and the long evaporation time of new complexes' solutions.

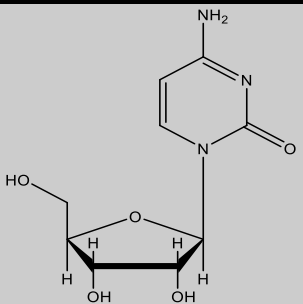
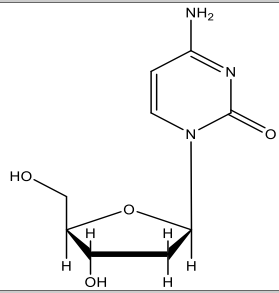
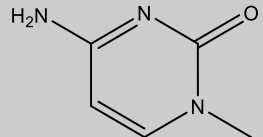
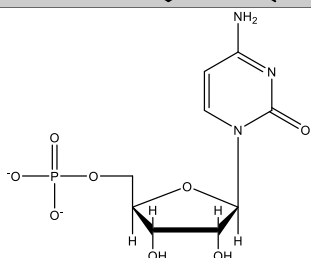
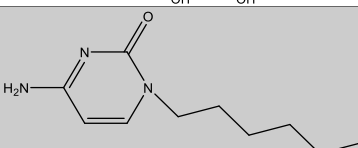
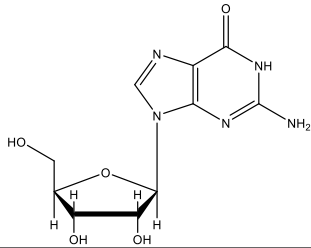
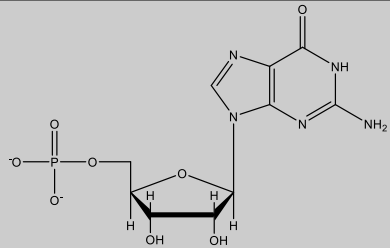
This work enhances the knowledge of the gold interaction with nucleic bases and opens new perspectives for futures work in this field that to this day so much is still yet unknown. In concrete the possibility to crystalize a 1:2 derivative of cytosine with gold would be a major hit, as it would possibly resemble DNA structure.

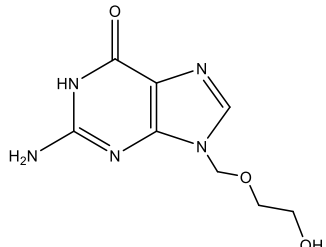
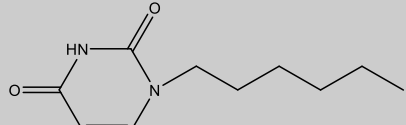
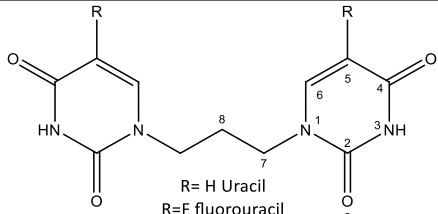
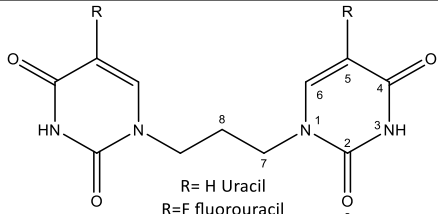
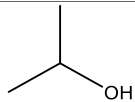
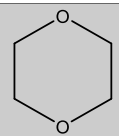


## 6 Annexes

## 6.1 Annex I: Abbreviations

Table 21 Most used reagent's abbreviations, complete names, and structures

Abbreviations	No abbreviated form	Structure
<b>Cyd</b>	Cytidine	
<b>dCyd</b>	2' deoxycytidine	
<b>MeCyt</b>	Methyl cytosine	
<b>CMP</b>	Cytidine monophosphate	
<b>CytC6</b>	N <sup>1</sup> -hexylcytosine	
<b>Gua</b>	Guanosine	
<b>GMP</b>	Guanosine monophosphate	

<b>Acv</b>	Acyclovir	
<b>UraC<sub>6</sub></b>	N <sup>1</sup> -hexyluracil	
<b>Ura<sub>2</sub>C<sub>3</sub></b>	N <sup>1</sup> , N <sup>1</sup> -trimethylene-bis-uracil	
<b>(F-Ura)<sub>2</sub>C<sub>3</sub></b>	N <sup>1</sup> , N <sup>1</sup> -trimethylene-bis-(5-fluorouracil)	
<b>iPrOH</b>	2-propanol	
<b>MeOH</b>	Methanol	<b>CH<sub>3</sub>OH</b>
<b>MeCN</b>	Acetonitrile	<b>CH<sub>3</sub>CN</b>
<b>DIO</b>	1,4-dioxane	

## 6.2 Annex II: IR spectrum

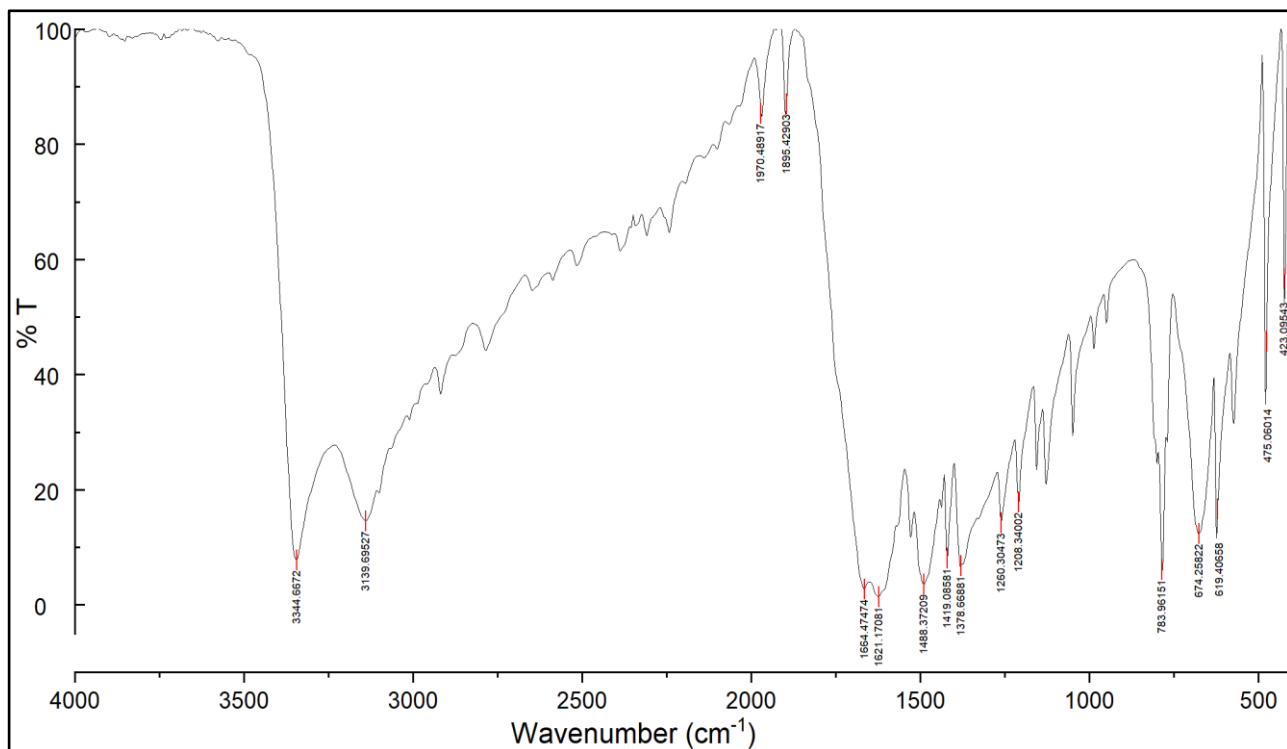


Figure 48 1-methylcytosine (commercial reagent)

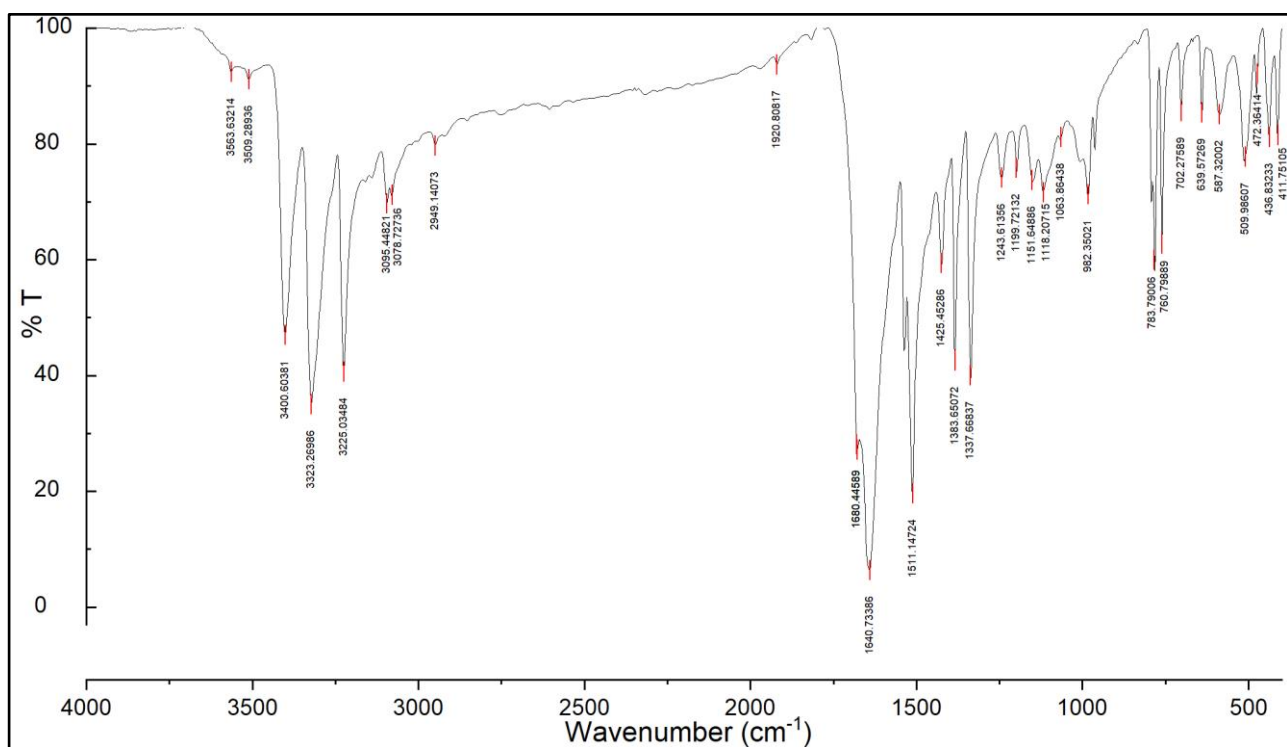


Figure 49 Complex I AuCl<sub>3</sub>MeCyt

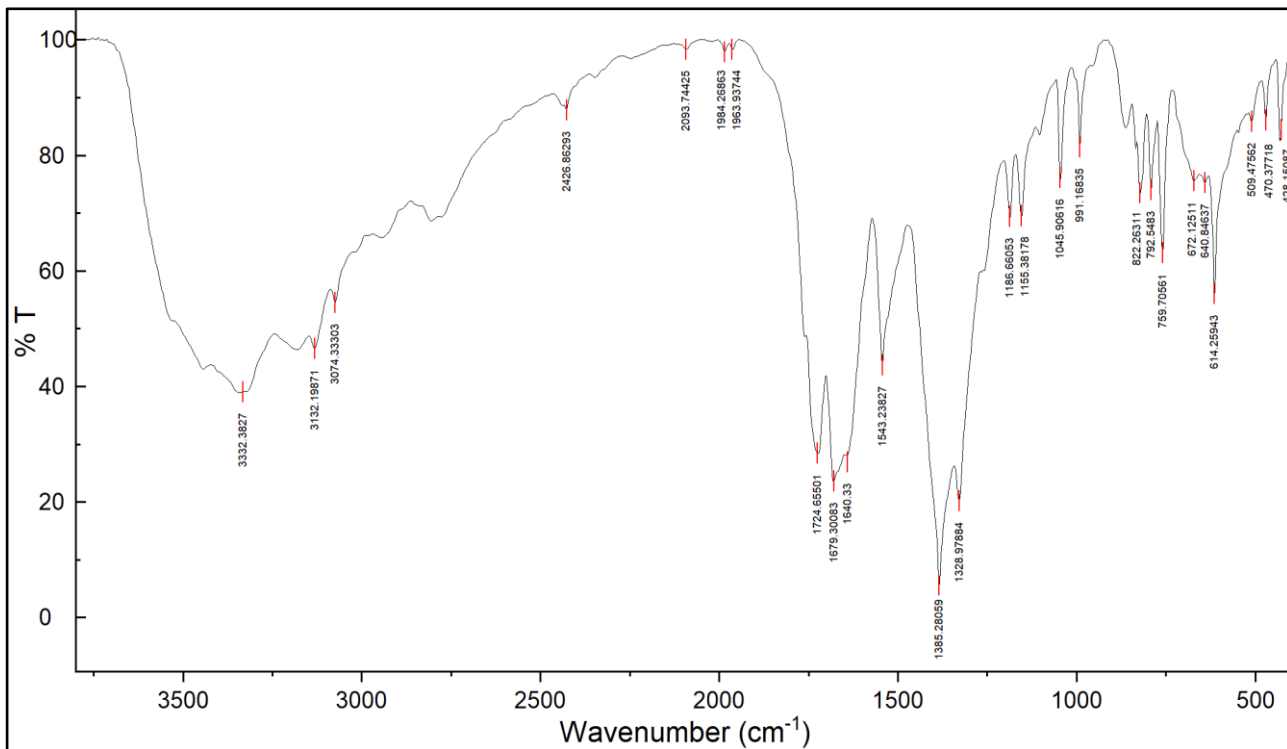


Figure 50 Complex II  $\text{AuCl}(\text{NO}_3)_2(\text{MeCyt})_2$

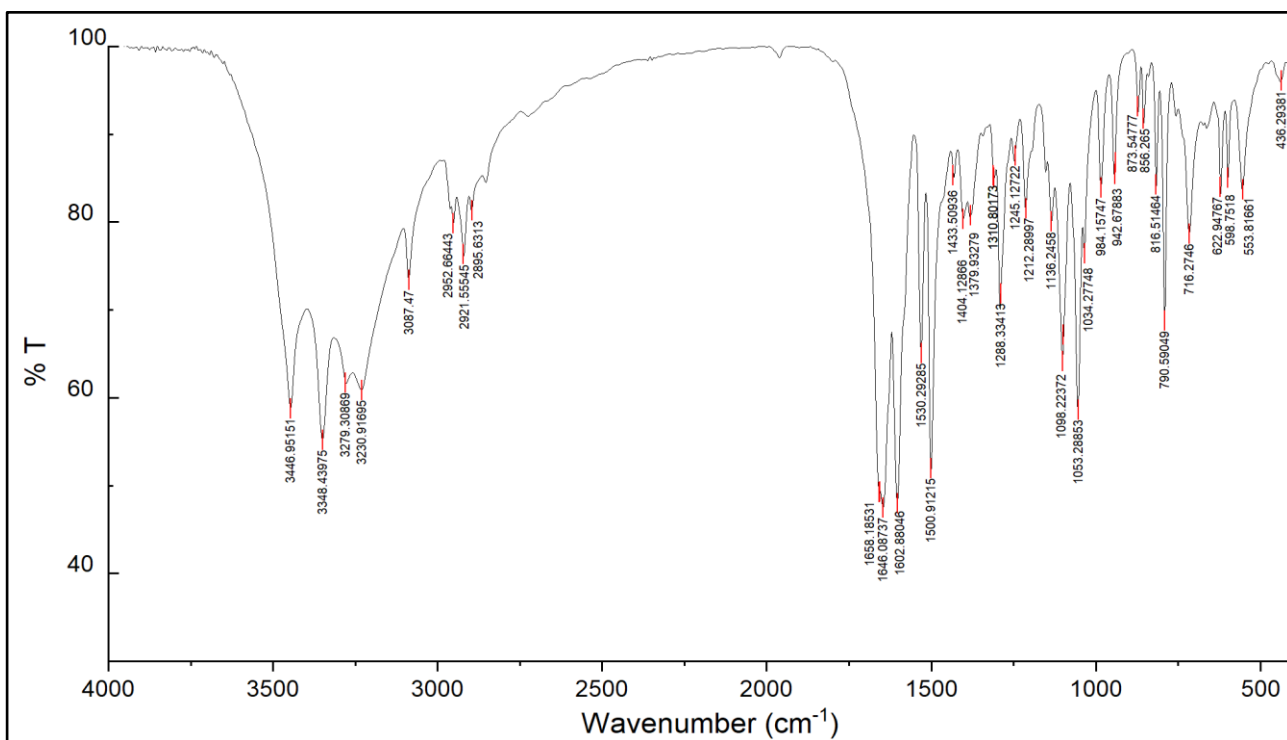


Figure 51 Cyt (commercial reagent)

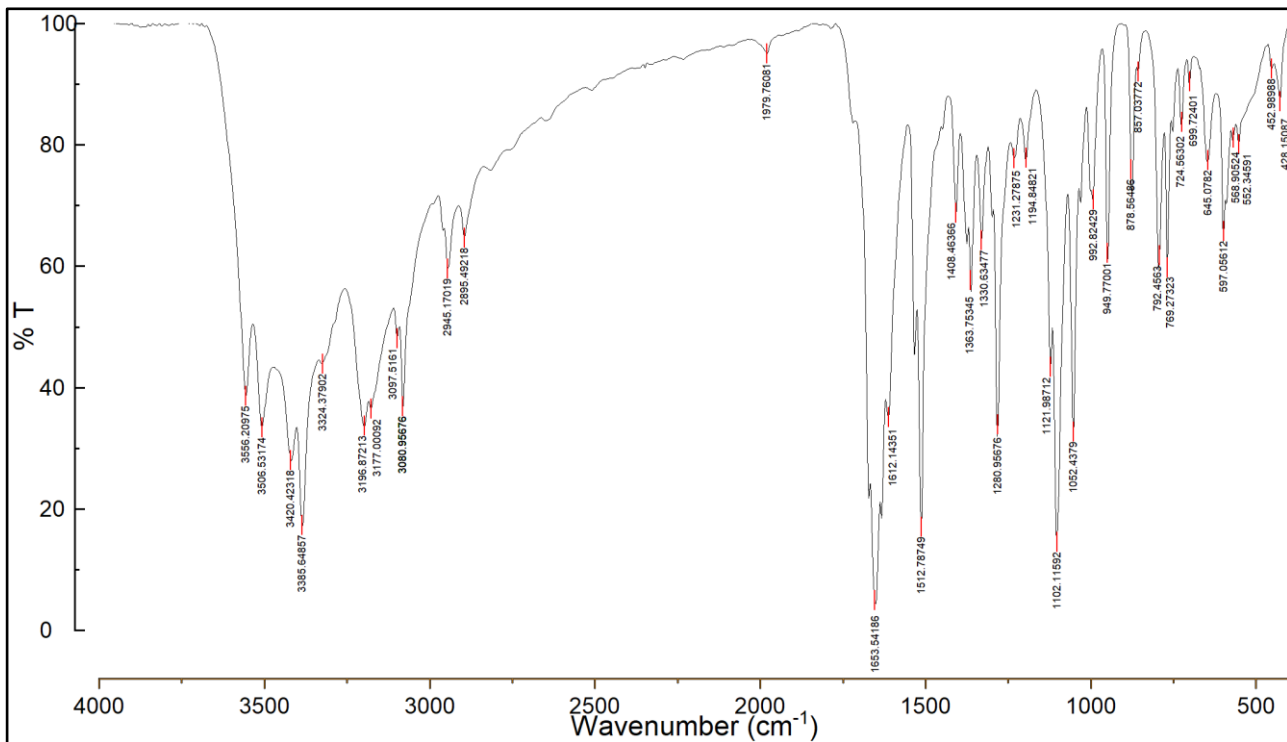


Figure 52 Complex III AuCl<sub>3</sub>Cyd

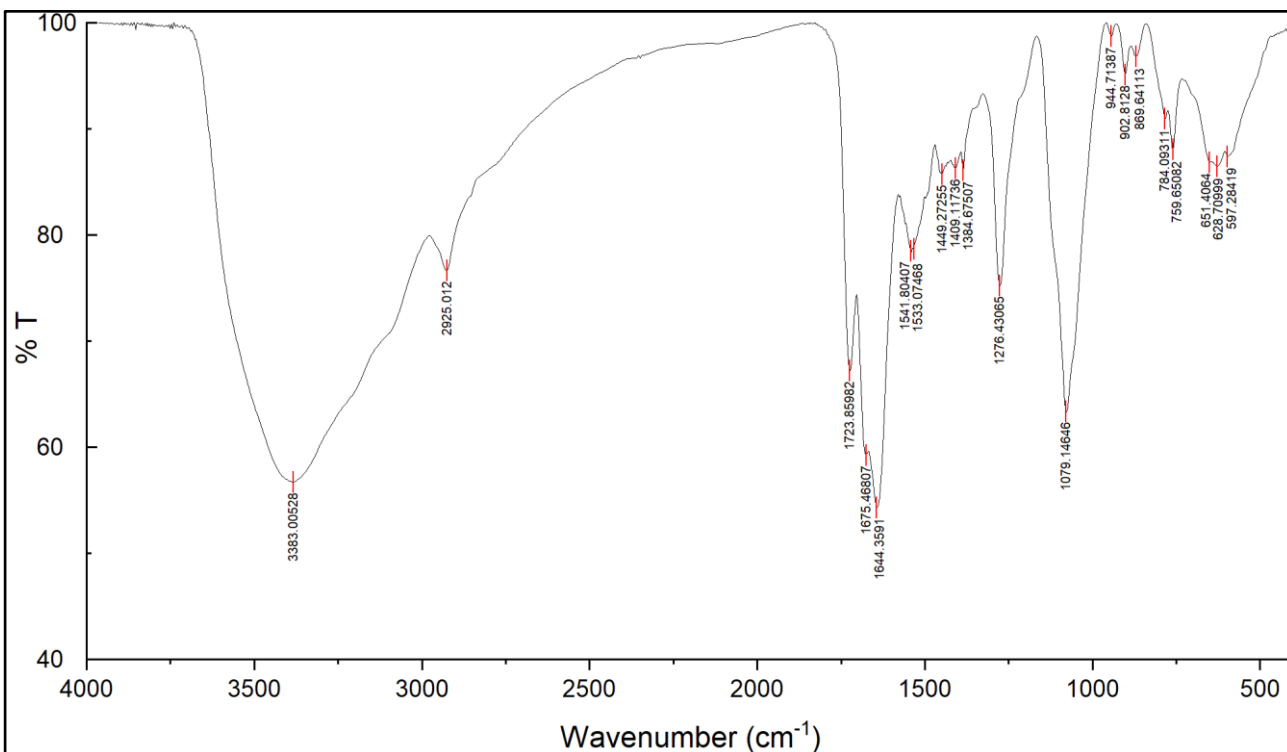


Figure 53 Complex IV Na[AuCl<sub>2</sub>Cyd<sub>2</sub>(SbF<sub>6</sub>)<sub>2</sub>]



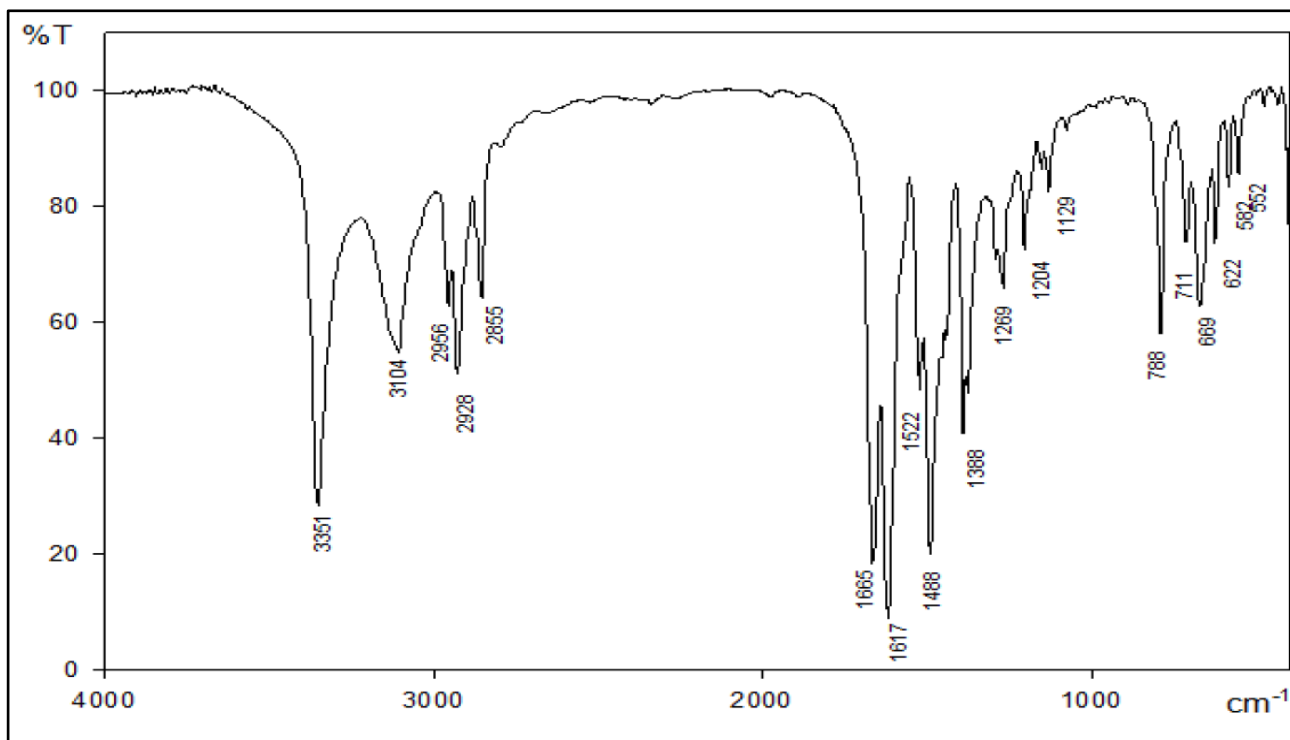


Figure 54 CytC<sub>6</sub> (IR spectrum from A. Baquero thesis<sup>39</sup>)

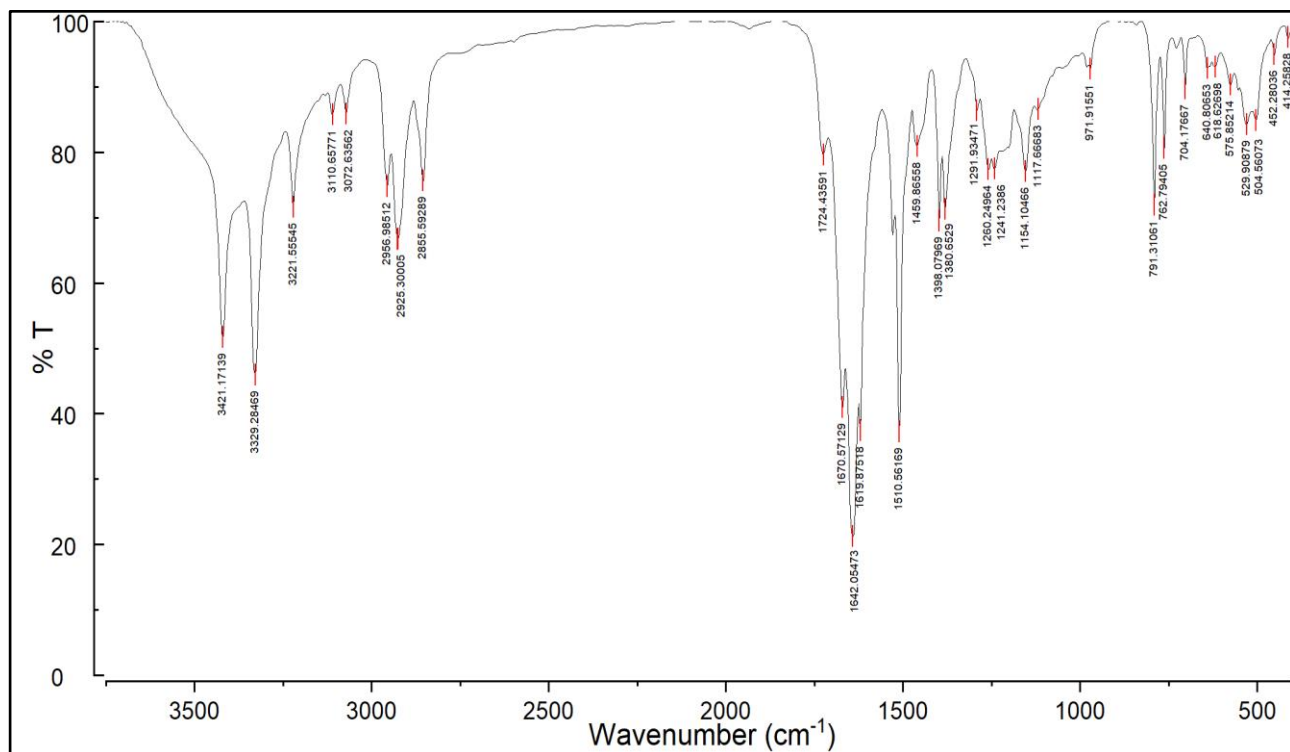


Figure 55 Complex VI AuCl<sub>3</sub>CytC<sub>6</sub>

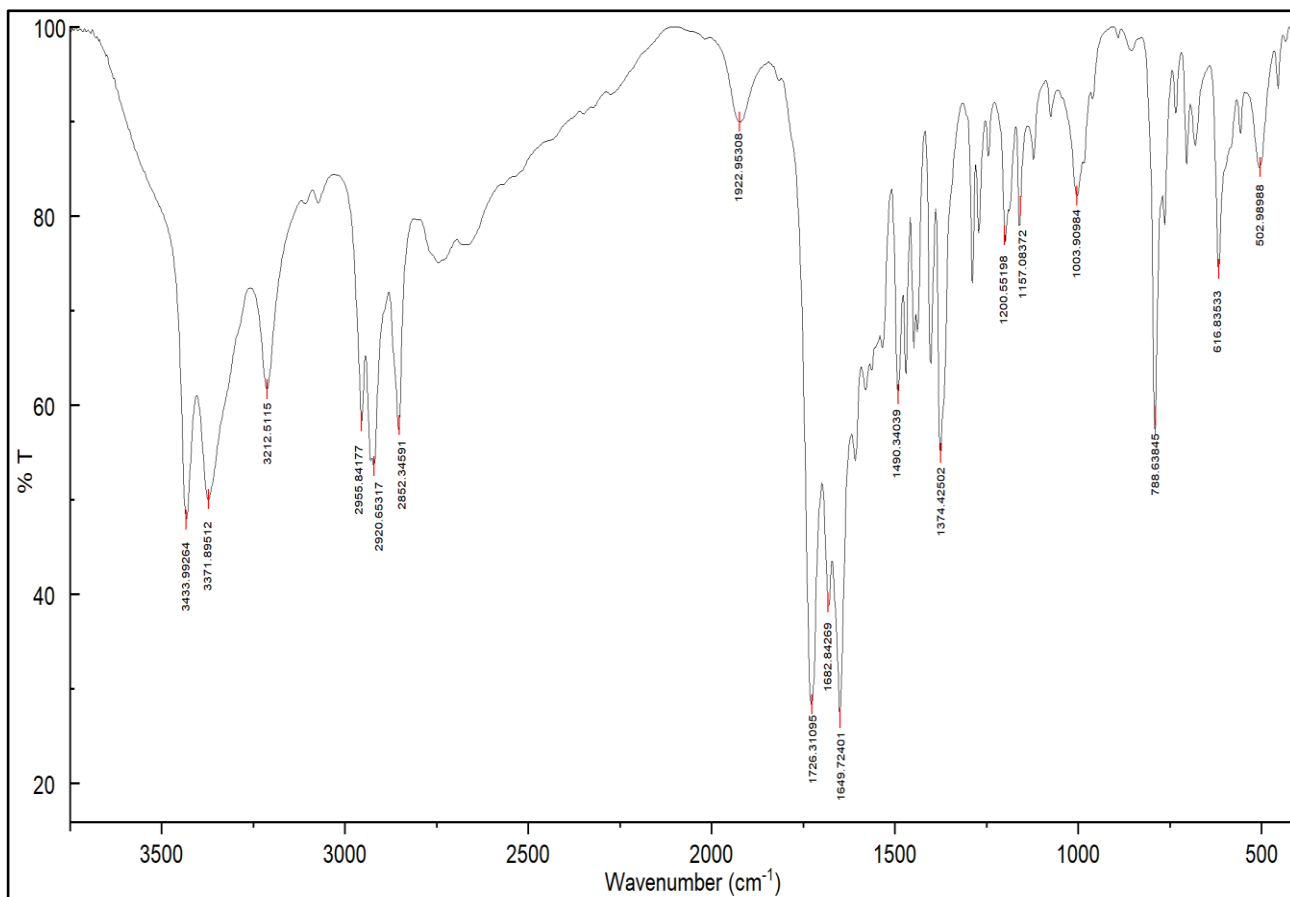


Figure 56 Complex VII ( $\text{HCytC}_6$ )<sub>2</sub> [ $\text{AuCl}_4$ ] Cl

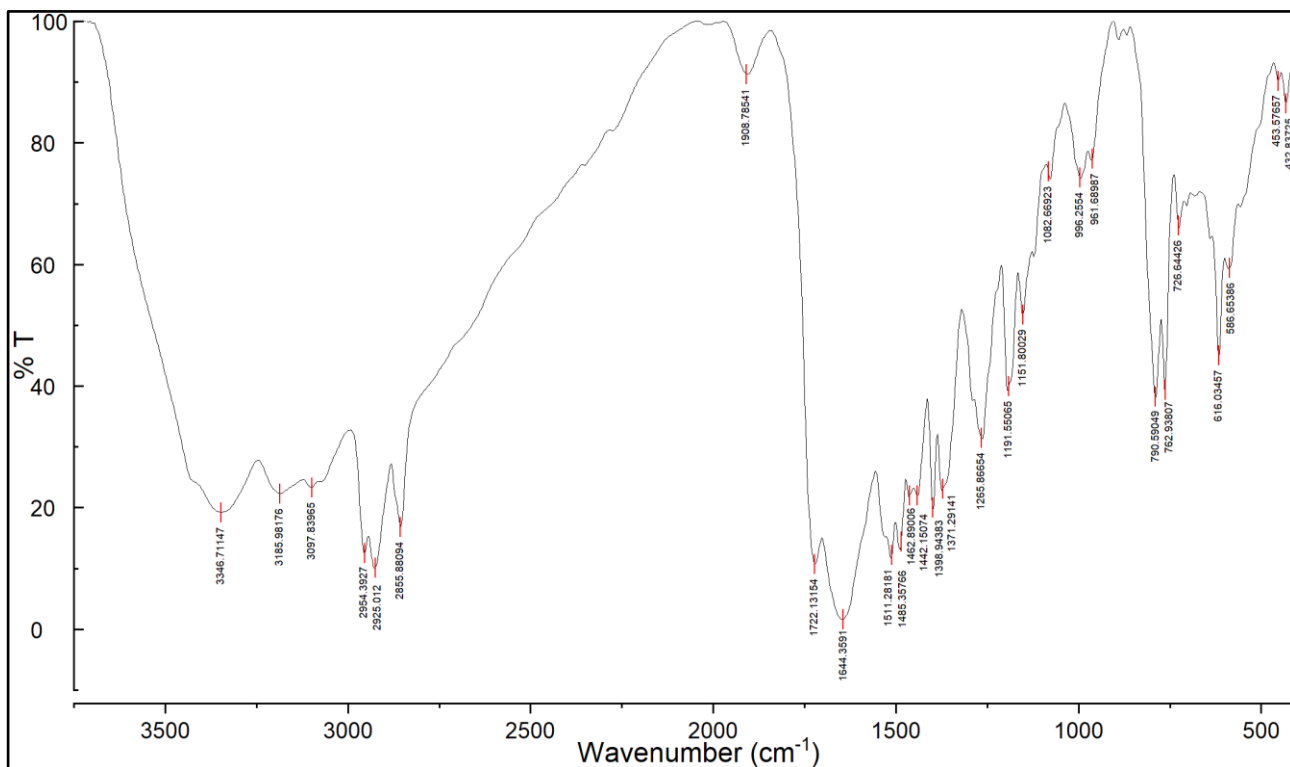


Figure 57 Complex VIII  $\text{AuCl}_2(\text{CytC}_6)_2$

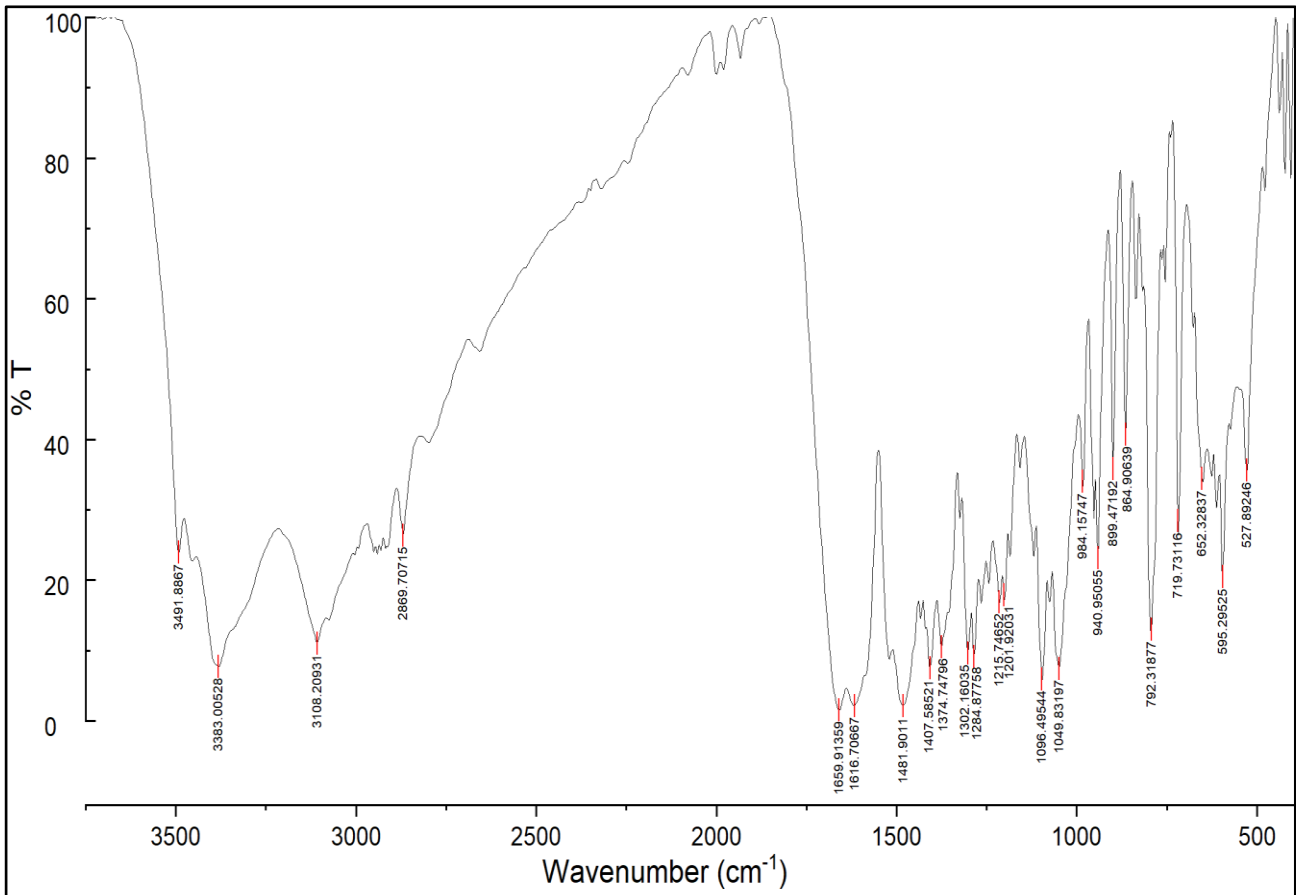


Figure 58 dCyd (commercial product)

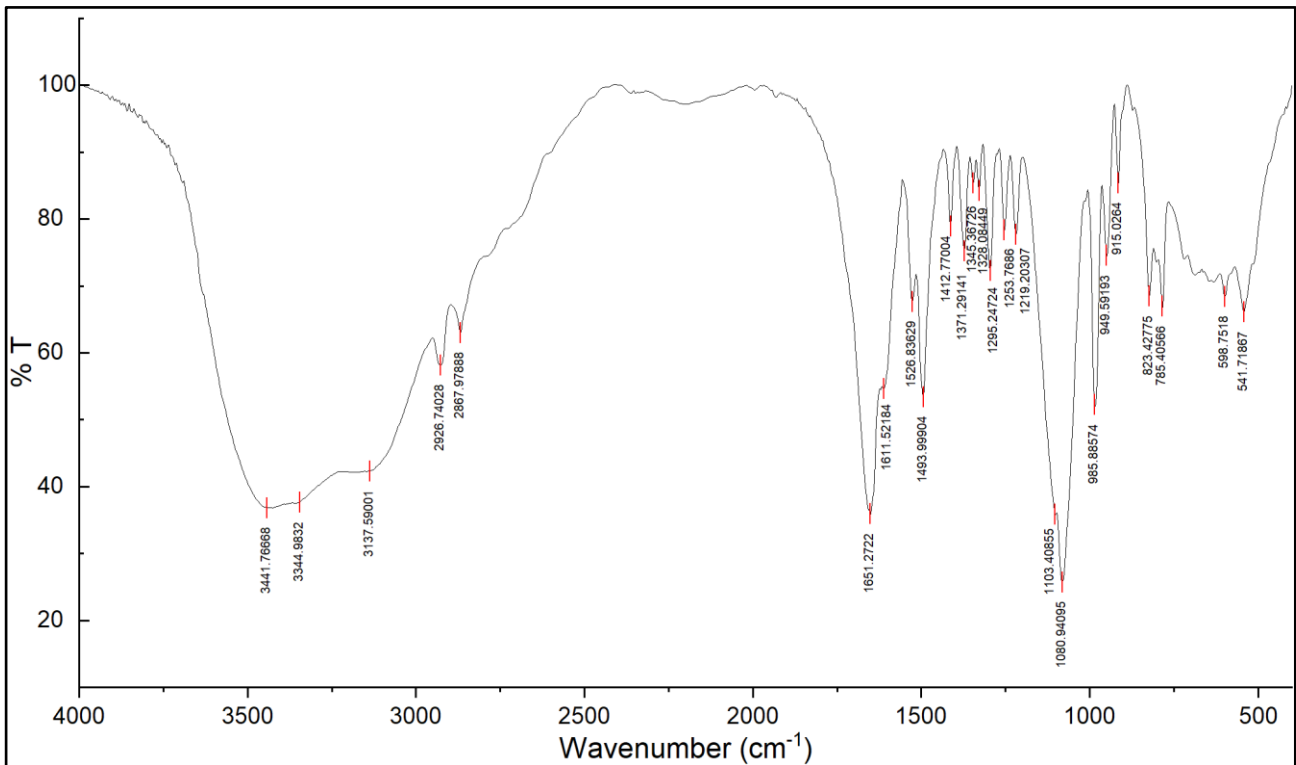


Figure 59 CMP (commercial product)

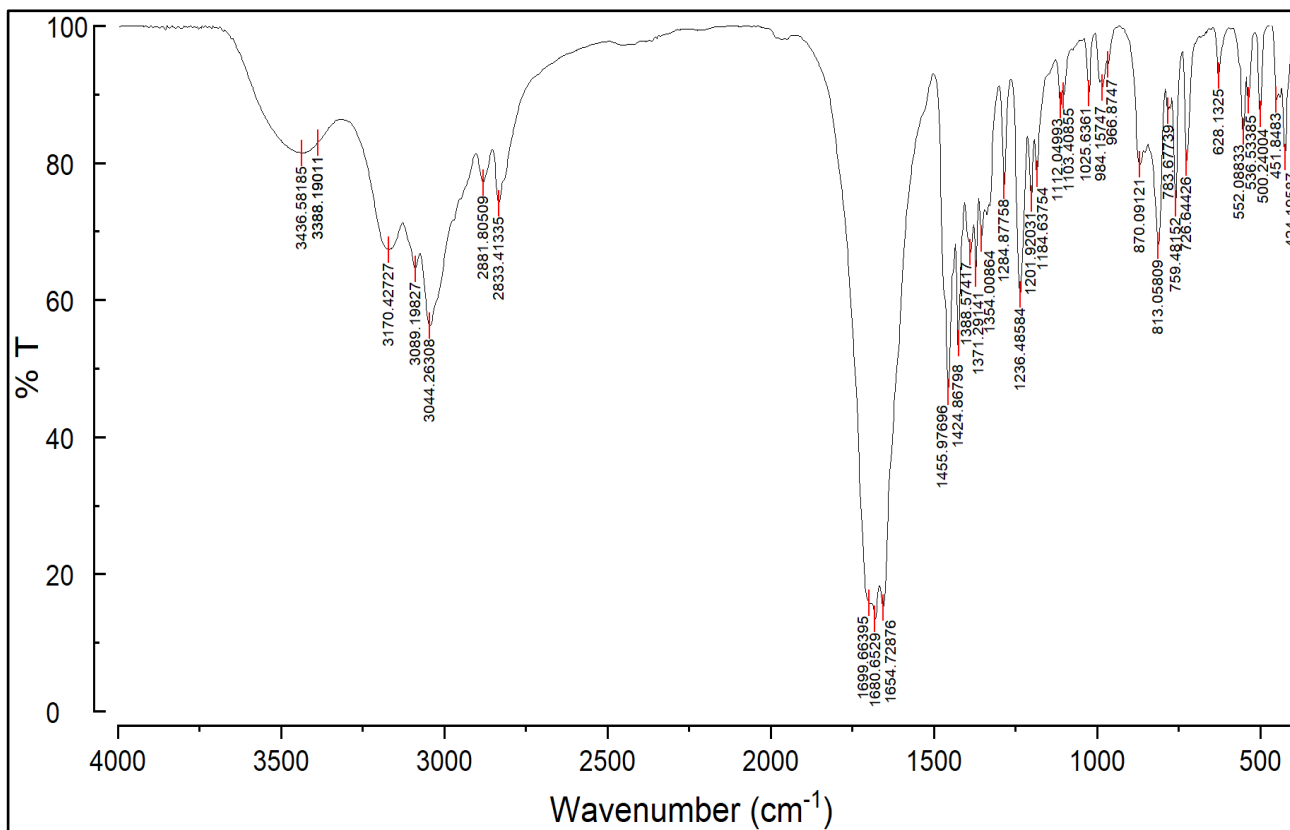


Figure 60 Ura<sub>2</sub>C<sub>3</sub> obtained as in bibliography<sup>41</sup>

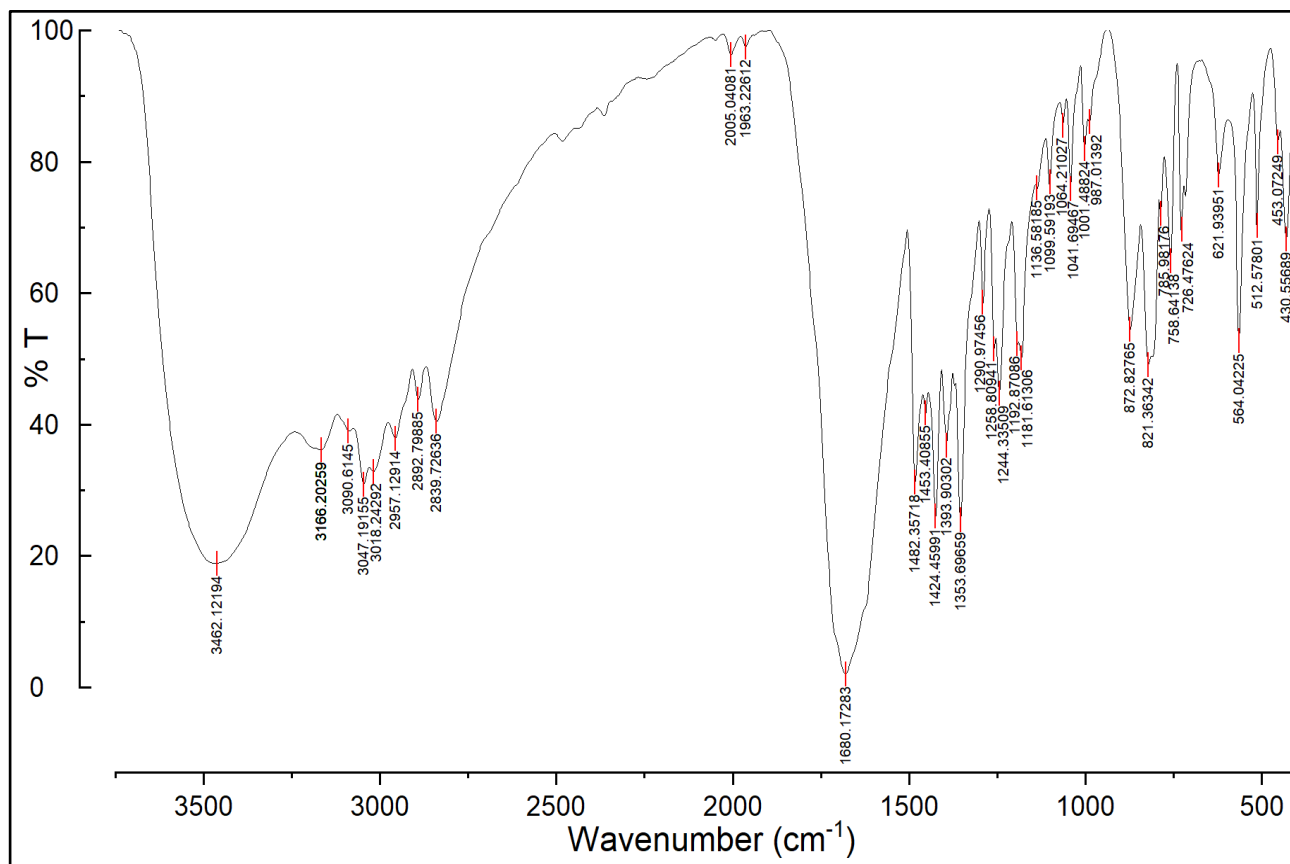


Figure 61 Complex XI AuCl<sub>3</sub>(Ura<sub>2</sub>C<sub>3</sub>)

### 6.3 Annex III: $^1\text{H}$ -NMR spectrum

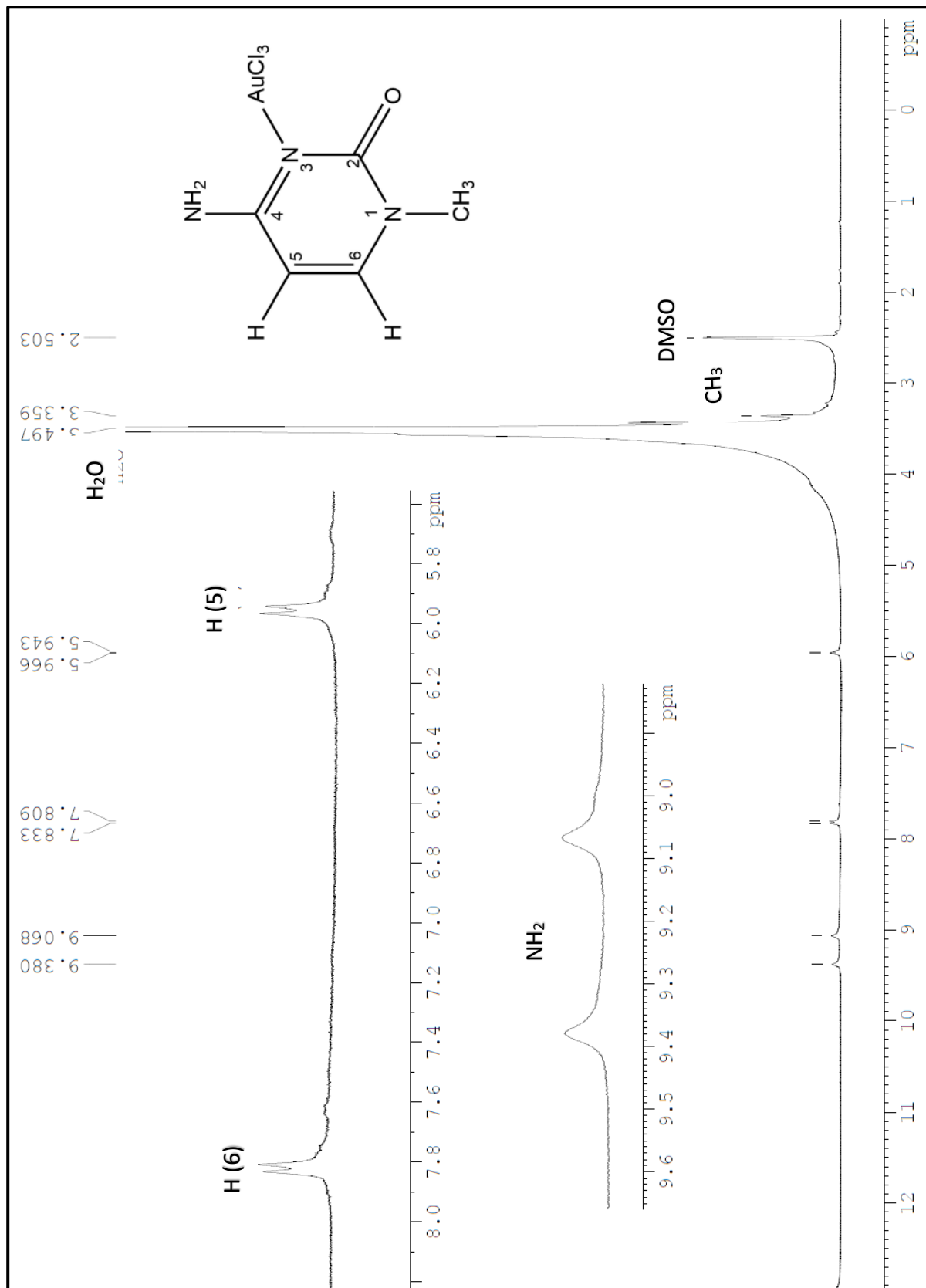


Figure 62 Complex I Au(MeCyt)  $^1\text{H-NMR}$

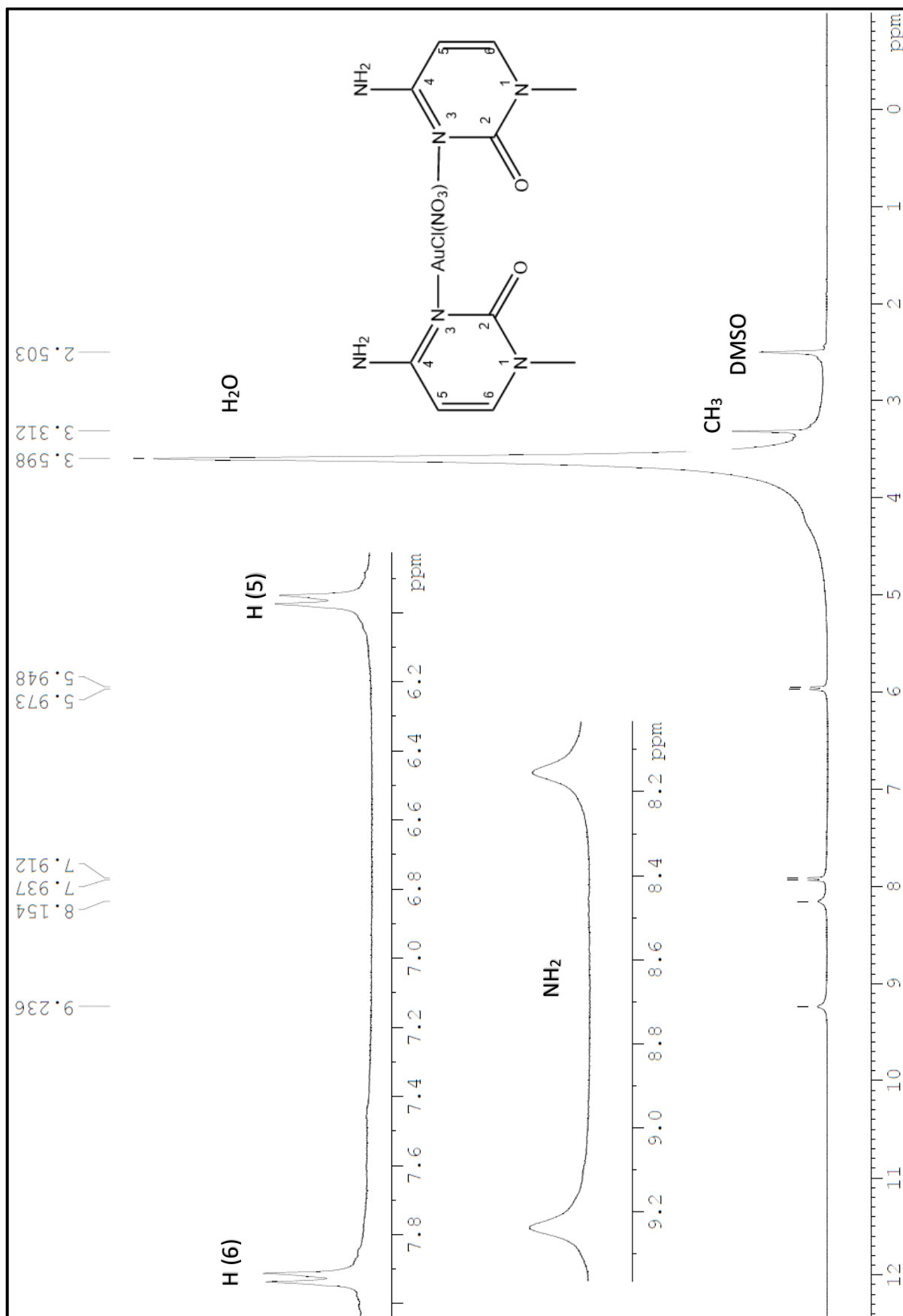


Figure 63 Complex II  $\text{Au}(\text{MeCyt})_2$   $^1\text{H-NMR}$

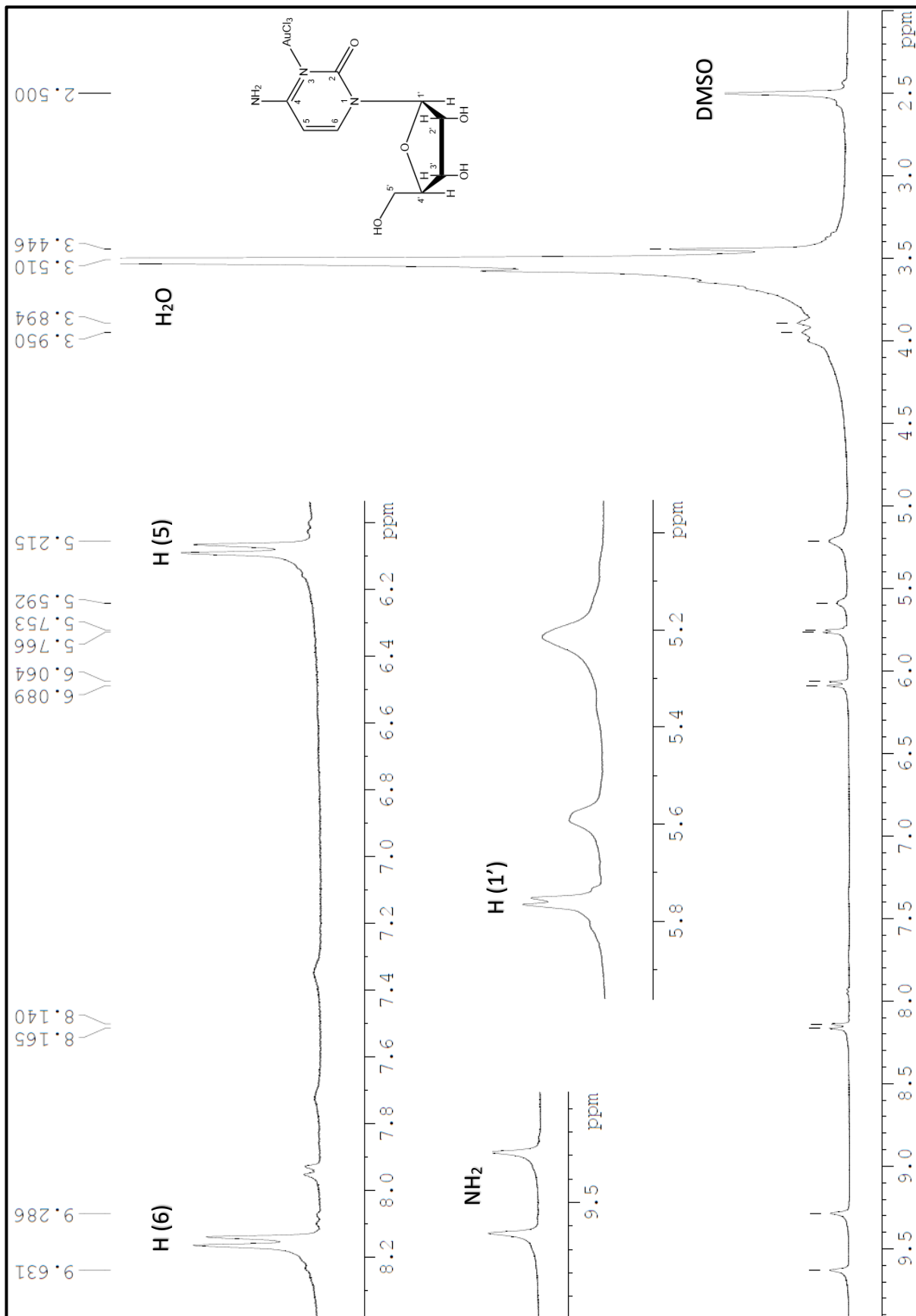


Figure 64 Complex III Au-Cyd  $^1\text{H-NMR}$



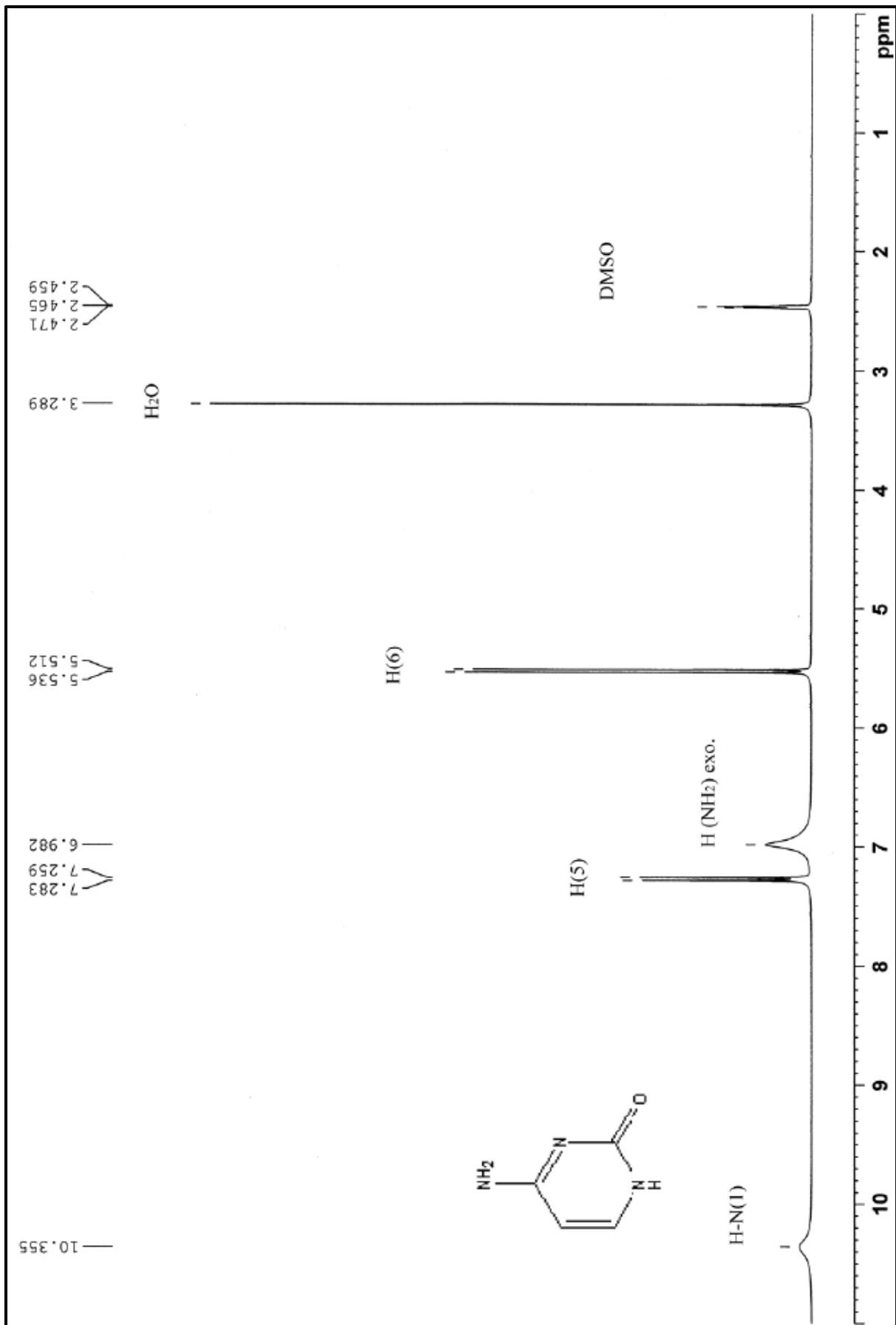


Figure 65 Cytosine <sup>1</sup>H-NMR ( extracted from A. Baquero thesis)

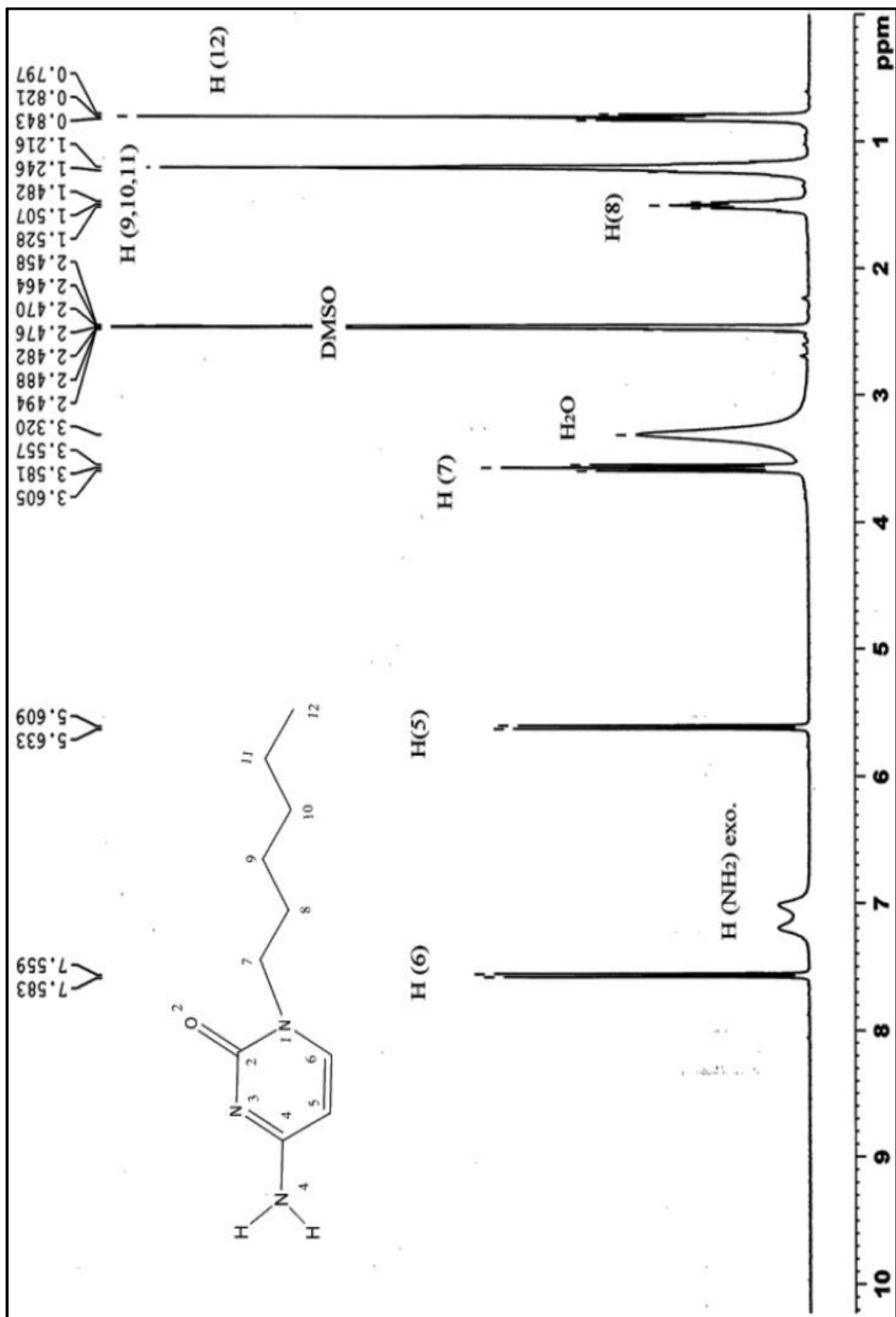


Figure 66 CytC<sub>6</sub> 1H-NMR ( extracted from A. Baquero thesis)

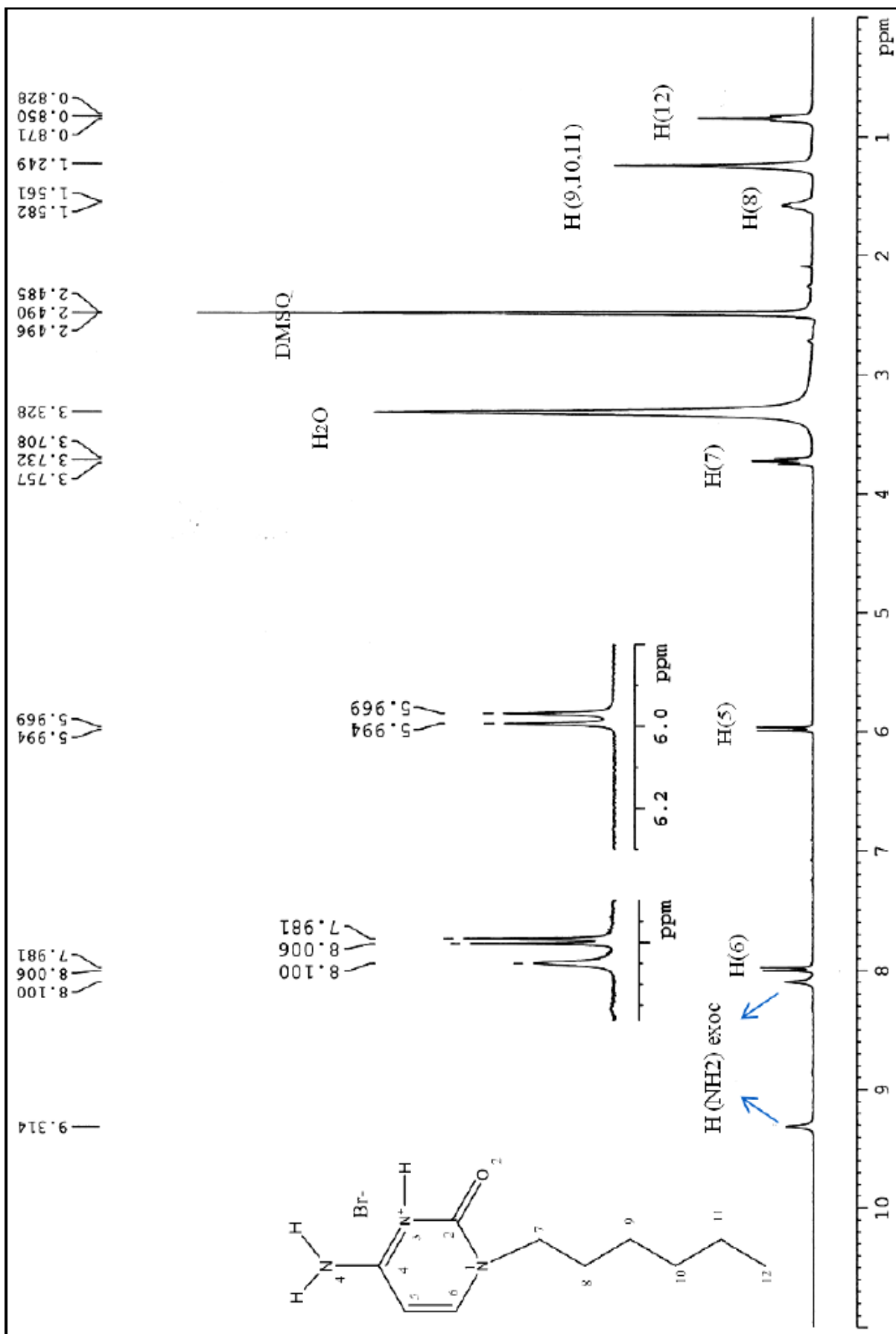


Figure 67 CytC<sub>6</sub>HBr <sup>1</sup>H-NMR (extracted from A. Baquero thesis)

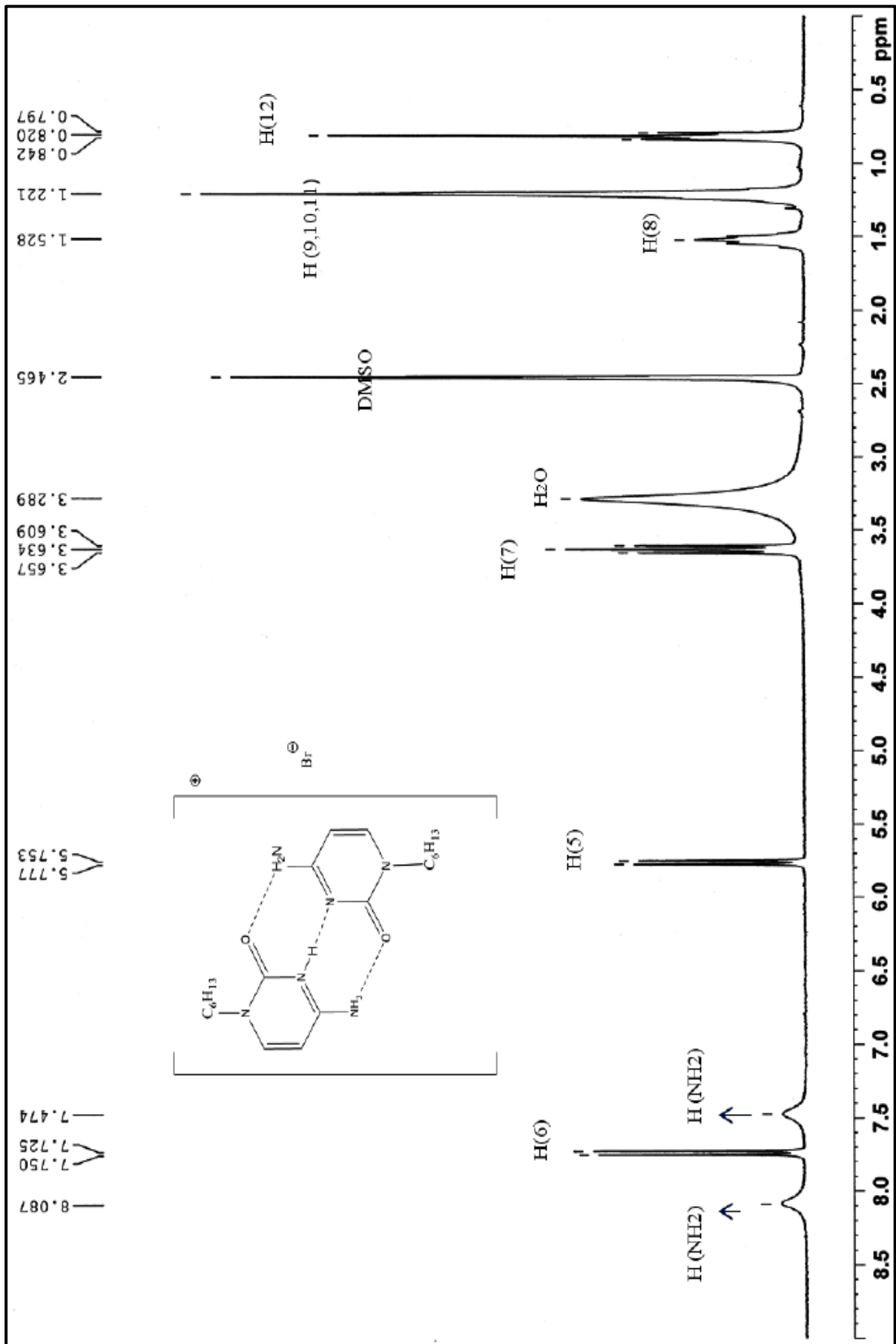


Figure 68 [CytC<sub>6</sub>-H-CytC<sub>6</sub>]Br <sup>1</sup>H-NMR (extracted from A. Baquero)

## 6.4 Annex IV: ESI-HRMS spectrums

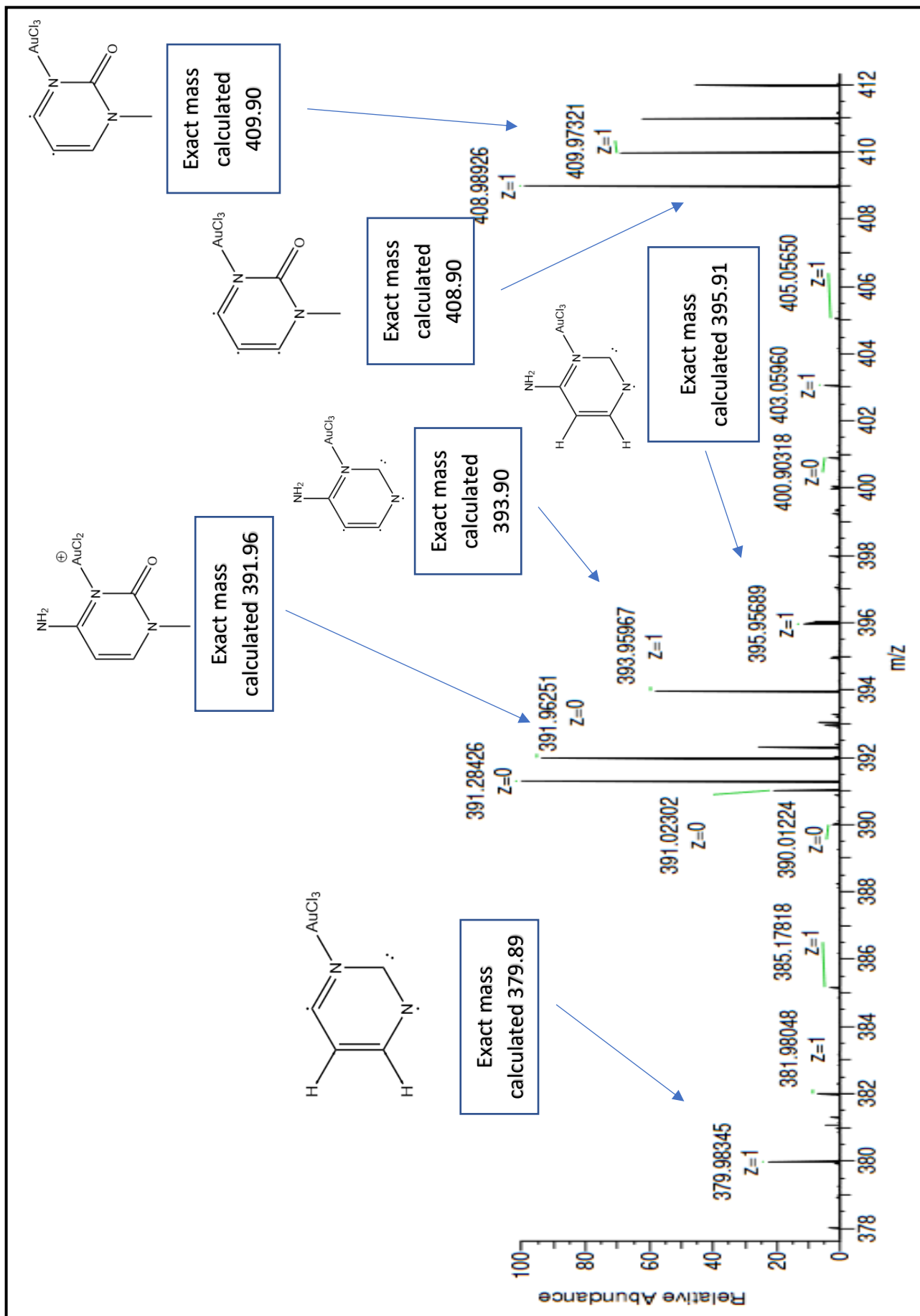


Figure 69 ESI-HRMS of complex I AuCl<sub>3</sub>(MeCyt)

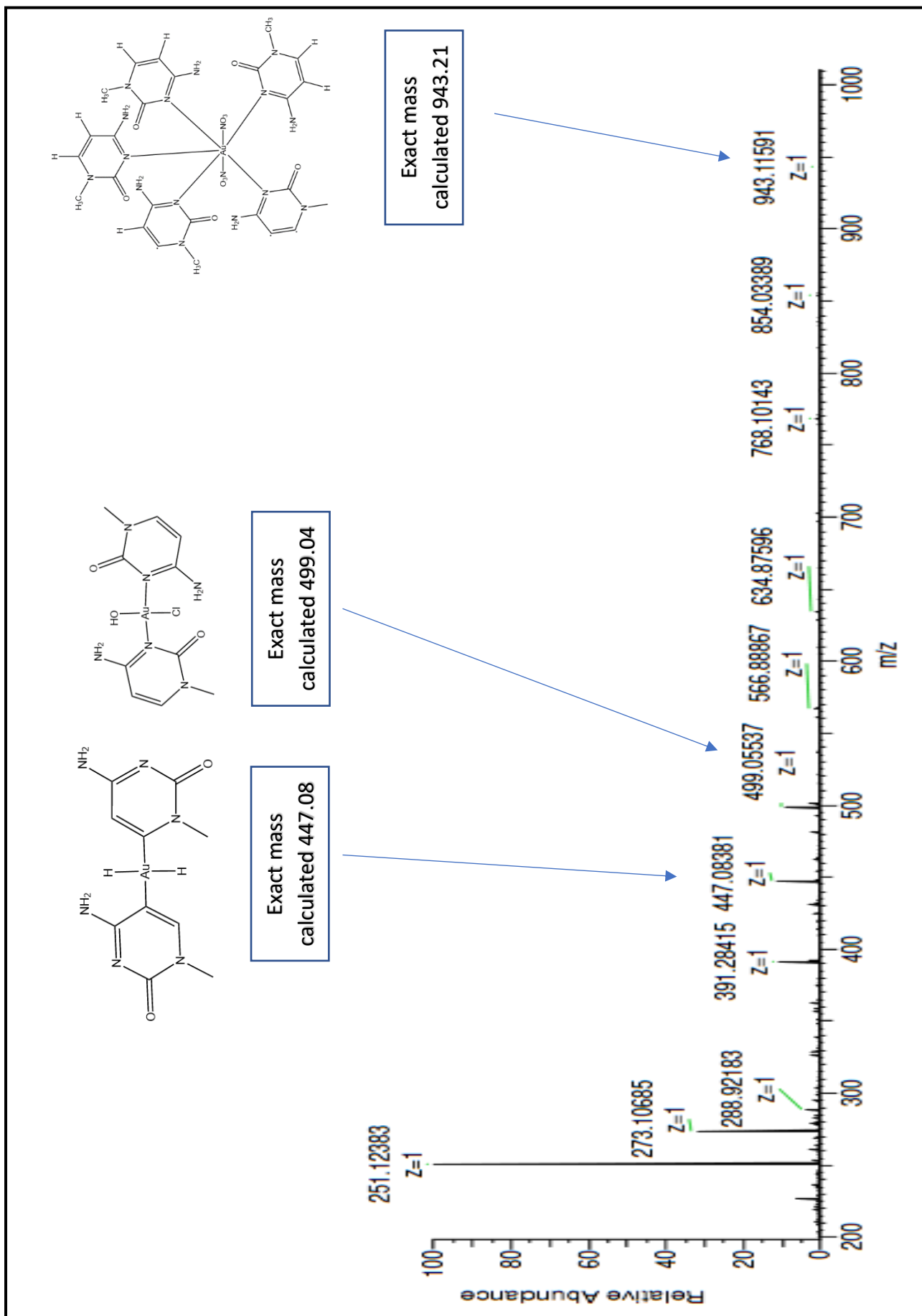


Figure 70 ESI-HRMS of complex II  $\text{AuCl}(\text{NO}_3)(\text{MeCyt})_2$

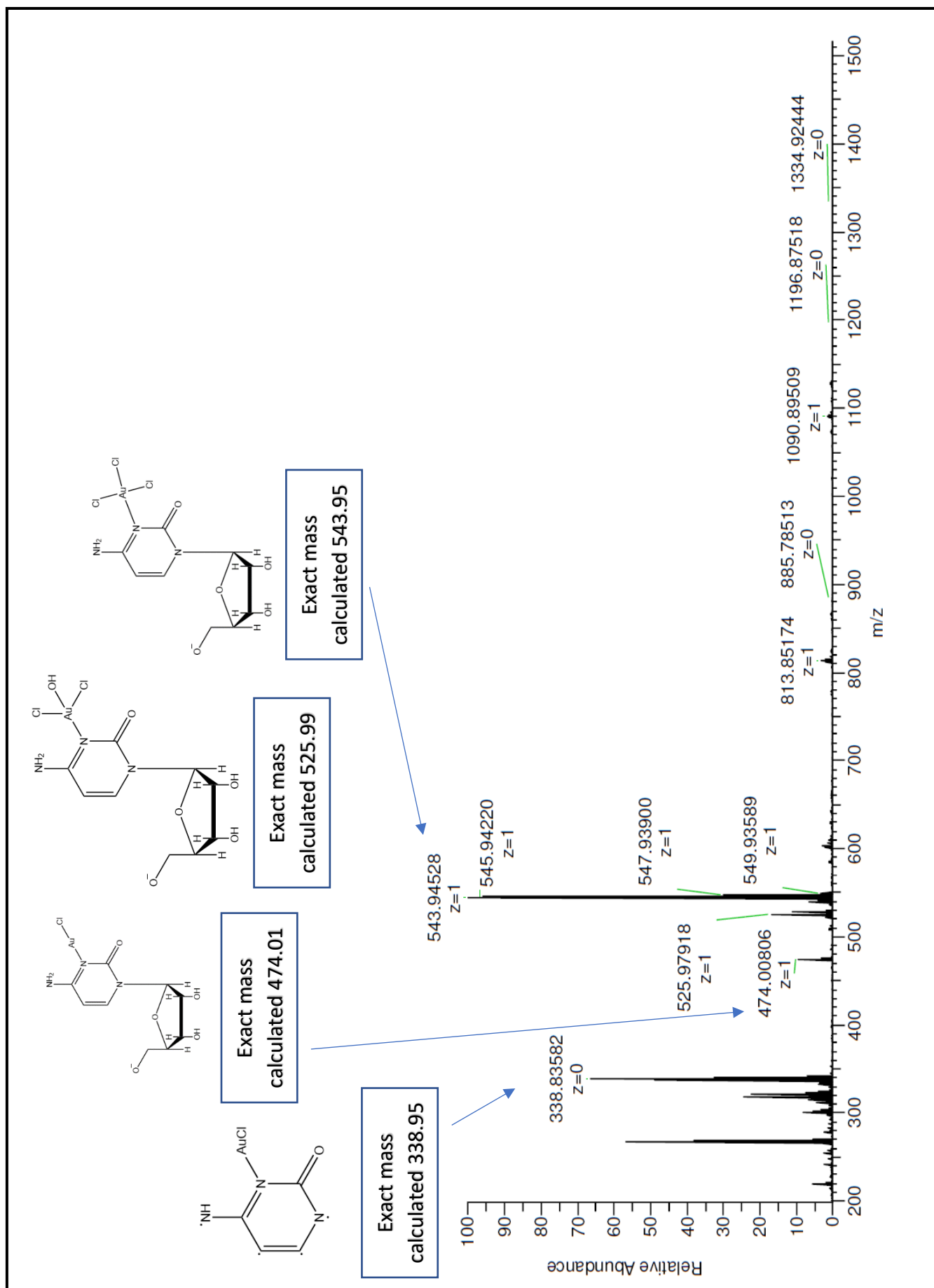


Figure 71 ESI-HRMS of complex III AuCl<sub>3</sub>Cyd



## 6.5 Annex V: Crystallographic data and X-Ray structures

Table 22 Crystallographic data of obtained complexes

Compound	AuCl <sub>3</sub> CytC <sub>6</sub>		AuCl <sub>3</sub> CytC <sub>6</sub>		(HCytC <sub>6</sub> ) <sub>2</sub> [AuCl <sub>4</sub> ]Cl	
	Complex VI		Complex VI (polymorph)		Complex VII	
Formula weight	498.58		498.58		766.77	
Temperature (K)	300(2)					
Wavelength (Å)	0.71073					
Crystal system	Monoclinic		Monoclinic		Triclinic	
Space group	P 21/c		P 21/c		P 1	
Unit cell dimensions	a (Å)	7.0041(19)	a (Å)	16.1471(11)	a (Å)	6.8686
	b (Å)	15.654(4)	b (Å)	8.4748(5)	b (Å)	10.7183
	c (Å)	16.326(4)	c (Å)	11.769(79)	c (Å)	20.600
	α (°)	90	α (°)	90	α (°)	84.71
	β (°)	115.405(8)	β (°)	105.40	β (°)	86.89
	γ (°)	90	γ (°)	90	γ (°)	72.36
	Volume (Å <sup>3</sup> )	1617.0(7)		1552.7		1438.57
Z	4		0			
Density (calculated) (Mg/m <sup>3</sup> )	2.048					
Absorption coefficient (mm <sup>-1</sup> )	9.586					
F(000)	944					
Crystal size (mm <sup>3</sup> )	0.200 x 0.070 x 0.070					
Theta range for data collection (°)	1.897 to 28.508					
Index ranges	-9 ≤ h ≤ 9					
	0 ≤ k ≤ 20					
	-21 ≤ l ≤ 21					
Reflections collected	7301					
Independent reflections	3861 [R(int) = 0.0687]					
Completeness to theta = 25.242° (%)	100.0					
Absorption correction	Semi-empirical from equivalents					
Max. and min. transmission	1 and 0.628					
Refinement method	Full-matrix least-squares on F <sup>2</sup>					
Data / restraints / parameters	3861 / 46 / 164					
Goodness-of-fit on F <sup>2</sup>	0.880					
Final R indices [I > 2σ(I)]	R1	0.0516				
	wR2	0.0975				
R indices (all data)	R1	0.1145				
	wR2	0.1136				
Largest diff. peak and hole (e·Å <sup>-3</sup> )	0.969 and -1.958					

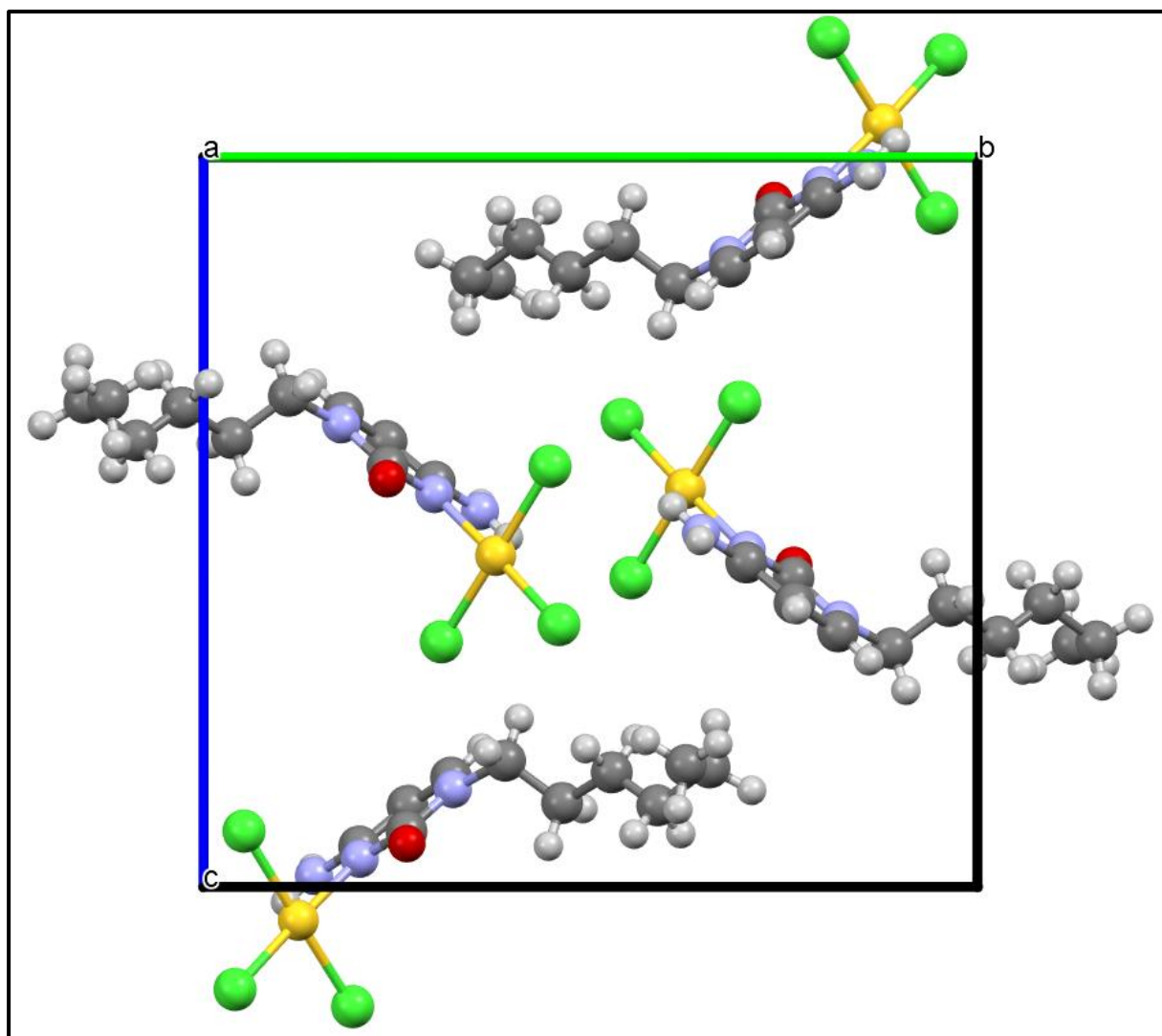


Figure 72 View of X-ray structure of Complex VIa along "a" axis

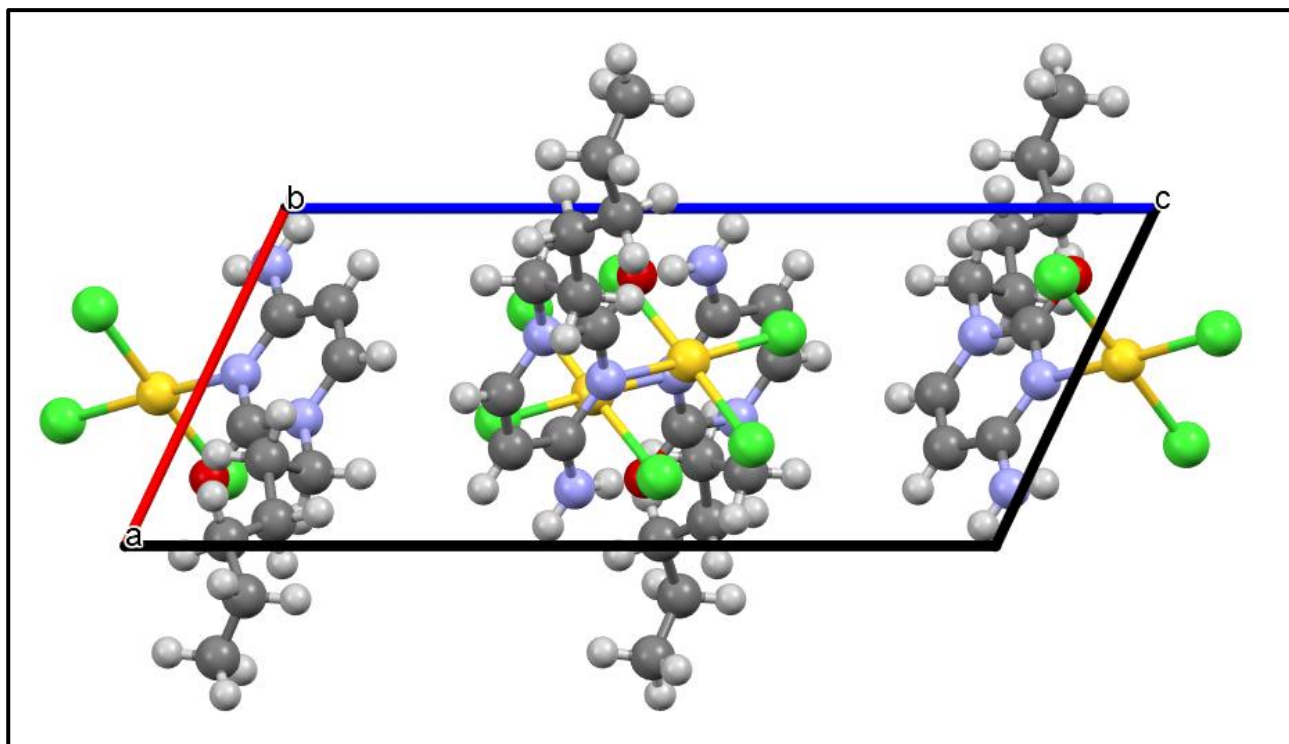


Figure 73 View of X-ray structure of Complex VIa along "b" axis

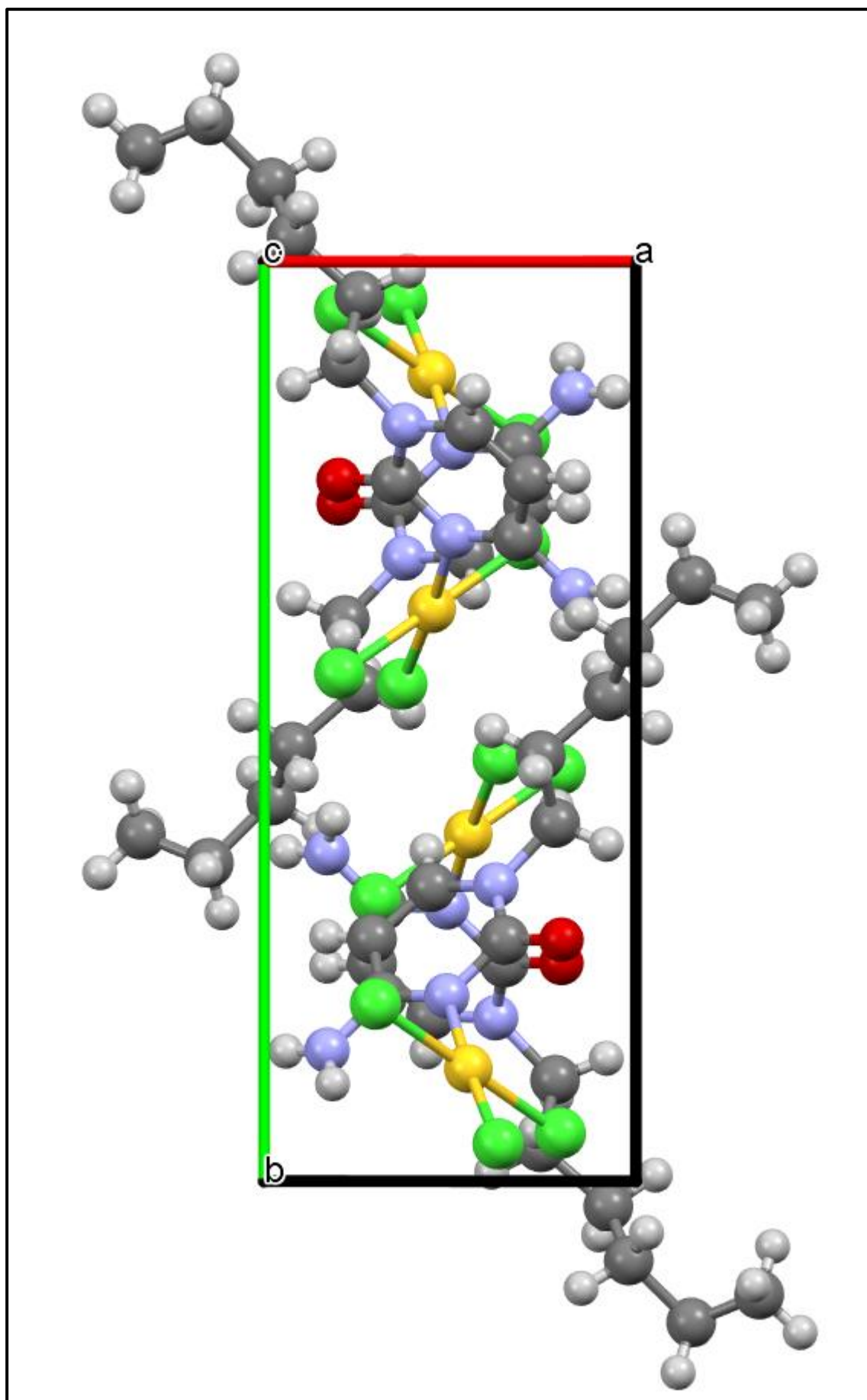


Figure 74 View of X-ray structure of Complex VIa along "c" axis

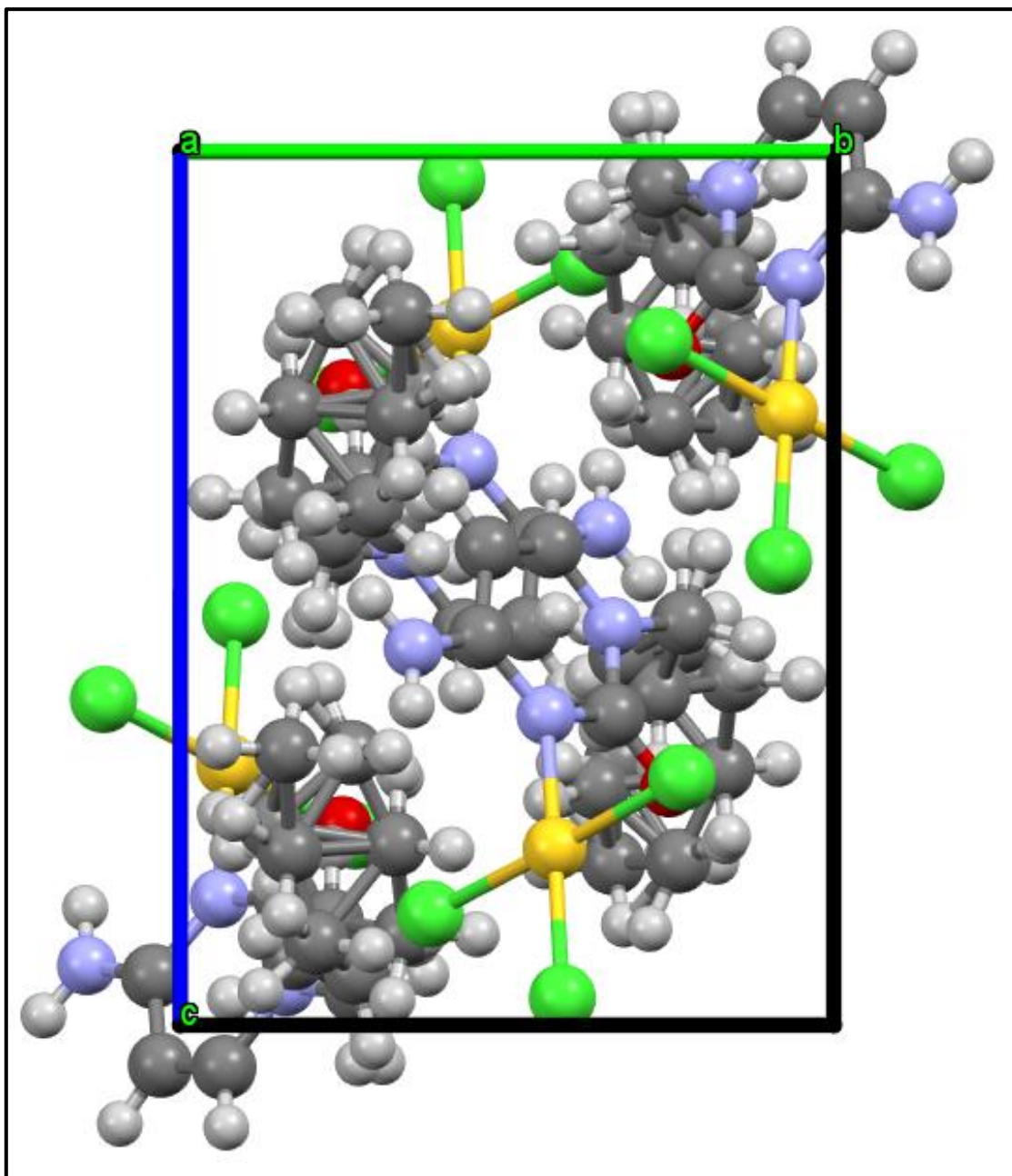


Figure 75 view of X-ray structure of Complex VIb along "a" axis

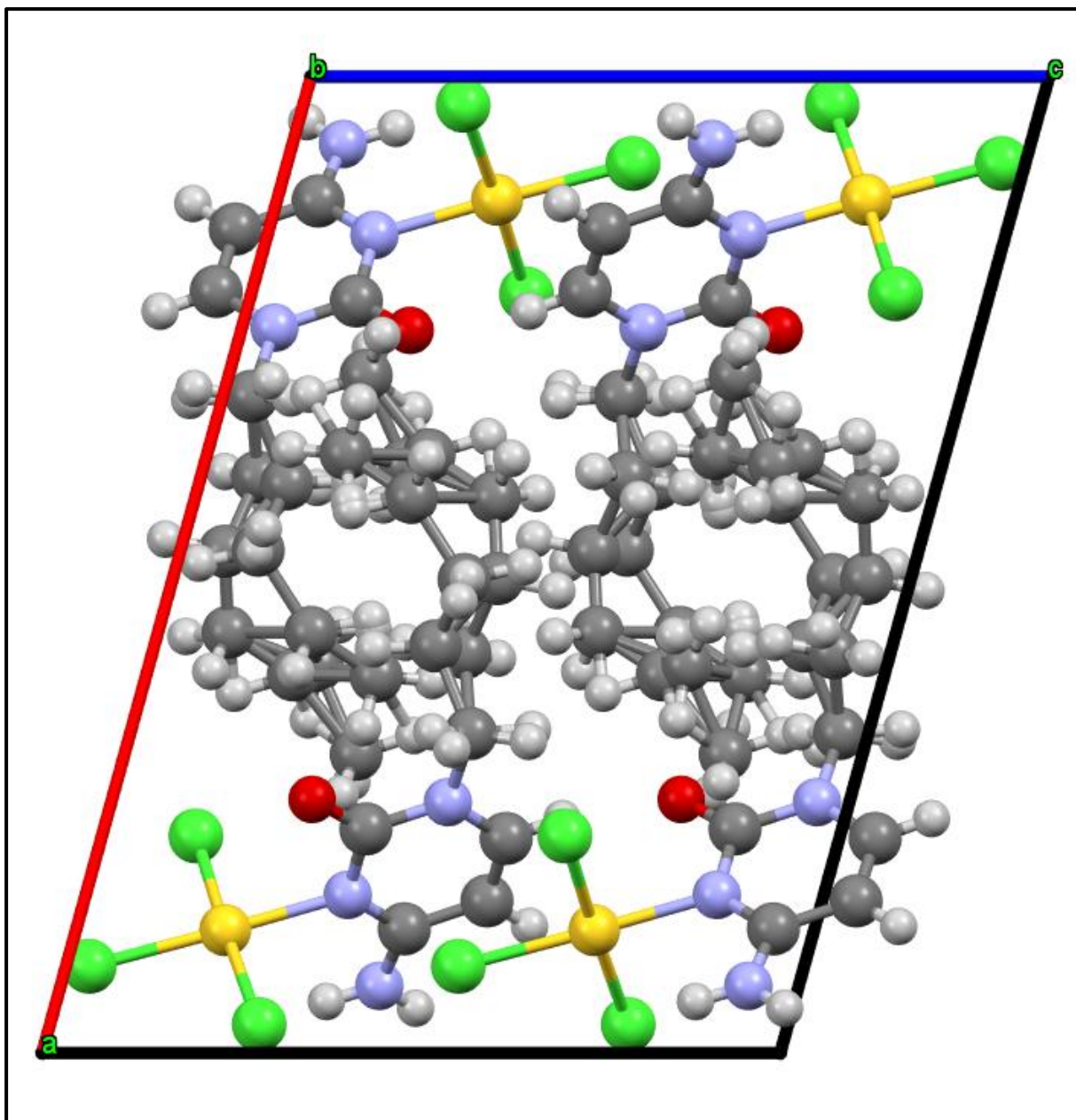


Figure 76 View of X-ray structure of Complex VIb along "b" axis

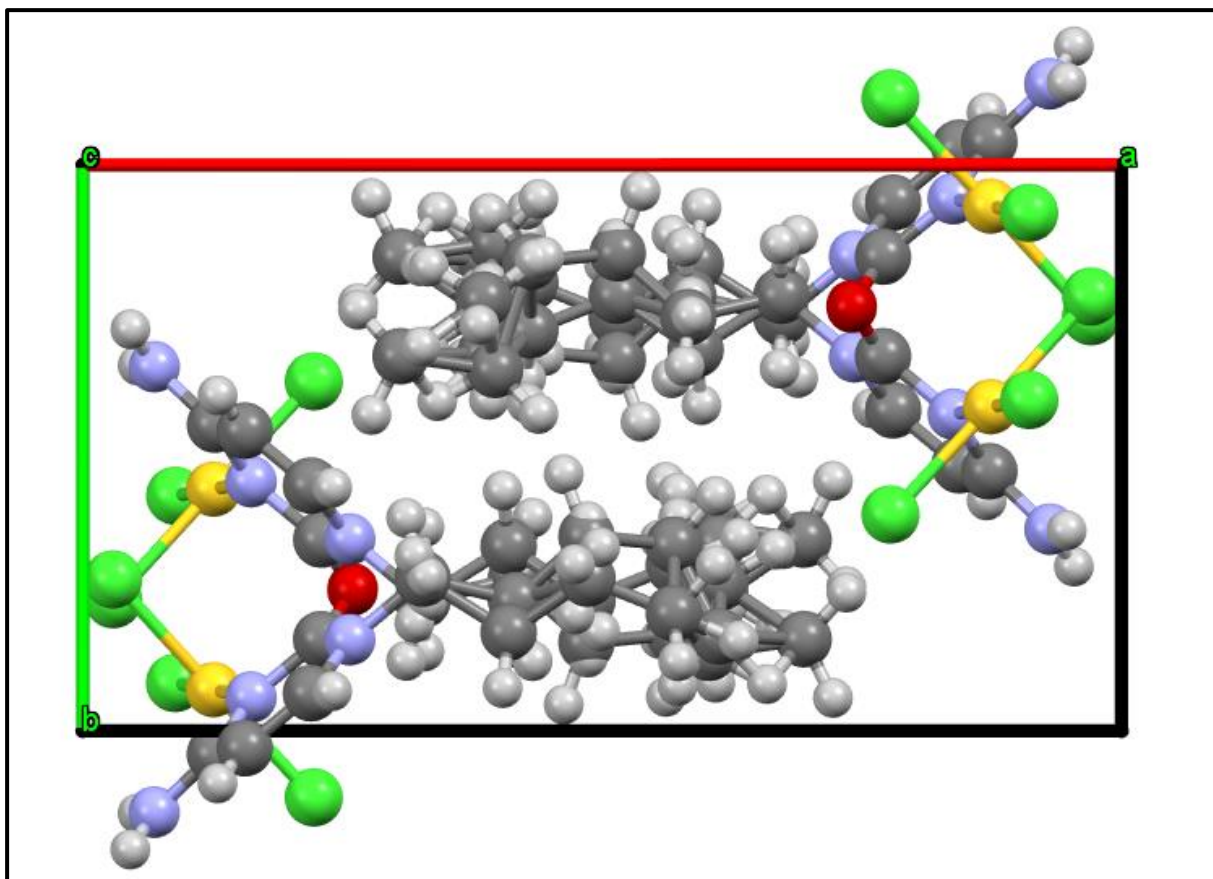


Figure 77 View of X-ray structure of Complex VIb along "c" axis



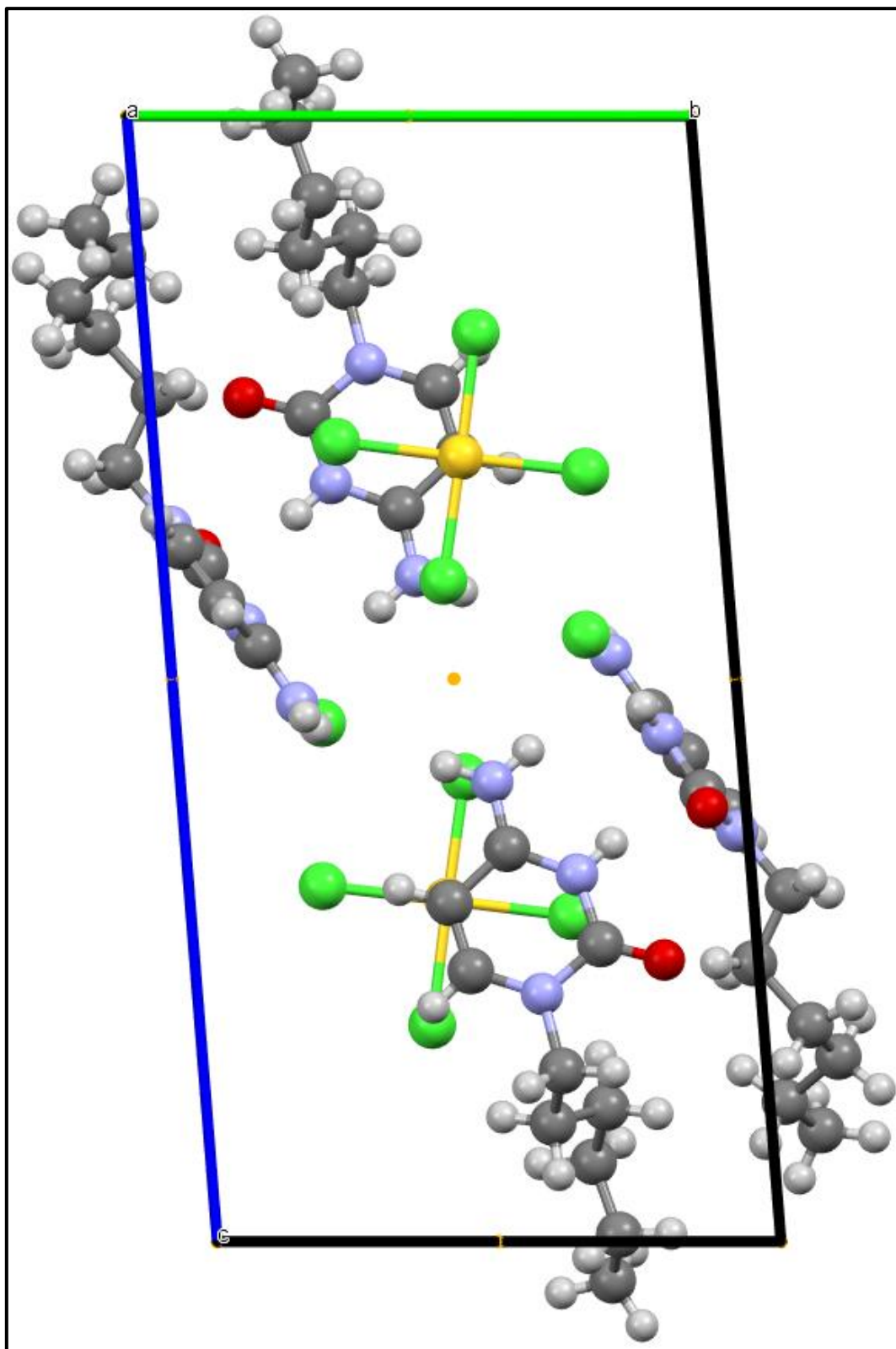


Figure 78 View of X-ray structure of Complex VII along "a" axis

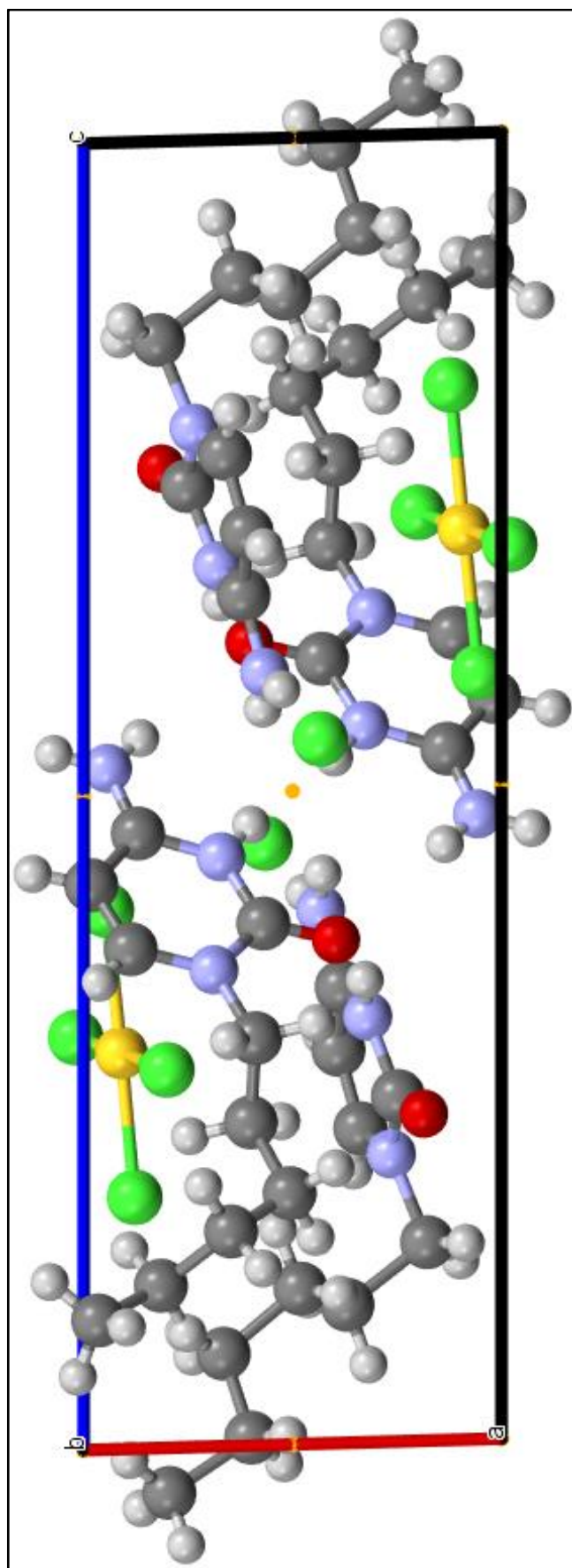


Figure 79 View of X-ray structure of complex VII along "b" axis

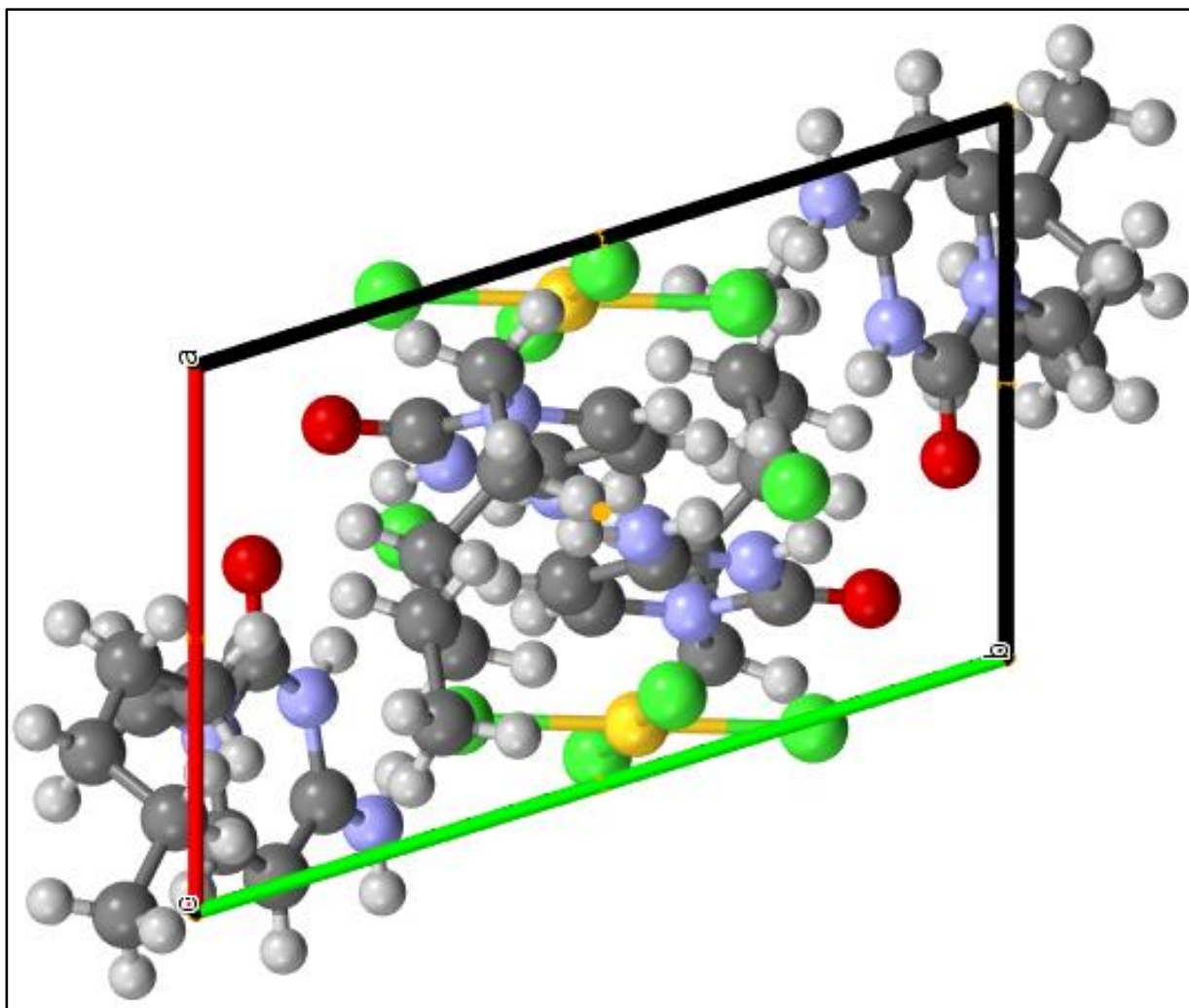


Figure 80 X-ray structure of complex VII along "c" axis